EFFECTS OF ENGINEERED LOG JAMS ON CHANNEL MORPHOLOGY, MIDDLE FORK OF THE JOHN DAY RIVER, OREGON

by

JENNA LAREE DUFFIN

A THESIS

Presented to the Department of Geography
and the Graduate School of the University of Oregon
in partial fulfillment of the requirements
for the degree of
Master of Science

June 2015

THESIS APPROVAL PAGE

Student: Jenna Laree Duffin

Title: Effects of Engineered Log Jams on Channel Morphology, Middle Fork of the John Day River, Oregon

This thesis has been accepted and approved in partial fulfillment of the requirements for the Master of Science degree in the Department of Geography by:

Dr. Patricia McDowell	Chairperson
Dr. Mark Fonstad	Member

and

Scott L. Pratt	Dean of the Graduate School

Original approval signatures are on file with the University of Oregon Graduate School.

Degree awarded June 2015

THESIS ABSTRACT

Jenna Laree Duffin

Master of Science

Department of Geography

June 2015

Title: Effects of Engineered Log Jams on Channel Morphology, Middle Fork of the John Day River, Oregon

Engineered log jams (ELJs) were constructed on the Middle Fork of the John Day River in eastern Oregon as part of a large restoration project. These log structures were designed to address many of the restoration goals including creating scour pools, inhibiting bank erosion, creating and maintaining a sinuous river planform, and increasing complexity of fish habitat. This study uses geomorphic change detection techniques to monitor topographic change under and around the 26 log structures in two different river reaches over a six to seven year period. This study finds that the ELJs are remaining stable within the river and maintaining deep pool habitat. The study provides insight into which log structure variables are most related to the patterns and amounts of aggradation and degradation. Understanding the geomorphic changes to the riverbed in response to the placement of the ELJs can influence the design and future effectiveness of ELJs.

CURRICULUM VITAE

NAME OF AUTHOR: Jenna Laree Duffin

GRADUATE AND UNDERGRADUATE SCHOOLS ATTENDED:

University of Oregon, Eugene, OR
Boise State University, Boise, ID

DEGREES AWARDED:

Master of Science, Geography, 2015, University of Oregon
Bachelor of Science, Geoscience, 2012, Boise State University
Bachelor of Arts, Spanish, 2012, Boise State University

AREAS OF SPECIAL INTEREST:

Fluvial Geomorphology
River and Habitat Restoration

PROFESSIONAL EXPERIENCE

Research Assistant, Boise State University Geoscience Department, 2012-2013

GRANTS, AWARDS, AND HONORS:

Graduate Teaching and Research Fellowship, Geography, 2013- 2015

ACKNOWLEDGMENTS

I would like to thank my advisor Patricia McDowell for training me to be a geomorphologist. She has spent countless hours in the field and in the office providing me guidance on how to approach problems and conduct my own research. Not only has Pat helped me learn the foundations of the science, she has also helped me learn to think critically about how natural systems function. I would also like to thank my committee member Mark Fonstad for introducing me to many new technologies used to conduct research and for providing feedback on my project throughout the whole process. Special acknowledgement is given to my fellow classmates for support and encouragement along with technical help. I would also like to thank the University of Oregon, Department of Geography for conference support. This research would not be possible without all of Pat's field crews from 2008 to 2014 who collecting the data I used in this project. This work was directly supported by Oregon Watershed Enhancement Board grant 212-920-10248 to the University of Oregon. I want to thank the Middle Fork John Day Intensely Monitored Watershed, the Confederated Tribes of the Warm Springs Indian Reservation, Oregon Watershed Enhancement Board, and the U.S. Bureau of Reclamation for project funding and support.

TABLE OF CONTENTS

Chapter Page

LIST OF FIGURES

Figure	Page

LIST OF TABLES

Table | Page

CHAPTER I

INTRODUCTION

In the past humans have viewed rivers as resources to be used, altered, and manipulated to address human needs. After westward expansion in the 1800s, rivers systems began to be heavily altered both directly and indirectly. As river floodplains were converted to agriculture and grazing, trees were harvested for wood, and riparian vegetation was reduced by grazing. Rivers were used to suit the needs of the area. They were straightened for navigation and flood control and mined for gold. Dams were built to store water and prevent flooding, and water was diverted for cities and irrigation. Practices like these devastated the fluvial systems, causing pollution and destroying the natural ecosystem function in Oregon and the rest of the county.

As a response to this ecological and geomorphic degradation, people have started to restore river systems. The number of river restoration projects implemented in the United States has increased exponentially between 1990 and 2005, with over $1 billion spent on these projects annually (Bernhardt et al. 2005). Restoration has been particularly prominent in the Pacific Northwest in response to the listing of five salmonid species under the Endangered Species Act (Katz et al. 2007). The listing of these anadromous fish species increased awareness of river degradation and the need to improve migration and spawning habitat.

Traditionally 'hard' engineered structures are built in streams to accomplish restoration goals such as grade control, energy dissipation to prevent bank erosion, and localized deposition and aggradation. Small weirs and dams are used to create step-pool features, and groins and dikes can be used to divert flow away from banks. These structures are traditionally built from large rocks or gabions. The structures are often successful at meeting their engineering goals, but do not always provide ecological benefits like increased fish habitat.

These traditional 'hard' restoration techniques focus on controlling the river, but often the goals of restoration include improving fish habitat and therefore returning the system to a more "natural" condition or assumed pre-disturbance condition. This is best accomplished through the use of natural materials and the simulation of the stream's natural processes (Abbe, Brooks, and Montgomery 2003). Focusing on emulating the natural system shifts the restoration strategy to emphasize the function of the river opposed to trying to solve one aspect in isolation of the rest of the system.

The restoration efforts in the Pacific Northwest have been at the forefront in incorporating and studying the effects and advantages of large wood as a 'soft' engineering method to emulate these natural river processes. Large wood is found naturally in rivers with forested floodplains and acts as grade control, prevents erosion, creates habitat diversity, and provides nutrients to streams (Abbe and Montgomery 1996; Keller and Swanson 1979; Manners and Doyle 2008, Nakamura and Swanson 1993). Studies have been conducted to understand the specifics of these effects and how best to emulate them in natural systems. In the Northwest, log structures are currently being used in many restoration projects, but there is a need to monitor these structures to understand if they are producing the desired effects. Many studies have looked at the hydraulic effects of log structures and there is a general understanding of the hydraulics and geomorphic features in isolated, simplified systems. There is still a lack of studies that directly measure the instream channel morphologic results.

The aim of this research is to better understand the effectiveness of engineered log jams (ELJs), or designed and human-built log structures, in river restoration (the terms 'ELJ' and 'log structure' will be used interchangeably throughout the rest of this paper to refer to ELJs). These structures are used in restoration projects as means of bank stabilization, pool creation, and fish habitat improvement. There is a need for more detailed understanding of ELJs channel morphologic effects and how site-specific characteristics and differences in log jam structure interact to create in-channel geomorphic features over timescales longer than a few years. There are multiple approaches to evaluating the effectiveness of these log structures. The paper will focus on the changes in channel bed topography around the structures to address whether these structures are meeting the intended restoration goals including developing and maintaining fish habitat. It will explore how engineered log jams control local scour and deposition patterns on the Middle Fork of the John Day River over multiannual timescales. To do this, the following research question will be addressed in this study:

> How does the log jam structure (number of logs, structure volume, etc.), its location along meander bend, and the dug pools drive patterns of aggradation and degradation?

CHAPTER II

BACKGROUND

River Restoration

River restoration is often thought of as a way to return a system back to its 'natural' state or condition before human interference. This definition is contentious, due to the uncertainty in defining the actual natural state of many rivers. Managers often identify a hypothetical 'natural form' to work toward in river restoration; emphasis on form often ignores restoring the natural function of the river, which includes physical and biological processes working together and a river system with lateral, vertical and longitudinal connectivity (Wohl et al. 2005). Wohl explains the issues that rise with the contradiction between form and function (Wohl 2005).

> A segment of river can meet many people's expectations of a healthy river if the water is clear and the stream banks are not rapidly eroding. However, the function of such a healthy-looking river can be highly compromised if flow and sediment are no longer moving downstream so that the habitats needed for diverse aquatic and riparian communities are not being maintained. (p. 1)

Successful river restoration focuses both on form and function in order to achieve the goals of ecological process.

River management as a whole and river restoration have generally followed two main trends throughout the world. The first of these trends is an engineering-focused view of river control management (Gomez 2000; Hillman and Brierley 2005). This is a reductionist approach to using the river as a resource to fulfill anthropocentric goals such as navigation, irrigation, power generation, and flood mitigation. Within this framework the river is no longer viewed as a natural system, but as hydraulically smooth channels, to minimize resistance and maximize the movement of water and waste (Hillman and Brierley 2005). The river is perceived as nature to be controlled and utilized, and potential negative aspects can be addressed through further engineering.

This technocratic approach started to lose traction when environmental concerns were on the rise in the 1970s. Changing world view and policy reflected the need to protect the natural systems and improve the previously abused and degraded systems. Emphasis was placed on river restoration and ecosystem rehabilitation. In many cases, management practices started to include ecosystem function and health as important variables along with more traditional management goals. Engineering became a tool that could be used in the restoration process, but less so as the definitive mode of management (Hillman and Brierley 2005).

Now, river restoration is broadly used to refer to many different types of projects with broad similar goals of reducing human caused degradation and improving instream habitat. Projects can be reach scale or multi-reach scale; they can be centered on the channel, or address the entire watershed as a whole. Project types include flow modification, instream habitat improvement, floodplain connectivity, riparian and wetland planting, erosion control, bank stabilization, grade control, channel reconfiguration, channel construction, dam removal , fish passage, culvert removal and replacement, and water quality management (Bernhardt et al. 2007; NOAA Fisheries).

Middle Fork of the John Day River

Geography

The Middle Fork of the John Day River (MFJDR) is located in Grant County in eastern Oregon (Figure 1). MFJDR is part of the John Day River, one of the longest free flowing rivers systems in the continental United States with headwaters in the Blue Mountains in Malheur National Forest (Bureau of Land Management).The John Day River is designated a National Wild and Scenic River and an Oregon Scenic Waterway.

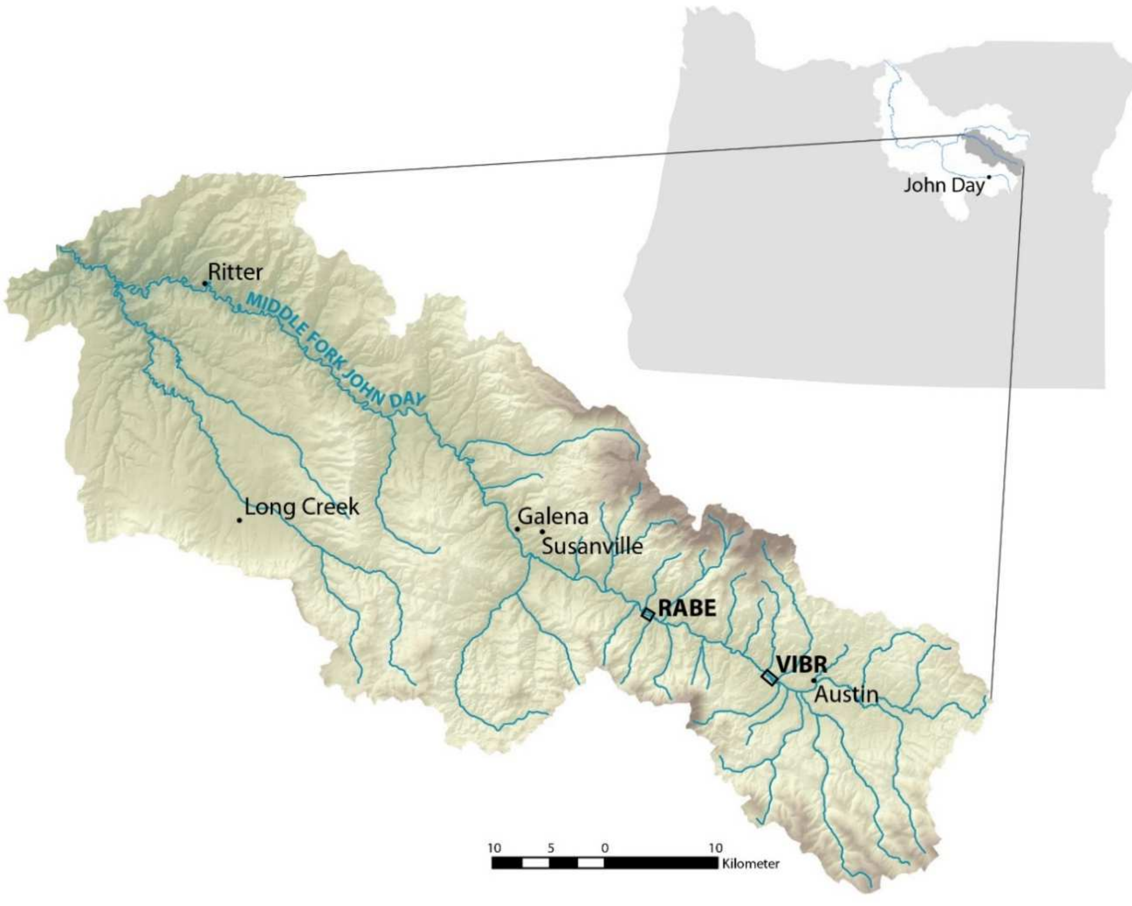

Figure 1: Middle Fork John Day basin location map-- from headwaters in the southeast to the confluence with the North Fork of the John Day River in the northwest. The study reaches, VIBR and RABE, are shown in black boxes.

The Middle Fork of the John Day is crucial habitat and spawning habitat for many fish including some listed under the Endangered Species Act. The river runs 120 km to its confluence with the North Fork of the John Day River north of the town of Monument. The North Fork of the John Day River flows into the main stem of the John Day River, which is a tributary to the Columbia River. The MFJDR basin has a drainage area of 2088 square kilometers. This description will focus on the upper MFJDR basin, upstream of Camp Creek (Figure 1)

The MFJDR is a meandering, gravel bed river, with a series of confined and unconfined reaches. Elevations range from 2500m at its headwaters to 670m at the confluence. Temperature and precipitation vary greatly with the large range in elevation. The basin receives around 100cm of precipitation annually at the headwaters and 25cm annually in the lowlands (Bureau of Reclamation 2008a). Most of this precipitation occurs in the form of snow in the winter, with episodic thunderstorms in the summer. The MFJDR has a snow-dominated hydrograph, usually some with rain on snow events, resulting in high discharge peaks in the early spring and larger than average winter and spring flood events. The discharge at Ritter, Oregon, in the lower part of the basin, peaks in late spring from snowmelt runoff and experiences the lowest flows in August and September, supported by groundwater and natural spring inputs (Figure 2).

The upper MFJDR naturally flows through grassy floodplains with dense riparian vegetation consisting of variety of shrubs and deciduous trees, such as cottonwood (*Populus trichocarpa*) and western hemlock (*Tsuga heterophylla*). Naturally, on the wide floodplains and hillsides were patches of conifer forests with predominately pine trees, such as ponderosa pine (*Pinus ponderosa*) (Bureau of Reclamation 2009).

Currently the riparian zone has less woody vegetation than historically and the previously forested floodplains have been cleared for agricultural and grazing land (Bureau of Reclamation 2009).

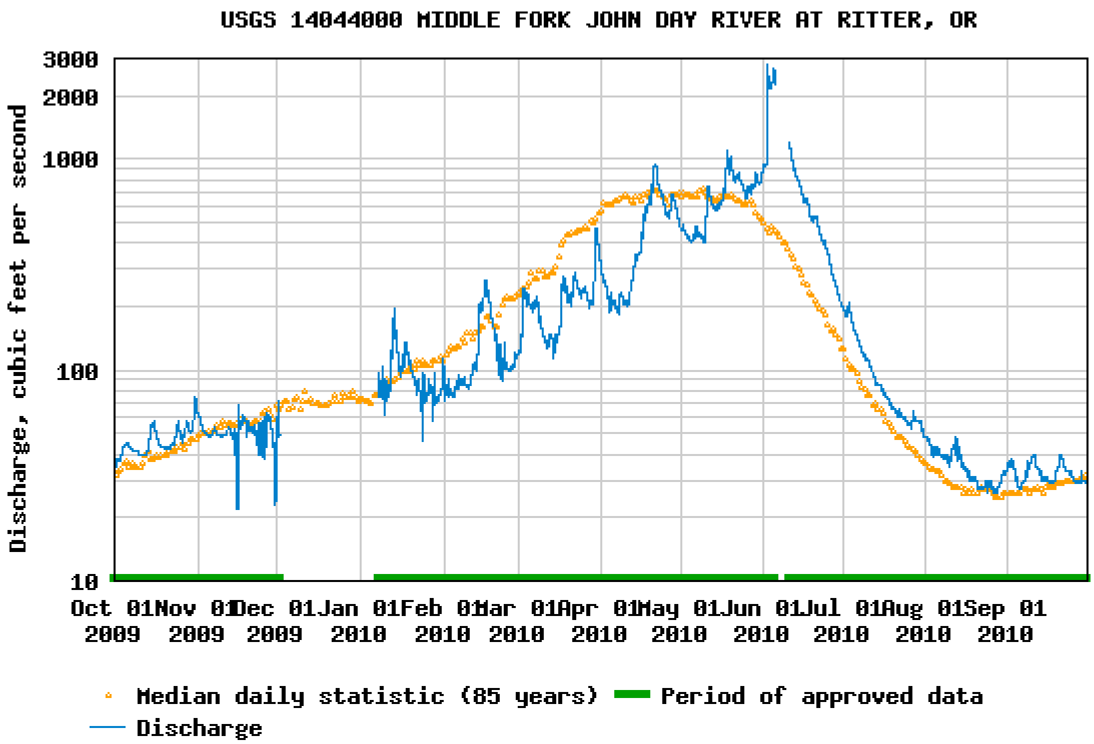

Figure 2: Hydrograph of the 2010 water year at the Ritter gauging station. The yellow line represents the average daily flow. Most recent water years, including 2010 (which has the smallest gap), have missing water data in the winter. Source: waterdata.usgs.gov

Salmon are native to the river, and in this area spring Chinook salmon (*Oncorhynchus tshawytscha*) and summer steelhead (*Oncorhynchus mykiss*) are the most common species. Chinook are found in the mainstem and larger tributaries, while steelhead are found in the mainstem and most tributaries. Bull trout (*Salvelinus confluentus*) are also found in cooler waters throughout the system (Bureau of Reclamation 2010). For this area of the Columbia Basin steelhead and bull trout are listed as threatened species under the Endangered Species Act (US Fish and Wildlife Service n.d.; NOAA Fisheries n.d.).

Geology and Geomorphology

The upper MFJDR basin is in the Greenhorn Range of the Blue Mountain physiographic province. This province was formed by a series of accretionary terranes joining onto the North America Continental Plate at a subduction zone. The oldest bedrock in the MFJDR formed 375 to 200 million years ago (Ma) during the Baker Terrane accretion. The Baker Terrane is composed of highly metamorphosed deep ocean sediment and volcanics. There are ophiolite deposits from oceanic crust uplift, and argillite deposits from the accretionary prism of the mid-ocean basin (Orr and Orr 2012). From 165 to 130 Ma these rocks were altered by the heat and pressure of a batholith intrusion composed of diorite and gabbro, which also now forms part or the bed rock in the area. The alteration of the oceanic crust rocks led to the crystallization of quartz along with heavy minerals, like gold (Oregon Department of Geology and Mineral Industries n.d.).

Widespread volcanism from 54 to 40 Ma covered much of the area in layers of volcanics known as the Clarno Formation. This is a series of andesite, tuff, breccia, and conglomerates, along with thick lahar flow deposits (Orr and Orr 2012; Oregon Department of Geology and Mineral Industries). The diverse makeup of the Clarno deposit, with stronger and weaker layers, makes it prone to landsliding (Bureau of Reclamation 2009). From 17 to 6 Ma, flows from the Strawberry Mountain volcanics, composed of basaltic andesite interbedded with ash, poured into the area (Orr and Orr 2012). Together Clarno and Strawberry Mountain volcanics underlie the majority of the modern upper MFJDR basin. Mazama ash from 7.7 thousand years ago (ka) is present in the deposits and serves as an important dating layer (Bureau of Reclamation 2009).

Since the deposition of the Strawberry Mountain Volcanics in the area, landscape development of the basin has been dominated by erosive and deformation processes. The main processes have been fluvial as the MFJDR and its tributaries have carved out the landscape and created the terraces and floodplains seen today. Late Pleistocene glaciation affected some of the upper parts of the tributary basins, providing sediment to the tributaries and their alluvial fans (Bureau of Reclamation 2009). Currently, the river is a meandering, gravel-bed, pool-riffle dominated channel, which flows through a series of confined and unconfined reaches, which are controlled by the geology of the areas and the erosivity of the exposed rocks (McDowell 2001). The modern floodplain is a medium energy non-cohesive floodplain (Nanson and Croke 1992) composed of alluvial deposits. These deposits are mainly cobbles and gravels along with sands and overbank fines. This floodplain has been occupied by the river for around the last 1000 years. Three well-preserved terrace surfaces were identified by Bandow (2004), with the youngest being 1-1.5 m higher than the active channel and likely 1,200 years old, and the oldest being 2-2.5 m above the active channel and dating from about 8 to10 ka.

In some cases, the location of the river within the valley has been controlled by landslides and alluvial fans. Between the two study reaches in this study, a large landslide made its way to the valley floor and controls the course of the river (Bureau of Reclamation 2009). They also provide sediment to the stream, along with boulders that are larger than the river is competent to move. Stream-dominated and debris-flow-dominated alluvial fans have also altered the river’s path in the valley. The river is diverted to flow around these fans at the mouths of the tributaries (Jett 1998). Sediment in the channel is likely sourced from a combination of tributary input, floodplain erosion, and alluvial fans (Bureau of Reclamation 2009). Prior to human impacts the river appears to have been in at least short-term equilibrium (100s to few 1000 of years); the river has been migrating laterally and vertically, not actively incising or aggrading, and creating a low gradient meandering, gravel-bed river, with pool-riffle sequences.

MFJDR Human Impacts

The MFJDR basin has been altered by non-Native American people since the early 1800s; Native Americans likely altered the landscape, but it was likely less intensive. There have been many human actions that have directly and indirectly affected the fluvial processes and channel conditions. The first non-Native American human alteration, and the least understood in this area, was beaver trapping in the early 1800s (Bureau of Reclamation 2008a). Beavers are native to this area and are important actors in providing instream wood, sediment storage, floodplain habitat, and increased local water tables. When over-trapping removed all the beavers from the ecosystem, these instream processes were lost.

Human alterations in the valley became much more visible and direct after the 1862 Homestead Act that brought people west and into the MFJDR basin. Miners were the first immigrates into the valley in the 1860s, followed by homesteaders. The floodplain and terraces were mined and mining continued in the valley throughout the next century. The floodplains and terraces were also good for grazing cattle and agriculture. Timber harvesting started in the valley and Bates, a lumber mill and company town, was built along the river, channelizing parts of it, and using the water for their mill ponds.   With the influx of people and economy came the needs for transportation. A railroad was built in 1910 along the south side of the valley. This required further timber harvest, but also channelized the river. River meanders were cut off to make room for the tracks. The rail only operated until the 1930s. Roads were built in the 1950s, and continued this pattern of channelization. Bank hardening structures were placed in the channel to decrease channel migration and protect the roads. These structures included riprap, thumb-jetties, and cabled-in logs; they resulted in reducing the channel's ability to meander and decreasing floodplain and habitat (McDowell 2000).

The most visible and direct of all the human alterations in the valley was gold mining. This started in 1860s with instream placer mining and bank and terrace hydraulic mining. These forms of mining directly disturb the channel bed and sediment supply. Fines are exposed and washed away and natural banks and floodplain surfaces are disturbed. From 1933 to 1942 a several segments of the river was dredge mined (Figure 3). This devastated the channel and floodplain.

Figure 3: River channel pre and post dredge mining. In 1939 the channel meanders along the southern part of the floodplain. After dredge mining (1956) the channel is left abandoned and the channel runs straight alongside the tailing piles, which are the white areas. Source: Bureau of Reclamation 2008a.

The dredge moved through the valley, digging up wide swaths of the channel and surrounding floodplain, while processing the sediment for gold. It then dumped the unwanted sediment in tailings piles on the side of a now straight, narrow, deep channel that was no long able to laterally or vertically migrate because it was not competent enough to move the coarse sediment that was dug up from deep in the floodplain. The river was left channelized and disconnected from its floodplain and alluvial fans.

MFJDR Restoration Project

These human alterations have left the river disconnected from its floodplain, straightened and with a generally degraded ecosystem and habitat. In recent years there has been a large effort to address these concerns. The area is now designated an Intensely Monitored Watershed (IMW) by the Pacific Northwest Aquatic Monitoring Partnership and the Oregon Watershed Enhancement Board; and has been provided significant funding to improve fish habitat and channel function (Middle Fork Intensively Monitored Watershed, n.d.). The central restoration actions are designed to reconnect habitat; restore hydrologic, geologic and riparian processes; and enhance instream habitat (Curry, Bennett, and Bouwes 2011). Passive restoration has included adding grazing exclosures. Some phases of the project have been active restoration, which included intense channel reconstruction—building pool-riffle sequences, meanders, side channels, and placing ELJs. The phases of the project discussed in this paper did not include channel reconstruction but, included the placement of engineered log jams as a more natural way to stabilize banks, but also add complex fish habitat. Old bank hardening structures have been removed and there are many planting efforts to add woody riparian vegetation. Table 1 shows some of the geomorphic and physical habitat restoration objectives and response hypotheses, along with monitoring techniques.

Table 1: Geomorphic and physical habitat monitoring hypotheses. Shows the restoration objective and action along with the response hypotheses and how they will be assessed with monitoring. The monitoring techniques are XS (cross section surveys), GC (gravel counts), FC (Fish cover surveys), LS (log structure surveys), and ground and aerial imagery. Source: McDowell, Pers. Comm.

Objective and Action	**Indicator/hypothesis**	**XS**	**GC**	**FC**	**LS**	**Imagery**	**Other**
Increase aquatic habitat quality: Place LWD	Pools/km ↑, Deep pools/km ↑						X
	Habitat units/km ↑						X
	Sinuosity ↑					X	
	Embeddedness ↓, % Fines ↓		X				
Increase fish cover: Place LWD	Pools/km ↑, Deep pools/km ↑						X
	Fish cover ↑			X			
	% undercut bank ↑						
Move toward natural channel morphology: Place LWD	Wbf ↓, Dbf ↑, W:D ↓	X					
	Sinuosity ↑					X	
Increase floodplain access: Place LWD; remove rock;	Stage ↑ for a given Q						
	Flow in side channel ↑						
Increase lateral migration: Remove rock	Lateral migration rates ↑	X				X	
Reaches are dynamically stable: All restoration activities	XS area relatively stable	X					
LWD will assemble in relatively stable and complex	Self-formed LWD accumulation					X	
	New accumulations persist					X	

The two reaches included in this study include VIBR (from **Vi**negar Creek to **Br**idge Creek) and RABE (from **Ra**gged Creek to **Be**aver Creek) (Figure 4). The VIBR reach is located in the Forrest Conservation Area (an area owned by the Confederated Tribes of the Warm Springs Reservation of Oregon and managed to protect and enhance fish habitat) just downstream of Bates, Oregon (Figure 1). The project section of VIBR is about 1.9 river km long and has an average active channel width of around 8m. The overall slope of the reach is about 0.5%. The restoration in VIBR was completed in 2008. The main goals were to reconnect the channel to its floodplain and increase fish habitat. To do this, riprap was removed from the stream banks, vegetation was replanted in riparian zone, and log structures were placed along the channel and pool were dug under them. There were several goals for the log structures in this reach including side channel and overflow channel creation for high flow refugia, deep pool development, bank stabilization, fish cover, and channel shading (Bureau of Reclamation 2010).

The RABE reach is located in the Oxbow Conservation Area (an area owned by the Confederated Tribes of the Warm Springs Reservation of Oregon and managed to protect and enhance fish habitat) about 13km downstream of the VIBR reach. RABE is about 0.8 river km long and has an average bankfull width of 13m. The overall slope of the reach is 0.6%. The restoration in RABE occurred in 2009 and included rock spur removal, planting of riparian zone vegetation, historic meander/secondary-channel reconnection, mid-channel bar creation, log structure placement, and scour pool excavation. In this reach, log structures were placed to increase perennial access to side channel, recruit spawning gravels, create fish habitat, and maintain scour pools (Bureau of Reclamation 2008b).

The ELJs constructed in the MFJDR consist of anchored logs and racked members, which are either woven into the structure or loose. The structures are not cabled into the bank or to each other, but instead rely on the anchored logs to fix them in place. The anchored logs are buried around 6 meters into the bank of the channel and into the floodplain, generally with rootwads extending into the channel. Cobbles or compacted soils were used bury the logs in the floodplain. In some jams, footer logs are used, which run parallel to the bank and help to elevate the end of the anchored logs in the channel. The racked logs form the body of the structures. The structures in VIBR are smaller and sometime are only composed of a few anchored logs; structures are on average 5 m long by 3 m wide and average bankfull width for the channel was 8 m. The RABE structures were larger on the most part with many anchored logs and racked members placed parallel to the flow; structures are on average 8 m long by 4 m wide and average bankfull width was 14 m. Some structures in RABE also use vertical pilings to pin the structure in place. Similar sized anchor logs were used in both VIBR and RABE, despite VIBR having a much smaller channel and smaller log structures. The diameter at breast height (dbh) of the logs ranged from around 30 cm to 45 cm (Bureau of Reclamation 2007; Bureau of Reclamation 2008c).

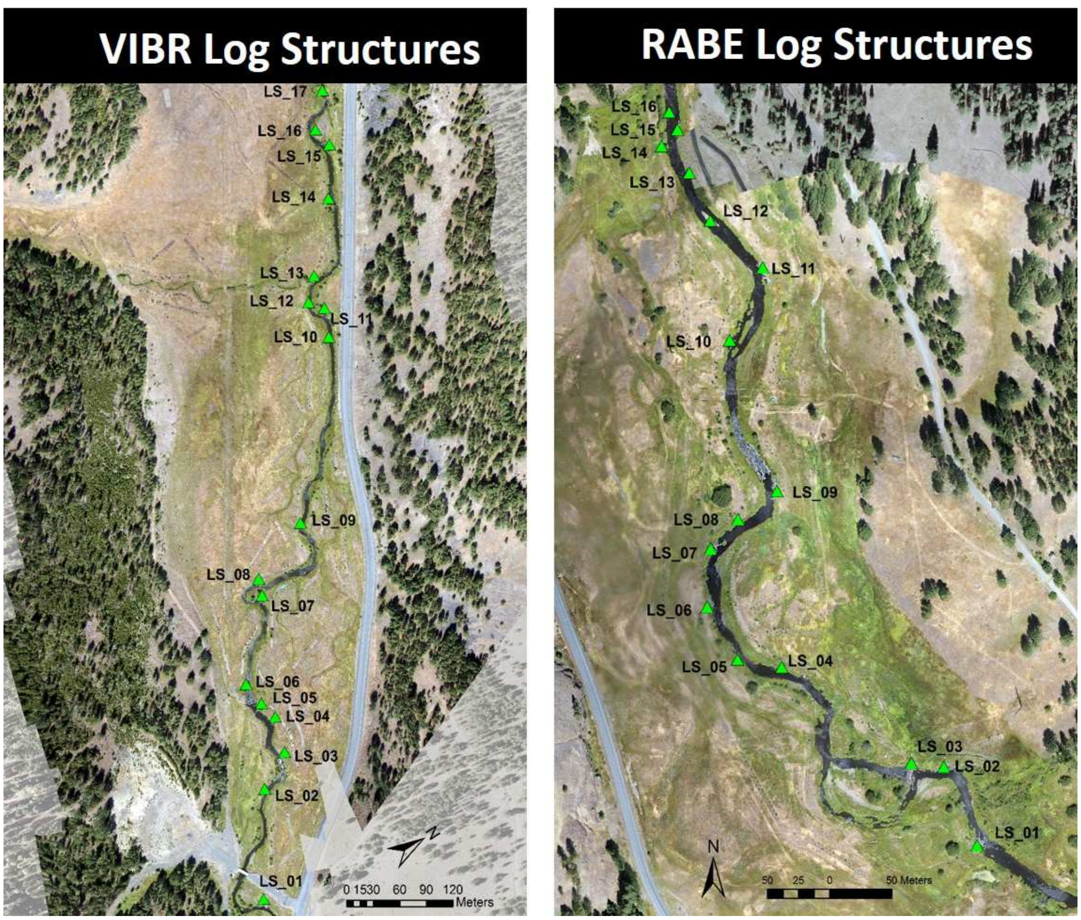

Figure 4: VIBR and RABE project reach maps with log structures labeled.

CHAPTER III

LITERATURE REVIEW

Wood in Rivers

The effects of log jams in rivers have been studied a number of different ways. Natural wood accumulations have been studied in channels to understand the geomorphic effects. Flumes studies have been conducted to link the geomorphic effects seen in natural streams to the hydraulic conditions producing those effects. Studies from natural log jams coupled with the flume studies have been used to design ELJs used in restoration. There is also a group of studies that have looked at the geomorphic and ecological effects of these designed structures. All of these aspects are important for understanding if ELJs are meeting their restoration goals.

Natural Large Woody Debris

Many studies have been conducted to understand the controls that natural large woody debris (LWD) structures impose on fluvial channel form and processes. Large woody debris and jams in low gradient (slopes of a 1-3m/km) meandering rivers are associated with changes in stream width, side channel formation, and the formation of more LWD jams downstream. In high gradient forested rivers, LWD produces long-term sediment storage, changes stream gradient by forming steps, and dissipates energy, which enhances fish habitat (Keller and Swanson 1979; Nakamura and Swanson 1993). LWD has been found to have differing effects on bank erosion depending on location and flood magnitude. Erosion decreased when wood obstructions caused zones of turbulence and dissipated energy, but erosion increased in low gradient streams when the wood acted as deflectors and directed flow toward the banks (Keller and Swanson 1979).

LWD also has effects on channel morphology. Wood jams, especially bar apex jams, have been shown to be associated with the formation of downstream bars and permanent features around the LWD where recruitment of other wood, energy dissipation, and sediment storage results in more stable mid-channel structures (Abbe and Montgomery 1996; Keller and Swanson 1979). LWD has large impacts on scour pool formation, frequency, and spacing (Buffington et al. 2002; Montgomery et al. 1995). This is especially common where in-channel wood forces scour pools by acting as local obstructions. The obstruction-forced pools were found to be the most common means of pool formation, which were often associated with logs that are oblique or perpendicular to flow, according to Montgomery et al. (1995). The angle of log to the flow has been found to have a larger impact on drag, or the fluid resistance, than the size of the log. Drag was higher with logs that were near perpendicular or perpendicular to flow (60° to 90° to the flow) and drag was high when the log was parallel to the flow and there was a bluff face of the end of the log obstructing the flow (Gippel et al. 1996). Another study showed that radius of curvature was lower in meanders with natural log jams, than those without jams, because of reduced channel migration from bank hardening (Abbe, Brooks, and Montgomery 2003).

Log Jams and Flow Hydraulics

Log jams, formed from the accumulation of woody debris, have significant effects on stream flow and hydraulics. Log jams have been studied in natural systems, but scientists have also worked to isolate effects by testing downscaled simplified structures in flumes. In streams, log jams and woody debris act as roughness elements to dissipate energy, increase drag, and help to break up areas of strong flows (Daniels and Rhoads 2004; Manners and Doyle 2008). Log jams serve as anchors to contribute to bend development by causing flow separation at the frontal jam area, which breaks the flow into eddies and deflects high velocities from the outer bank toe. Reduced velocities along the bank toe help reduce bank failure and lateral channel migration, assisting in channel stabilization (Daniels and Rhoads 2004; Shields, Morin, and Kuhnle 2001). These flow structures have been replicated in flumes with simplified single-log structures, specifically with downstream-oriented logs (logs attached to bank with the trunk extending in the downstream direction). The structures in these experiments produced less scour and scour area along the bank than banks without logs by deflecting flow away from banks, thus increasing bank stability (Biron et al. 2005; Cherry and Beschta 1989).

Flume studies of simplified flow obstruction have shown that there are areas where aggradation and degradation is the most common. Manners et al. (2007), showed that aggradation occurred directly upstream and downstream of the jam from backwater effects and velocity reduction downstream. There was also a patch a degradation at the tip of the structure because of flow coverage. Flow obstruction models presented in Buffington et al. (2002) demonstrate how flow might interact with different kinds of obstructions and result in upstream and downstream eddies, along with concentrated flow adjacent to and under the structures. These flow patterns help interpret the patterns of aggradation and degradation.

Flume studies also found that logs and rootwads with perpendicular and upstream orientations to flow create the greatest flow disturbance, forcing water around and under the obstruction while producing eddies downstream, resulting in larger scour holes directly under and upstream of the obstruction (Biron et al. 2005; Svoboda and Russell 2011), but can also increase potential of bank erosion from flow deflection (Cherry and Beschta 1989). Cherry and Beschta also found upstream-oriented logs produced deeper scour depths and perpendicular-oriented logs produced larger surface area of scour; the deepest scour was found just downstream of the dowel tips and farther downstream there was aggradation. This study also showed that partially elevated logs created more localized scour (large magnitude of scour over a smaller area) than logs in contact with the channel. Similar results have been shown in other studies; however, in some cases overtopping flows created higher disturbance and could result in more area of scour (Beschta 1983; Biron et al. 2005).

Log jam porosity, the amount of open space within the jam not filled by logs, debris or sediment, has also been found to have important effects on patterns of scour and aggradation. Manners et al. (2007) looked at natural instream structures with varying levels of porosity. The lowest porosity was represented by a structure wrapped in plastic, increasing porosity was represented by a natural log structure; a structure with the small woody, soil, and leaf litter removed; and the high porosity was represented by a structure with all woody except for the key members removed. Manners et al. found that complexities in patterns of erosion and deposition are dependent first on porosity. They show that jams with very low porosity have random distribution of erosion and deposition and that jams with higher porosity have increased downstream velocities and decreased velocities adjacent to the structure. They also show that high porosity jams have smaller backwater effects upstream or areas of very low flow which result in aggradation. Svadoba and Russell (2011) found in their flume experiment that using additional logs in the structure had little effect on scour and deposition and appeared to block and divert flow away from the structure. It is important to note that many studies of woody debris effects are conducted with single-log models, and Manners et al. (2007) found that there is a complex non-linear relationship for stream hydraulics between single log and debris jams.

Engineered Log Jams and Restoration

Large woody debris and debris jams are being emulated in restoration to recreate the natural effects of woody debris. These structures are referred to as engineered log jams (ELJs). In some cases, ELJs are designed to reduce bank erosion and are considered an alternative to traditional stream stabilization and hardening methods. One study, Drury et al., 1999, used ELJs in place of rock groins to protect a bridge pier and prevent avulsion, but also to enhance salmon habitat. Post-project monitoring showed that the structures created flow separation and turbulence at the frontal area of the structure and redirected flow from the bank, reducing bank erosion. The structures were also successful at creating scour pools upstream and adjacent to the ELJs, which enhanced fish habitat. They found that spacing between consecutive structures could be greater than that for rock structures for reducing bank erosion along long stretches of bank.

There is concern about the longevity of placed wood structures. In one study, the first year of monitoring showed positive results; the structures were reducing bank erosion in an incised channel (Shields, Morin, and Kuhnle 2001). Additional years of monitoring showed these results were temporary as the structures failed within the next few years (Shields, Knight, and Stofleth 2006). Studies have identified the importance of a fixed key member in log jams for stability and longevity (Abbe, Brooks, and Montgomery 2003; Nakamura and Swanson 1993). This suggests these stability problems could be addressed with improved designs of the way logs are anchored into the banks.

Engineered log jams have also been used in degraded river systems to help stabilize the stream and create complex fish habitat. Brooks et al. (2004) monitored the geomorphic effects of introducing ELJs in the William River in Australia. Within one year they found that deflector jams created scour pools upstream and adjacent to the jams along with aggradation in riffles upstream of many types of ELJs, resulting in an increase in pool-riffle amplitude throughout the reach. Further monitoring (five years after implementation) showed a continuation of these patterns, but also an increase in pool and bar area throughout the reach (Brooks et al. 2006).

Although Brooks et al. (2006) found that the structures produced an increase in pools and riffle area, they did not find an increase in fish assemblages within the five years of their study. Brooks suggests that some levels of degradation may not be fixed quickly even with high degrees of intervention. In the another ELJ placement project, Pess et al. (2012) found higher juvenile fish densities in stream units with log jams. (Roni et al. 2002) reviewed the results from many studies and found that log structures were successful at creating juvenile Coho habitat and increasing densities.

Synthesis

The importance of natural wood in creating and maintaining complexity and ecosystem health in fluvial systems is well understood. In recent years river restoration has worked to incorporate these ideas into projects in hopes of increasing success and longevity of the restoration. When river restoration projects build engineered log jams to emulate natural complexity, it is important to have a sound scientific understanding of the systems in order to fully grasp the potential for physical changes. When designed properly for the specific river and conditions, engineered log jams can increase channel complexity, hydraulic roughness, pool frequency, and sediment storage. They can also help to control river gradient, bank erosion, meander curvature radius, and water velocity.

The degree to which these effects actually occur is not understood in all situations. Studies like Abbe and Montgomery (1996) have developed simplified flow obstruction models for understanding the effects of naturally formed log jams on channel morphology. By understanding the channel hydraulics and log jam structure, they identified predictable patterns for channel morphologic change including pool and bar formation. Location and degree of scour can be predicted by empirical models developed from experimentation. Although studies like this lay a foundation for understanding general patterns, these situations are simplified and the nature of what actually will occur when attempting to engineer these natural situations is not known. As more river restoration projects incorporate log jams, it becomes important to know the actual physical effects.

Some projects have attempted to quantify the channel morphologic change in river restoration projects. Monitoring ELJs in the field is important, and positive geomorphic and biologic results have been shown (Brooks et al. 2004; Drury et al. 1999; Pess et al. 2012). Studies like these do not attempt to link the results to how the structures are producing the change. The ability to link simplified flow obstruction models to the design and implementation of engineered log jams (Abbe et al., 2003;

Brooks et al., 2004) would allow for better understanding of the physical results and development of restoration techniques that produce desired effects.

DEM of Difference Method

Error Assessment for DEM of Difference

New technologies have made four dimensional monitoring possible in rivers. RTK-GPS provides an easy way to collect high density point clouds in the field in a short amount of time. These point clouds can be interpreted into surfaces that represent the channel bed. By using two data sets from the same area, but in different years, the rasters can be subtracted from each other to create a difference of DEM (DoD) to compare areas over time (Brasington et al., 2000).

When creating DoDs, it is important to account for the error associated with the creation of each surface, because when they combine, the errors propagate. There are two general methods for accounting for this error–- uniform error assessment and spatially distributed error assessment. All of these methods can be completed on the same data, but difference information is extracted and processed depending on the method. The simplest of these methods, uniform error assessment, involves quantifying the error through root-mean square error (RMSE) calculations based on the inherent surveying error. When using this with DoDs, a minimum level of detection (LoD) or a set threshold where real change can be distinguished, is calculated by taking the RMSE for each surface to account for propagated error in both surfaces. The significance of the error from point density difference and grain size effects was tested on small subsamples from the dataset to help identify the threshold for the LoD (Brasington et al., 2000). The disadvantage of this method is that the RMSE is averaged over the whole surface. This results in over or under estimations of channel fill and scour, and especially a loss of information on smaller channel changes (Wheaton, 2010).

Errors within DEMs tend to occur where topography is rapidly changing. Uniform error assessments cannot account for this variability. Spatially variable error assessment addresses this issue. There are currently two main methods to implement for spatially distributed error assessment. Milan et al. (2011) introduced a method that uses a linear relationship established between the survey elevation error and the local topographic roughness. Elevation error is established by creating an interpolated surface from the survey points and comparing the interpolated values to the actual survey values. Local topographic roughness is established by taking the standard deviation of the survey points within some radius (usually encompassing no more than seven points) of each point to create a surface that represents the variation in topography. The linear regressions are applied to the map of local topographic roughness, creating a spatial error grid for each DEM. The RMSE is then calculated from these error grids to create a spatially distributed LoD grid for the survey. The LoD is then subtracted from the DoD to create a spatially thresholded surface. Incorporating the surface variability has been shown to better estimate sediment volumes and detect spatial patterns (Milan et al. 2011).

The other method of spatially variable error assessment was developed by Wheaton et al. (2010). They created a Matlab tool that allows for the creation of DoDs, integrating different methods of error assessment including uniform error assessment and two new alternative methodologies. To account for DoD uncertainty, they consistently use three steps: (1) quantify the uncertainly within each surface by looking at measurement errors, survey bias, and interpolation methods; (2) propagate error, using a root mean square error equation, into a DoD (using a different method than Milan et al. 2010); and (3) assess the significance of the uncertainly by applying a probabilistic threshold.

Wheaton et al. (2010) presented new methodologies that classify variables using fuzzy set theory. Slope, point density, and GPS point quality (error associated with instrument used to collect data) are the inputs into the system, and elevation uncertainty is the output. Milan et al. (2010) used topographic roughness instead of slope and surface interpolation error instead of measurement error (point density and GPS quality). Levels of elevation uncertainty were assigned to the surface based on fuzzy inference logic that combines the three inputs. This was done for each DEM and then the DEMs are combined with RMSE error propagation, resulting in a DoD based on the probably that the change is real. The second method extends this method using the spatial coherence of the erosional and depositional areas to increase the known area of change, through the use of Bayes' Theorem.

CHAPTER IV

METHODS

Creating the DEMs of Difference

Patricia McDowell's research group conducted field surveys from 2008 to 2014 to collect high resolution topographic data of the channel bathymetry. These surveys included latitude, longitude and elevation for points in an area around and under each log structure. The research group defined the survey areas for each log structure to include the river bed, banks, and start of the floodplain along the stretch of river from a few meters upstream of the structure to a few meters downstream. From 2008 to 2010 surveys, the group conducted the surveys with a total station, and from 2011 to 2014 the surveys were completed using an RTK- GPS. In the first two years of surveying, the group collected sparser point clouds with point spacing from 1m to 3m apart; the later surveys are higher density point clouds, with point spacing from 0.3m to 1m. Points in the surveys were taken as a series of cross sections running perpendicular to the log structure. Points along the cross section were spaced at 0.3 meters to 1m. Each cross section was 1m to 3m away from the previous cross section.

The research group collected as-built surveys around each log structures within a month following construction of the structures—VIBR surveys in 2008 and RABE surveys in 2009. They resurveyed these areas either once or twice in following years (Table 2). From 2008 to 2014, Patricia McDowell's group conducted a total of 71 surveys. A total of 27 log structures have repeat surveys and were used for analysis.

I imported the points collected from these surveys as point clouds into ArcGIS and converted each point cloud into a TIN (Triangulated Irregular Network), using break lines along the water surface edge. I corrected anomalies in the TIN surface by excluding points from the survey that did not appear to accurately represent the surface. I then interpolated the TINs into DEMs (Digital Elevation Models) with a resolution of 0.1 m x 0.1 m, using nearest neighbor interpolation, and clipped the DEMs to the channel area that was covered by the surveys for all survey years.

Table 2: Years of log structure survey; blue highlighted surveys have two survey years, orange highlighted have three surveys, and the non-highlighted were only surveyed once.

	2008	**2009**	**2010**	**2011**	**2012**	**2013**	**2014**
VIBR LS 1	x		x				x
VIBR LS 2	x					x	
VIBR LS 3	x		x			x	
VIBR LS 4	x		x			x	
VIBR LS 5	x		x			x	
VIBR LS 6	x						x
VIBR LS 7	x						x
VIBR LS 8	x		x			x	
VIBR LS 9	x		x			x	
VIBR LS 10	x						
VIBR LS 11	x						x
VIBR LS 12	x		x			x	
VIBR LS 13	x					x	
VIBR LS 14	x						x
VIBR LS 15	x					x	
VIBR LS 16	x					x	
VIBR LS 17	x						x
RABE LS 1		x		x		x	
RABE LS 2		x				x	
RABE LS 3		x					
RABE LS 4		x		x			x
RABE LS 5		x					
RABE LS 6		x		x			
RABE LS 7		x		x		x	
RABE LS 8		x				x	
RABE LS 9		x				x	
RABE LS 10		x				x	
RABE LS 11		x		x			x
RABE LS 12		x				x	

	2008	2009	2010	2011	2012	2013	2014
RABE LS 13		x					
RABE LS 14		x					
RABE LS 15		x					
RABE LS 16		x					x

To assess the change in the channel topography over time, I compared the DEMs for each log structure using the DoD method. In this method, two DEMs of the same area are compared by subtracting the earlier DEM from the later one. To account for uncertainty in these data sets the use of spatially variable error assessment is crucial when quantifying small topographic changes. I created the DoDs using the methodology presented in Milan et al. (2011). To create the DoDs, for each DEM I completed the following steps:

1. Established a linear relationship between the elevation error (survey point elevation minus the interpolated elevation) and the local topographic roughness (standard deviation of elevations within a radius around each point—the radius was determined for each survey based on point density so that no more than about 7 survey points were encompassed).
2. Applied the linear regressions to the map of topographic roughness, which creates a spatial error grid.
3. Calculated the root mean square error (RMSE) by combining the error grids from each year's DEM to create a spatially distributed LoD grid.
4. Subtracted the LoD from a basic DoD to create a thresholded surface with spatially distributed error.

DoDs were created for each log structure with multiple surveys. If there were three surveys at one structure, DoDs were created for each time step and the overall change (year 2 – year 1, year 3 - year 2, and year 3 - year 1). Each DoD was clipped to where the surveys overlapped and the channel bed extent so the in channel changes could be compared. I later used the area of these clipped DoDs, referred to as the survey area, to normalize the change in sediment volumes to make it comparable among surveys. Appendix A shows the resulting DoD and the linear regressions for each log structure and the values used in this methodology.

I then extracted quantitative information on topographic change from the DoDs and DEMS. I calculated total volume of sediment aggraded and degraded for each survey area along with the net change in volume. I also extracted pool areas and volumes for each survey and calculated the changes in pool area and volumes. I collected residual pool depth and changes in residual pool depth from the DEMs by identifying the deepest point in each pool and the pool tail crest elevations for each year (Lisle 1987).

Qualitative variables were also gathered from the DoDs. I described the dominant location and direction of change for each log structure; location of change was categorized relative to the log structure as downstream, upstream, outboard, under structure, along opposite bank, or along same bank as the structure. I also noted shifts in pool shape or location and identified changes in as narrowing/widening and shifting downstream, upstream, or laterally. Both the quantitative variables of volume and area of change and the qualitative variables patterns of change were used as response variables in the analysis.

Log Structure and Channel Characteristics

During 2014, I collected the characteristics of the log structures to be used as explanatory variables in the study. These were collected using field measurements and observations, as well as aerial imagery analysis. I noted log structure characteristics at each site; variables included the numbers of logs, logs anchored into the bank, logs woven into the structures, loose logs, logs perpendicular to flow, and rootwads. I collected these values for within bankfull, outside of bankfull, and total number. I noted information on the occurrence and location of logs in contact with the channel bed, and measure the height of the log structure with a stadia rod.

I also categorized log structures by ELJ type as either a meander jams (MJ), bar apex jams (BAJ), alcove jams (AJ), bar top jams (BTJ), or bank jams (BKJ). Meander jams are placed on the outside bank of meander bends and are composed of key anchored logs and racked members. Bank jams are built along semi-straight sections of the stream and are anchored into the bank. Bar apex jams are located on a central bar and have a key member oriented parallel to the flow, whereas bar top jams are logs, anchored or not, on the surface of an active bar. Alcove jams are built in an alcove or small side channel and do not extend far into the channel.

I also used georectified aerial imagery collected in 2009 and 2013 to collect log structure and site characteristics. The 2009 photography was taken from a tethered balloon and has very high resolution (<5 cm processed resolution) (Russell and Bauer 2009). This imagery represents the as built structures in RABE and the structures after one year in VIBR. The 2013 photography was taken from a helicopter; the processed imagery is 10 cm resolution (Dietrich 2014). From these photosets, I measured log structure width and length, and I identified active channel boundary, referred to as bankfull in this study, along each reach from the 2013 photoset and complementary DEMs and extracted bankfull widths at each log structure survey. I drew centerlines for each reach between each bankfull line and used them to calculate radius of curvature at each log structure. I calculated radius of curvature (centered on each log structure) by drawing a circle arc connecting three points—one centered on the log structure and points located 1.5 reach-averaged bankfull widths upstream and downstream (average bankfull for VIBR is ~ 8m and RABE is ~14m). I then calculated radius of curvature from the arc length and the chord length between the endpoints of the arc. Variable names and descriptions are summarized in Appendix B.

Data Analysis

Starting with the variables discussed in Appendix B, I converted all field data values that were counts (i.e., the number of rootwads) to proportions of the total number of logs in each structure, to make them comparable. The new set of variables is displayed in Table 3. To assess the distributions of the data, I made histograms for each variable and calculated the variable means by reach. The univariate results and discussion consists of these histograms and the discussion of the distribution and reach differences. These histograms and the rest of the analysis were completed in R.

Table 3: Variables used for analysis

Variables	Units	Description	Transfor-mation
ls_type	Qualitative	Log jam categories: MJ- Meander jams, BAJ- Bar apex jam, AJ- alcove jam, BTJ- Bar top jam, BKJ- Bank jam	None
vol_ls_log	m^3	Volume of log structure (length x width x height)	Log
area_ls_log	m^2	Area of log structure (length X width)	Log
porosity	m^3/count	Volume of log structure/ number of logs	None
anch_tot	Proportion	Proportion of logs that are anchored	None
perp_tot	Proportion	Proportion of logs that are perpendicular to the flow	None
rw_tot	Proportion	Proportion of logs that have rootwads	None
bc_tot_sqrt	Proportion	Proportion of logs that are in contact with the bed	Square-root
bf_tot	Proportion	Proportion of logs that are in within bankfull	None
ch_obs	Proportion	Proportion of the channel obstructed by the structure	None
roc_log	m	Radius of curvature at the log structure	Log
por_area_chg	Proportion	Proportion of the survey area that shows real change	None
por_area_agg	Proportion	Proportion of the area of real change that is aggradation	None
agg_area_sqrt	m	Volume of aggradation/survey area	Square-root
deg_area_sqrt	m	Volume of degradation/survey area	Square-root
net_per_area	m	Volume of net change/survey area	None
chg_pd_por	Proportion	Change in residual pool depth as a proportion of the initial pool depth	None
chg_pa_por	Proportion	Change in pool area as a proportion of the initial pool area	None
chg_pv_por	Proportion	Change in pool volume as a proportion of the initial pool volume	None
pool_depth	m	Final residual pool depth	None
pool_area	m^2	Final pool area	None
pool_vol	m^3	Final pool volume	None
sed_pat_1	binary	1 means that the survey shows degradation on the bank or under the structure and aggradation outboard or along the opposite bank, 0 means it does not show this pattern	None

I needed to assess the normality of the distributions and reduce the number of explanatory variables to perform multivariate analysis, I created correlations matrices for both the explanatory and response variables and, to normalize the data, I transformed variables that displayed curvilinear relationships with other variables. Variables that were actual values were log-transformed and proportions were square root transformed. The correlation matrix was remade for all the variables (Appendix C).

I then performed principle component analysis (PCA) on the explanatory variables to assess the correlation among them. Components with standard deviations greater than one were considered significant in this study. For further anlysis, I used the variable that was most highly loaded on each component, along with variables that were not highly loaded on any component and variables that were associated with a component, but did not seem to be conceptually associated with the other component variables. PCA was also completed with the response variables to see which appeared to be associated, but all of the variables were used for further analysis and PCA results were considered later in the analysis.

I used a Generalized Additive Model (GAM) to create multivariate models for each response variable. GAMs are a form of multivariate analysis that allow for non-linear relationships to be assessed between a response variable and multiple explanatory variables. They also allow for use of binary qualitative data. The individual effects of each explanatory variable can be examined, while holding the other explanatory variables constant. These results are displayed as partial residual plots. To assess the combined effects of the predictor variables, I displayed the models as 3-D surfaces using vis.gam in R.

First, I created a model of each response variable with five explanatory variables identified from the PCA analysis. For each model, the two explanatory variables with the lowest p-values were used to create another multivariate model that could be visualized on a 3-D surface. In some cases, other explanatory variables, besides those identified in the first GAM, were tested in the models in order find the highest correlation that also made conceptual sense for the response variables. I removed outliers from some models to create smoother fit curves that better explained the majority of the data. Correlation values for the models and p-values for the individual variables in the models were also calculated.

CHAPTER V

RESULTS

Structural Changes to ELJs

There have been few structural changes to the log structures constructed on both reaches of this restoration. Most of the structures were designed to remain stable under high winter and spring flows, with logs anchored into the bank and most logs woven within the structures. Other structures were not as well anchored and consisted of loose logs to be mobilized during high flows. Structural changes in the log structures were assessed by comparing aerial photos from 2009 and 2013 (see changes for each of the following structures in Appendix D and structure characteristics in Appendix E). In that time frame, four log structures (VIBR 7, VIBR 11, VIBR 16, and RABE 8) endured minor changes with a few of the loose logs missing. The bank jam RABE 10 was completely rearranged and lost four logs. Two structures, VIBR 10 and RABE 16, were completely removed. VIBR 10 was a bank jam structure with three loose logs located on top of the bank near a small alcove; all of the logs have been washed out and the alcove has been filled. RABE 16 was a single log bar apex jam with a rootwad anchored into a mid-channel bar, and the log and the bar have been completely washed out. In 2011, there was a large flood event with discharges far above average all winter and spring along with several peak flood events (Figure 5). The 2011, 1.0 m resolution, aerial imagery, was too coarse to confirm that the minor changes in the log structures occurred during the flood, but showed that the flood was responsible for the washing out VIBR 10 and RABE 16 and caused the changes to RABE 10.

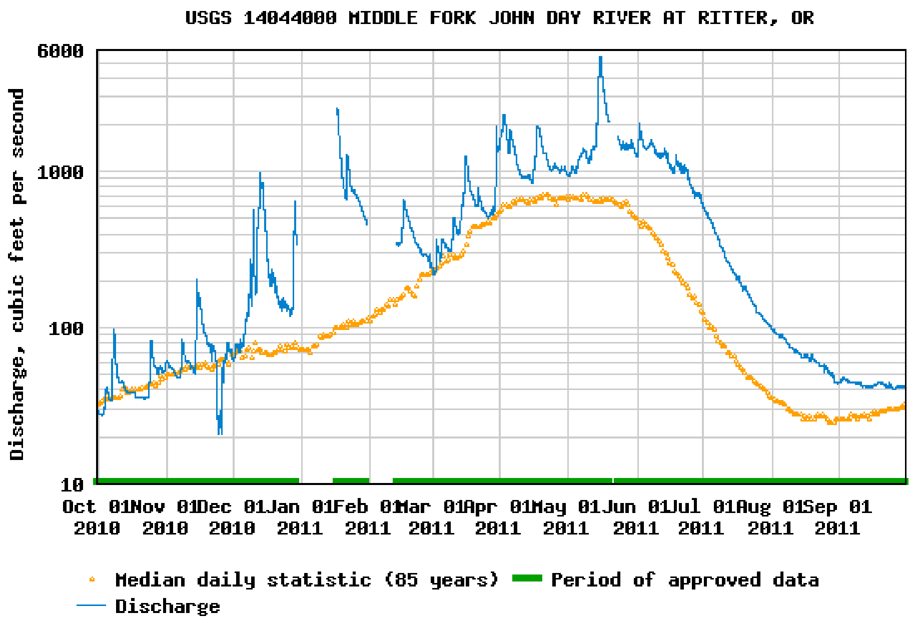

Figure 5: Hydrograph of the 2011 water year on the Middle Fork of the John Day River in Ritter, Oregon. Winter and spring, and summer flows remained above the 85-year median. There were several large events in December, January, and May with flows 5 to 10 times higher than the median. Source: waterdata.usgs.gov

Univariate Results

Log Structure Composition Surveys

The field composition surveys provided information on the design of the ELJs and the structural characteristics that may have affected the geomorphic results from the topographic surveys. The table in Appendix B describes the variables that were collected during the composition surveys and the variables that were calculated from those data. The data from the composition surveys are summarized in Appendix E. There is a clear difference in the composition of the log structures between the upstream reach, VIBR, and downstream reach, RABE. Figure 6 and table 4 show that the structures in VIBR contain less than half the average number of logs than the structures in RABE. The VIBR structures also consist of less rootwads on average than RABE structures. Although RABE structures have greater number of logs and have substantially larger volumes than VIBR on average, they are slightly more porous on average than VIBR structures. When the volume of log structures are normalized by the reach average bankfull widths, the volume of log structures are still on average larger in RABE.

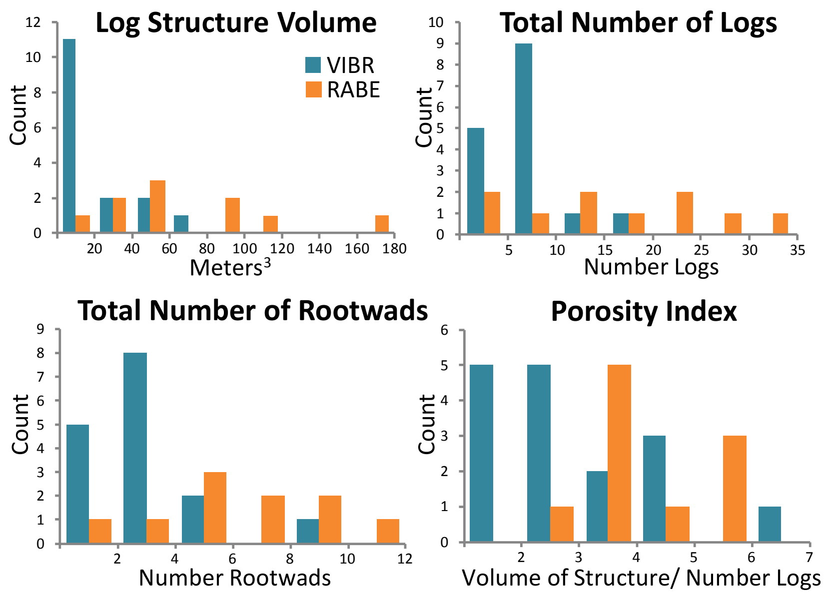

Figure 6: Log structure composition. Histograms for log structure volume, total number of logs in the structures, total number of rootwads, and the porosity index (volume of structure/number of logs).

Figure 7 and table 4 show that on average, the structures in RABE have a higher percent of logs within the defined active channel width, or bankfull, and a smaller percent of anchored logs than VIBR. The VIBR structures have a higher percentage of perpendicular bankfull logs than RABE.

In VIBR, the structures obstruct more of the bankfull width than in RABE, which is partly due to the smaller average bankfull width, but also the structure design (Table 4). Figure 8 shows the distribution of radius of curvature values for the locations of the structures in each reach. This shows that the structures in VIBR have smaller radius of curvature values overall than RABE. Both reaches have similar sinuosity ratios of around 1.2, therefore more structures in VIBR than RABE were built along tighter bends, with very few on straight sections of the channel. The radius of curvature values for RABE are more evenly spread across the histogram.

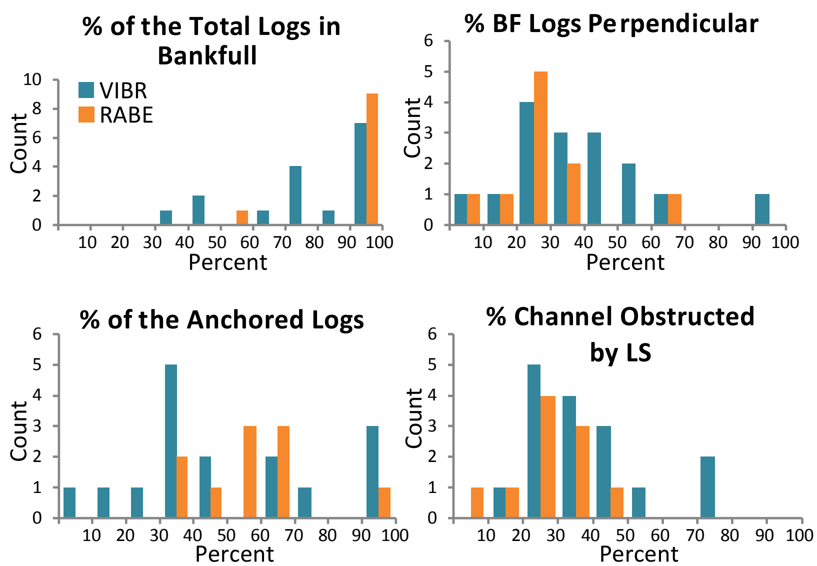

Figure 7: Log structure composition by percent. Histograms for percent total logs in bankfull, the percent bankfull logs that are perpendicular to flow, percent anchored logs and the percent of channel obstructed by the log structure.

There are several differences between the reaches. RABE structures are overall larger based on the number of logs and rootwads, along with the volume of the structures. Most of the RABE structures have all logs within bankfull, whereas VIBR structures have a range or percentages of logs within bankfull. Channel width obstruction was larger in VIBR, which has smaller channel width. VIBR also has overall smaller radius of curvature values because of the high sinuosity of the reach.

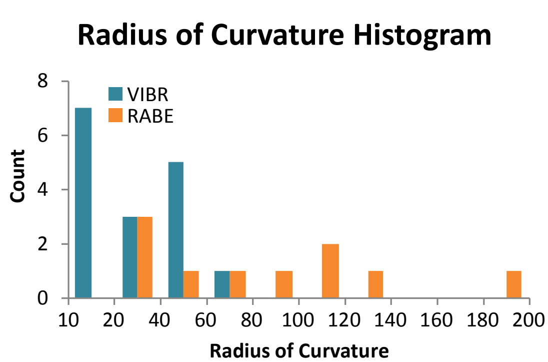

Figure 8: Radius of curvature values in meters for each log structure by reach (m).

Topographic Surveys

The variables collected from the DoDs show differences between the two reaches as well. Overall there was more aggradation per area than there was degradation per area (Table 4). This is also shown in figure 9, the average values for the net change for the reaches, which are positive for both, showing more aggradation overall. VIBR has less aggradation and slightly more degradation than RABE. Total change per area shows that on average there was a higher volume of sediment moved per survey area in RABE than in VIBR.

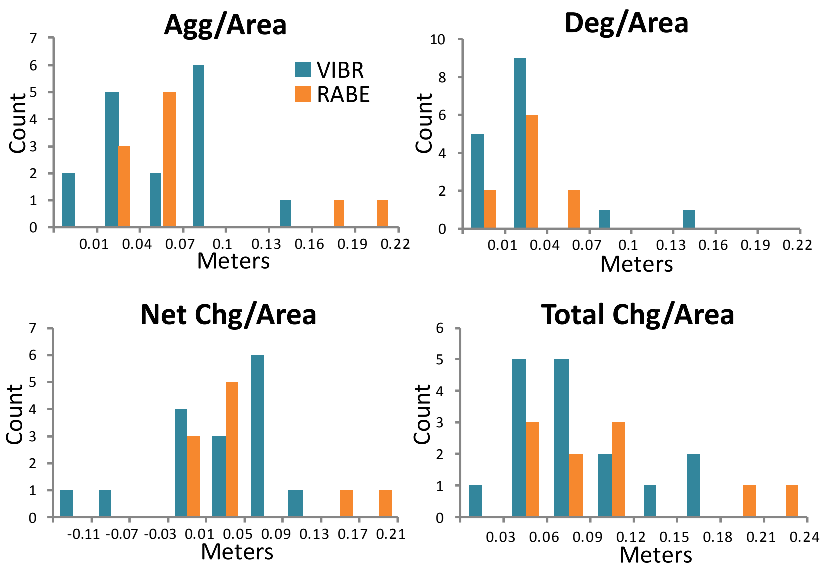

Figure 9: Sediment response around log structures. Histograms for both VIBR and RABE for aggradation per survey area (Agg/Area), volume of degradation per survey area (Deg/Area), net volume of change per survey area (Net Chg/Area), and total volume of change per survey area (Total Chg/Area). All have units of meters.

The overall higher amounts of aggradation around the structures in both reaches imply that the log structures are acting as flow obstructions and are overall reducing the velocity of the stream around the structures and resulting in sediment deposition. The higher sediment volumes changes in RABE may be due to the larger amount of the flow in this reach, or the larger log structures. The stream power in RABE at bankfull is calculated to be 491.2 W/m and larger than the stream power in VIBR at bankfull, which is calculated to be 276.7 W/m. Unit stream power for RABE is 110.4 W/m^2, which is lower than in VIBR (161.4 W/m^2). The lower unit stream power in RABE suggests the high sediment aggradation may be due more to log structure characteristics than to the more powerful flows.

Table 4: Reach averages for explanatory variables and sediment response variables.

	VIBR Reach Average	RABE Reach Average
Log Structure Volume (m^3)	20.63	67.45
Total Number of Logs	7.19	16.20
Number of Rootwads	3.44	6.50
Porosity Index	2.94	4.01
Percent Logs in Bankfull	79.90	93.71
Percent Anchored Logs	49.81	58.49
Percent Perpendicular Logs	41.11	28.17
Percent Channel Obstructed	38.68	25.94
Total aggradation/ total reach survey area (m)	0.053	0.076
Total degradation (+)/ total reach survey area (m)	0.029	0.026
Total net change/ total reach survey area (m)	0.024	0.050

Changes in pool depths from the first year of survey to the last year of survey are shown in Figure 10A. This histogram shows the values for both reaches, VIBR and RABE, in different colors. These data are shown for a total of 16 pools in VIBR and 9 pools in RABE, so relative shapes of the histograms can be compared, but not magnitude of the distribution. Figure 10A shows that the distribution of the change in pool depth is skewed to the left, displaying that more pools shallowed (negative values) than increased in depth. The peak of the histogram is from 0.0m to -0.05m of change for both RABE and VIBR. The average change in pool depth for VIBR is -0.07m and the average change in depth for RABE is -0.12m.

Although pools are shallowing overall, pool area is increasing. Figure 10B shows the histogram of change in pool area for both reaches. The histogram peaks between 0.0m^2 and 5.0m^2 increase in pool area for both reaches. The distribution for VIBR is fairly normal, centered on positive change, whereas the distribution for RABE is skewed to the left. In VIBR the average net pool change in positive, 4.06m^2, showing an overall 32% increase in pool area for the reach. In RABE the average net change in pool area is only 0.08m^2, but more pools are increasing in area than decreasing. Overall a total of 65.70m^2 of pool area was gained in both reaches around the log structures, most of which was gained in VIBR (64.96m^2); RABE gained quite a bit of pool area in some pools, but also lost a lot of pool area in others.

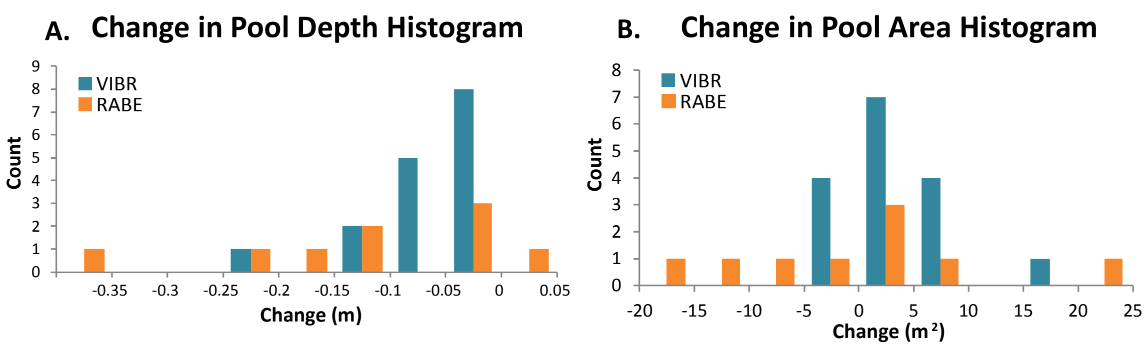

Figure 10: **A**. Histogram for change in pool depths for both reaches; **B**. Histogram for change in pool area for each reach.

Changes in pool volume show different patterns for each reach (Figure 11). Almost all pools in RABE decreased in volume (Figure 11). In VIBR there was on overall slight increase in total pool volume, but some pools gained volume, while others lost volume.

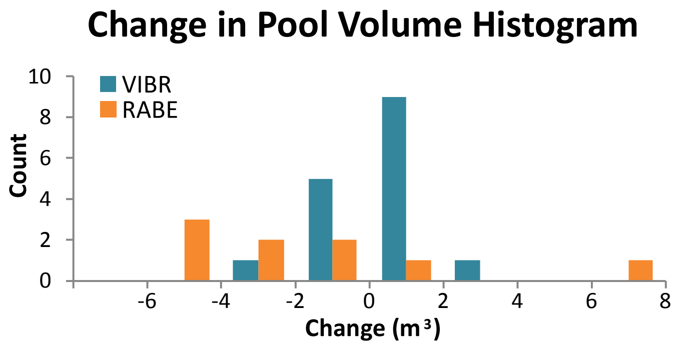

Figure 11: Histogram for change in pool volume for both reaches

Histograms of the initial and final values of the different pool characteristics demonstrate the initial and final differences in values by reach (Figure 12). Pool depths in VIBR were initially shallower than in RABE. The histograms for pool area show that pools were initially smaller in VIBR, but they are expanding more than RABE pools. Pool volume distributions do not change as much as the others, but pool volumes do appear to be increasing some in VIBR and decreasing in RABE.

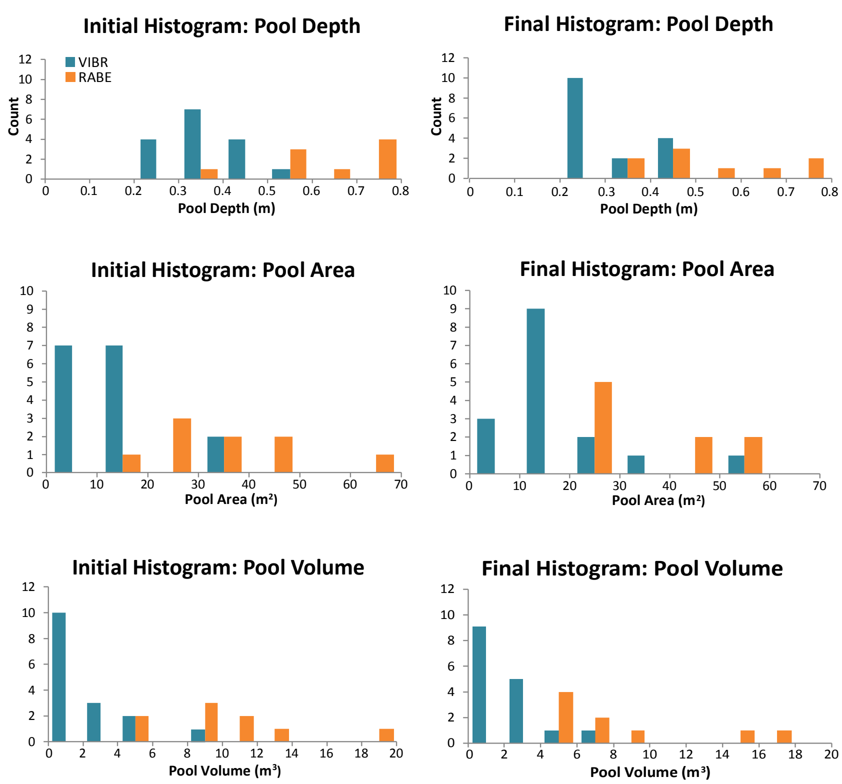

Figure 12: Histograms for the initial and final values of pool depth, pool area, and pool volume for each pool in each reach.

Multivariate Results

PCA

The PCA analysis for the transformed explanatory variables (Table 3) resulted in three components with standard deviations greater than one, which was used as a cutoff for this analysis (Figure 13). The first two components were comprised of log structure characteristics; the first component was heavily loaded by log structure volume (vol_ls_log), log structure area (area_ls_log), the proportion of anchored logs (anch_tot), the proportion of logs with rootwads (rw_tot), and the proportion of logs in contact with the bed (bc_tot_sqrt). The second component was heavily loaded by proportion of logs within bankfull (bf_tot), the proportion of perpendicular logs (perp_tot) and the proportion of logs in contact with the bed (bc_tot_sqrt). The third component included channel characteristics. Channel obstruction (ch_obs) and radius of curvature (roc_log) were most heavily loaded on this component. See Table 3 for summary of all variables. Appendix F shows the original PCA plot and loadings for all explanatory and response variables.

Volume of log structure, the proportion of logs in bankfull, and channel obstruction were the variables most highly loaded on each component and were used to represent the other variables that were associated with them. The proportion of perpendicular logs and radius of curvature was also included, because they are conceptually different than the other variables on component two. Porosity was not heavily loaded on any component and therefore was considered another unique variable to be used in the multivariate modeling.

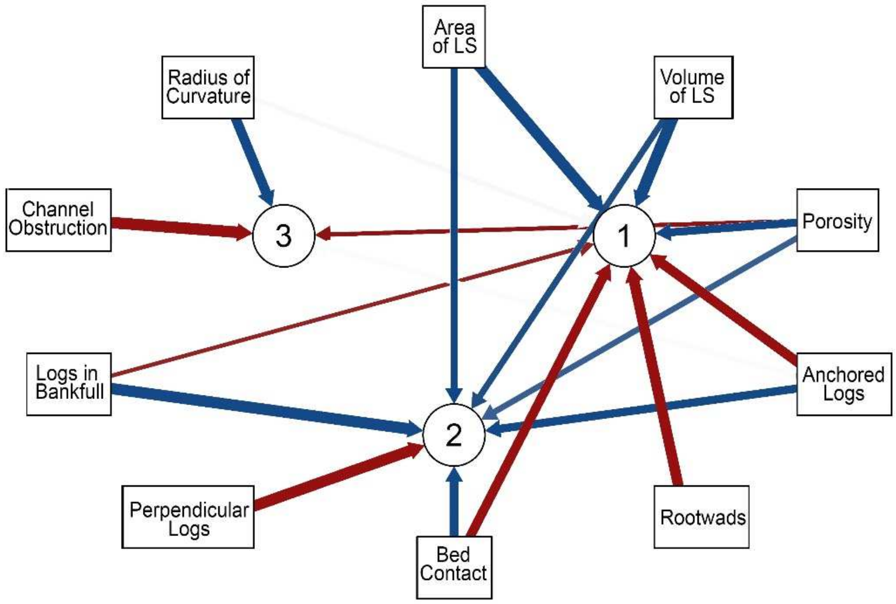

Figure 13: PCA components and their associated loadings for the explanatory variables. The circles are the components and the squares are the variables. Blue arrows indicate positive relationships and red arrows indicate negative relationships. The thickness and hue of the line signify the amount of loading on each component.

<u>Multivariate Regression</u>

Generalized Additive Models (GAMs) were used for the multivariate regressions in this study. GAMs allow for non-linear relationships between a response variable and multiple explanatory variables to be assessed. They also allow one to look at the relationship between individual explanatory variables with the response variable while the other variables are fixed. Models were made for all response variables, but not all were able to be explained through this method. A few of the multivariate GAMs showed interesting and noteworthy results and will be discussed here (Table 5).

Table 5: Summary of GAM models

Response Variable	**Explanatory Variable 1**	**p- value Variable 1**	**Explanatory Variable 2**	**p-value Variable 2**	**R^2 for equation**
agg_area_sqrt	porosity	0.058	vol_ls_log	0.070	.376
por_area_agg	porosity	0.030	bf_tot	0.068	.519
pool_depth	ch_obs	0.016	vol_ls_log	<0.001	.576

Response Variable	Explanatory Variable 1	p- value Variable 1	Explanatory Variable 2	p-value Variable 2	R^2 for equation
pool_vol	ch_obs	0.023	vol_ls_log	<0.001	.678
sed_pat_1	porosity	0.016	vol_ls_log	0.021	.530

Figure 14 shows the model for proportion of the area that showed aggradation for each structure (por_area_agg). Porosity and the proportion of logs in bankfull together best explained this variable; the other explanatory variables were removed from the model because they did not significantly contribute to the model. The model showed that when porosity of the log structure was very high or low, proportion area aggradation was higher. As the proportion of logs within bankfull increase, so does the amount of aggradation, until the proportion of logs in bankfull is equal to 1, where there is a wider range of outcomes. This may be due to the some of the smaller structures that are entirely within bankfull, but consist of fewer logs.

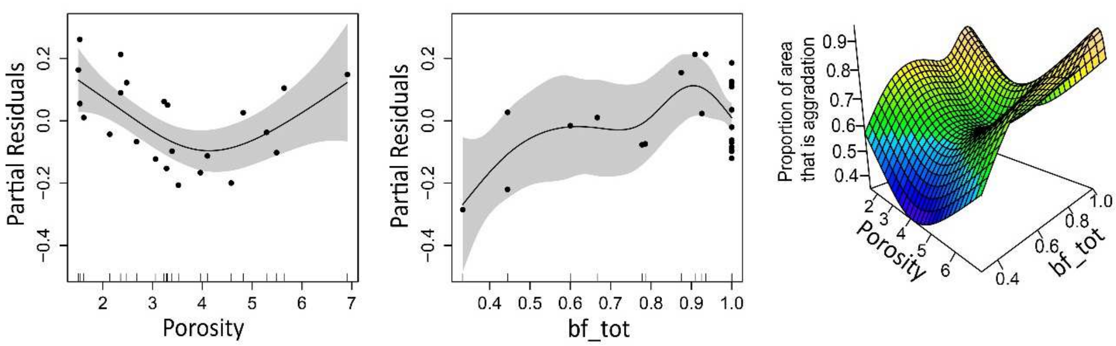

Figure 14: Multivariate model for proportion area aggradation. The first two graphs show the partial residual plots for the response variables and the third shows the predictor surface for the explanatory variable. Partial residual plots show the relationship between the response variable and one explanatory variable, given that there is another explanatory variable in the model. See Table 3 for variable names.

The two points with the lowest amount of aggradation were removed from the model to provide a better fit for proportion of logs in bankfull; VIBR 1 and VIBR 14 both showed very low aggradation areas compared to the other surveys and were skewing the model. Without these points, the p-values for both porosity and proportion of bankfull logs are relatively low. Low p-values show that the model functions better with both of these variables than it would without these variables. The R^2 for this model is 0.51, meaning that 51% of the structures can be explained by the model.

Examination of DoDs for log structures with high and low porosity helped in interpreting this model. For those log structures with low porosity and more areas of aggradation, the aggradation tended to be along the opposite side of the channel (VIBR 2, 3, and 8). This suggests that low porosity structures are obstructing the flow and reducing energy across the channel. There is still degradation under the structures, which could be caused from flow diverting under the structures when it encounters the low porosity structures. The log structures with high porosity shows large amounts of aggradation under the structure and upstream, downstream and opposite of the structure (VIBR 13 and RABE 2). Aggradation upstream and downstream of the structure is expected as the log structure interrupts the flow and a results in backwater upstream and slow water downstream, as shown in Figure 15.

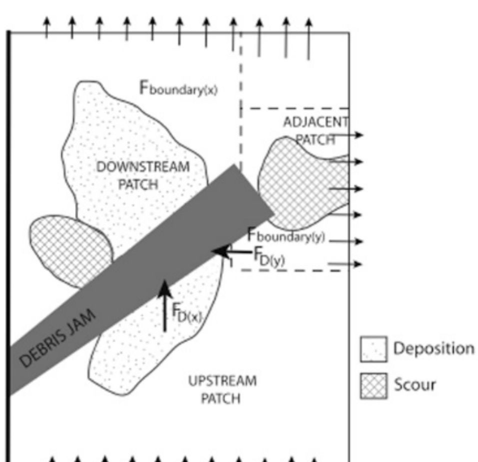

Figure 15: Schematic of areas of aggradation and degradation around a simplified log structure. Source: modified from Manners et al. 2007.

The aggradation seen under the highly porous structures could be explained by the water still being able to flow through the structures. The flow's energy would still decrease because of the increased turbulence, resulting in sedimentation.

This model was also affected by the proportion of the logs within bankfull flows. The structures with the smaller proportions of logs within bankfull showed less aggradation (VIBR 11 and 14). These are both alcove structures and therefore they obstruct less flow during lower flows, which leads to less turbulence and energy dissipation and, therefore, less aggradation.

The GAM for volume of total aggradation per survey area (agg_area_sqrt) is best explained by the combination porosity and volume of the log structure (Figure 16). When porosity is either high or low, aggradation/area increases, similar to the model for proportion area aggradation. As volume of the log structure increases, the aggradation also increases, but in a non-linear fashion, with a shallower slope around the mid-volumes. The p-value of porosity is 0.06 for this model and the p-value for volume of log structure is 0.07, which suggest that the model functions better with these values than it would without them. The R^2 for the whole model is 0.37. This value is low, but the model is still useful considering the complexities of natural systems.

This model for aggradation/area follows a similar relationship with porosity as the model for proportion of area that is aggradation. For the values with higher porosity, the pattern is not as strong because although there is more area of aggradation, it is not a large magnitude of aggradation for the most part (VIBR 13). Volume of log structure is more important in this model as well. In general, log structures with higher volumes resulted in larger volumes of aggradation (RABE 2 and 9). For the largest structures, the aggradation was generally upstream or downstream of the structures. The smaller structures with less aggradation were either alcove structures that did not protrude into the channel and therefore caused less energy dissipation and aggradation or had lower porosity which may have led to less aggradation (VIBR 11, 14) .

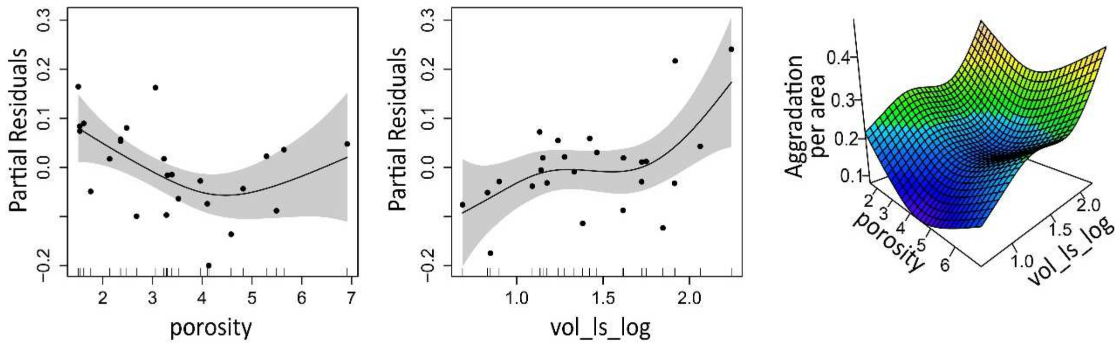

Figure 16: Multivariate model for aggradation per area. The first two graphs show the partial residual plots for the response variables and the third shows the predictor surface for the explanatory variable. Partial residual plots show the relationship between the response variable and one explanatory variable, given that there is another explanatory variable in the model. See Table 3 for variable names.

Figure 17 shows the GAM for final residual pool depth, which is modeled by a combination of log structure volume and channel obstruction. Pool depth has a positive linear relationship with the log-transformed log structure volume and a generally negative non-linear relationship with channel obstruction. Pools are generally deeper at log structures with less channel obstruction and shallower at higher channel obstruction. The p-value for volume of log structure is statistically significant at <0.001 and the p-value for channel obstruction is less significant at 0.16. The less significant p-value for channel obstruction suggests that the model could function without channel obstruction as a variable, but it does function better with it. The R^2 for the overall model is 0.58, which is higher than the R^2 for just the linear relationship between the log-transformed structure volume and final pool depth, which is 0.49.

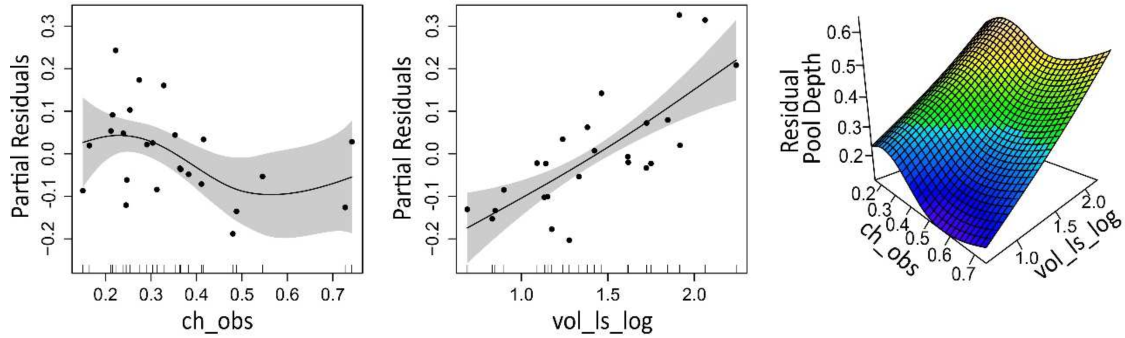

Figure 17: Multivariate model for residual pool depth. The first two graphs show the partial residual plots for the response variables and the third shows the predictor surface for the explanatory variable. Partial residual plots show the relationship between the response variable and one explanatory variable, given that there is another explanatory variable in the model. See Table 3 for variable names.

A similar model was created for final pool volume with the explanatory variables log structure volume and channel obstruction. As volume of log structure increases and channel obstruction decreases, the volume of the associated pool also increases (Figure 18). The p-value for log structure volume is <0.001 and the p-value for channel obstruction is 0.05, which shows that both explanatory variables are significant in the model. The model has a R^2 of 0.68 and therefore 68% of the results can be explained through this model.

Both final pool depth and final pool volume are correlated with the same variables in similar manners. Larger log structure volumes resulted in deeper and larger pools. This makes sense because the log structures with larger volumes generally spanned more channel length and resulted in longer pools. The larger structures also had more points of channel obstruction because they often consisted of more logs, resulting in more places for flow to be diverted around and resulting in scour. Pool depths and volumes also change with channel obstruction. More channel obstruction leads to small pool depths and volumes because there is more aggradation across the whole channel due to the larger area of obstruction. Overall, log structures with the largest volumes and least channel obstruction lead to deeper, larger pools.

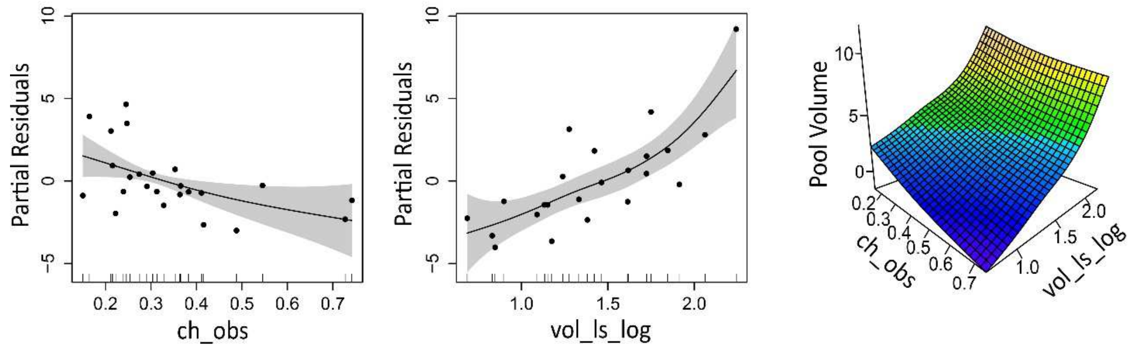

Figure 18: Multivariate model for pool volume. The first two graphs show the partial residual plots for the response variables and the third shows the predictor surface for the explanatory variable. Partial residual plots show the relationship between the response variable and one explanatory variable, given that there is another explanatory variable in the model. See Table 3 for variable names.

Pattern Description

Sedimentation Discussion

Each log structure shows unique patterns of change because of site specific characteristics and the unique arrangement of the log structures. Table 6 describes some of the specific change patterns seen at each log structure and any important site-specific characteristics that differ greatly from the other structure. The table also notes structural changes that were previously discussed and general pool changes.

In addition to these unique patterns, there are also some common trends in sedimentation that are seen around the structures. Approximately 85% of the log structures show aggradation directly upstream of the structure. Around 69% of the surveys show the channel is aggrading just downstream of the structures and 65% of the structures resulted in channel degradation outboard of the structure or along the opposite side of the channel. Patterns of aggradation upstream and downstream are common with log structures because they act as flow obstructions and dissipate energy of the water upstream and downstream of the structure leading to aggradation (Figure 15, Manners et al. 2007). Degradation is common outboard of the structure as the flow is diverted under the log structure, leading to the deep pools under and adjacent to the log structures, and around the log structure, leading to this degradation pattern that is seen in over half of these surveys.

From the DoD maps, the main areas of aggradation and degradation were noted for each log structure (Table 6). When the main area of degradation for the survey was along the same bank as the log structure or under the log structure, the main area for aggradation was either outboard of the structure or along the opposite bank (sed_pat_1). Bank scour happened only at bank jams, whereas scour under the structure occurred at many different type of jams. This suggests that flow is being diverted along the bank of some of these structures instead of the other side of the stream.

Figure 19 shows that the pattern of degradation on the structure side of the channel and aggradation on the opposite side (sed_pat_1) was most likely to happen at very low or high porosities, but also is dependent on the volume of the log structure. The response variable, the pattern of change, was a binary—a ‘0’ means the survey did not exhibit these patterns and a ‘1’ means the survey did exhibit the patterns. This model excludes VIBR 13, which has the highest porosity, because a tributary enters under the log structure. Mid-size structures with either high or low porosity resulted in degradation along the bank and under the structure (VIBR 2, RABE 4, and 8). This pattern of scour along the bank and under the structure was also seen in the low porosity structures in the models for por_area_agg and agg_area_sqrt. This does not explain, why the pattern is seen at higher porosity structures as well.

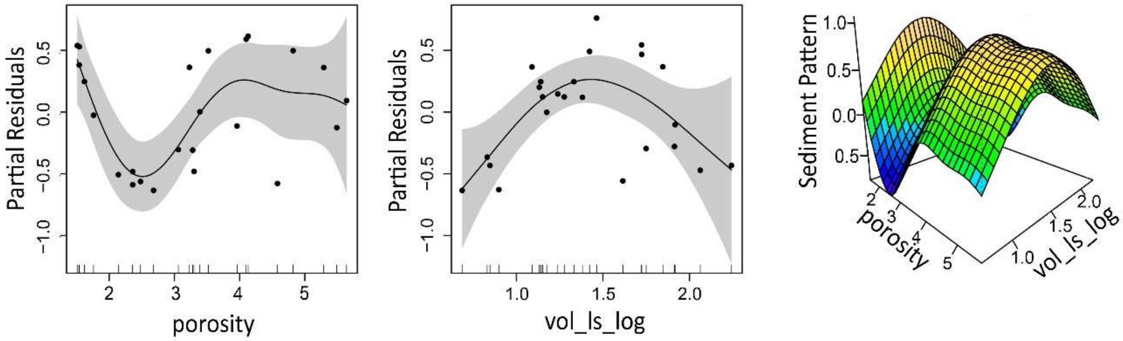

Figure 19: Multivariate model for sed _pat_1. The first two graphs show the partial residual plots for the response variables and the third shows the predictor surface for the explanatory variable. Partial residual plots show the relationship between the response variable and one explanatory variable, given that there is another explanatory variable in the model. See Table 3 for variable names.

When the area of degradation was outboard of the structure or along the opposite side of the stream/bank, the main areas of aggradation were usually under the structure. This pattern of sedimentation suggests that the flow is being diverted around the log structure as expected, with slower flows directly under the structure. This pattern of change occurred at all types of log jams.

Two explanatory variables, the proportion of perpendicular logs and radius of curvature, were not highly correlated with any of the models. From the literature, it was expected that the angle of the logs to the flow would have a large influence on scour and scour area (Gippel et al. 1996). Perhaps it did not in this situation because of the way it was measured. The log within 10° of perpendicular were counted, but this did not account for their location within the structure, or how exposed each log was to the flow. Radius of curvature was also not correlated, perhaps this was because the calculation did not occur for the location of the log structure along the meander.

Table 6: Log structures and channel changes. Symbols for channel change: A: significant aggradation; a: slight aggradation; d: slight degradation; D: significant degradation; '-': little change. Symbols for pool change: DN: expanding downstream; UP: expanding upstream; OB: expanding outboard of channel; UN: expanding under structure'-': little change. Upper-case characters indicate significant change; lower-case characters indicate slight change

Log Structure	Type	Up-stream	Down-stream	Under	Outboard /opposite bank	Along bank	Pool change	Comments
VIBR 1	MJ	D	d	D	a	D	-	
VIBR 2	MJ	a	-	D	A	D	DN	
VIBR 3	BKJ	a	a	d	A	d	OB	
VIBR 4	MJ	a	a	A	A	A	DN	-First of series of 3 log structures in a row
VIBR 5	BKJ	d	-	a	D	-	OB	-Just upstream of weir. -Second in series of 3 log structures in a row
VIBR 6	BKJ	a	d	d	-	-	-	-Just downstream of weir -Third in a series of 3 log structures in a row
VIBR 7	AJ	-	-	D	A	D	DN	-Logs spanning alcove entrance gone -Alcove is heavily scoured, could be from overbank flows running into it and the alcove acting as a plunge pool
VIBR 8	BKJ	A	A	D	a	D	UN	-Channel spanning log
VIBR 9	MJ	A	A	-	d	D	DN, OB	
VIBR 11	AJ	-	-	d	a	D	DN	-Six boulders at mouth of alcove -One loose log missing
VIBR 12	MJ	a	a	a	a	A	DN	

Log Structure	Type	Up-stream	Down-stream	Under	Outboard /opposite bank	Along bank	Pool change	Comments
VIBR 13	MJ	a	A	A	d	-	OB, UP	-Constructed over the top of a stream entrance
VIBR 14	AJ	-	-	a	d	-	DN	-Boulders along opposite bank
VIBR 15	MJ	-	a	a	d	A	OB	-Two boulders upstream of structure
VIBR 16	BTJ	-	a	A	d	-	OB	-Logs on opposite bank across from the log structure -Some loose bar top logs missing
VIBR 17	MJ	a	-	d	-	-	OB	-Boulders in channel
RABE 1	BKJ	A	D	d	A	-	UN, DS	-Riffle at upstream end of structure
RABE 2	MJ	a	A	a	a	-	UN	-Just upstream of side channel split, and large channel- spanning structure that diverts large amounts of flow
RABE 4	BKJ	-	a	d	a	D	UN	
RABE 6	BKJ	a	a	A	A	d	-	
RABE 7	BKJ	a	A	a	a	d	-	-Large Carex Nudata shrub in channel downstream of log structure
RABE 8	BKJ	a	a	A	d	D	DN	-Loose log parallel to flow missing
RABE 9	MJ	d	A	A	A	-	UP	
Log	**Type**	**Up-**	**Down-**	**Under**	**Outboard**	**Along**	**Pool change**	**Comments**

Structure		stream	stream		/opposite bank	bank		
RABE 10	BKJ	d	a	D	A	-	-	-Two Carex Nudata islands split flow upstream and at the log structure -Structure totally rearranged, new log upstream and ~4 logs missing
RABE 11	MJ	d	D	-	a	-	DN	-Large Carex Nudata shrub in channel upstream of structure
RABE 12	BAJ	a	a	D	-	-	NA	-Single log on mid-channel bar
RABE 16	BAJ	-	D	D	-	-	NA	-Single log on mid-channel bar -Log structure washed out, 2 side logs (not part of structure) also missing

Pool Changes Discussion

For this restoration project the pools were purposefully over-dug at each log structure to help create deeper pools faster. The over-dug pools are now adjusting to the stream conditions and this explains why most of the pools are shallowing even though log structures are known to create deep pools (Buffington et al. 2002; Montgomery et al. 1995). One of the goals of the restoration was to maintain these deep pools, specifically, deeper pools than pre-restoration conditions. The ultimate test for pool maintenance will be to compare residual pool depths before and after the restoration project construction, but these data are not yet available. Between the two reaches, 68% of the pools shallowed less than 20%, and 88% shallowed less than 30% of their initial depth. Average reductions in residual pool depth between the as-built and later surveys are 0.07m in VIBR and 0.12m in RABE. For most structures these reductions were relatively small compared to how deep some of the pools were initially dug, but 2 pools, VIBR 12 and RABE 1, decreased by around 50% of their depths, which is relatively large change. This suggests that log structures may be generally maintaining deep pools.

Residual pool depth histograms in figure 12 show that, within each reach, the minimum pool depths are similar for both the initial and final pool depths. In VIBR the initial pool depth range was between 0.27m to 0.54m and the final range was 0.20m to 0.44m. In RABE, the initial pool depth range was 0.37m to 0.79m and the final pool depth range was 0.32m to 0.75m.

Although the pools are generally shallowing, their areas are generally increasing. In most cases the pools are expanding out into the channel and many are shifting or expanding in the downstream direction, creating more natural shaped pools with long tails in the downstream direction and curved pool bottoms (Figure 20). Pool volumes only decreased 11% overall, even with the consistent decreases in residual pool depths. Most of the pools are now adjacent to or extend slightly downstream of the structures. This contradicts Brooks et al. (2004) findings that pools formed upstream of the log structures in their restoration site.

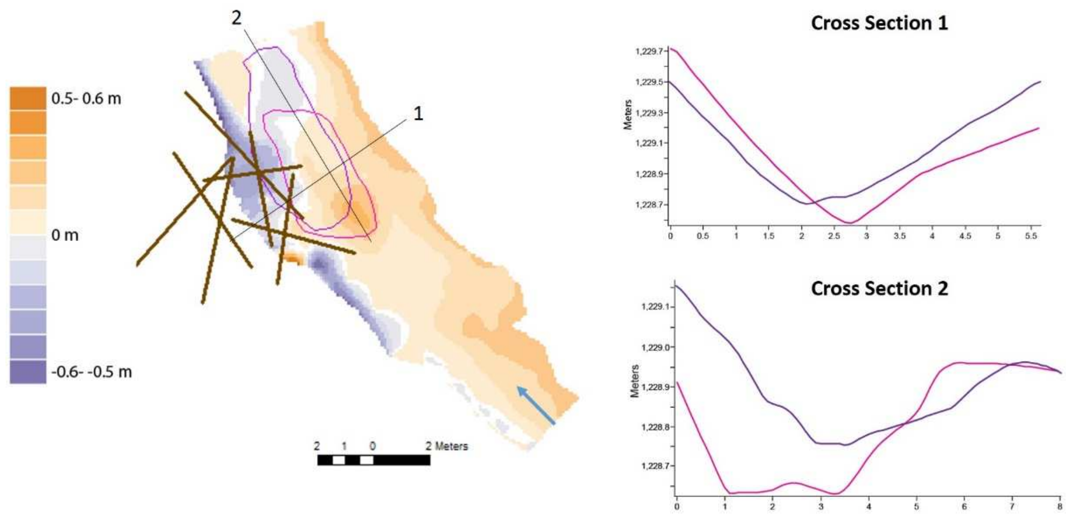

Figure 20: Pool cross sections at VIBR 2. DoD for VIBR 2 from 2008 to 2014, the pool area for 2008 is outlined in pink and the pool area for 2014 is outlined in purple. Cross section 1 is from left bank to right bank and cross section 2 is from upstream to downstream. Both cross sections show the 2008 pool in pink and the 2014 pool in purple.

Study Limitations

Although this study was designed to improve upon previous log structure research by looking at actual built complex structures instead of simplified models, using direct geomorphic measurement, and increasing study time, there were still limitations. One study weakness is differences in survey techniques from the first few years and the last few years of surveying. The 2008 to 2010 surveys were conducted at a coarser resolution than the surveys from 2011 on. The differing resolutions in the point clouds resulted in DEMs of different detail being compared. When creating the DoDs some of the resolution difference was accounted for when creating the topographic roughness surfaces, but beyond that the effects of these differences are unclear. On the other hand, the early surveys, done with a total station, have lower spatial error than those done in the later years with RTK_GPS. The error differences are not accounted for in this study.

Another limitation was the small sample size for statistical analysis. Many of the structure characteristics differed between the two projects, making it difficult to address differences based on classifications like log jam type. It is possible that a larger sample size would have reduced some of the variability in the data.

Effects of the ELJs on reach scale characteristics, such as the channel planform, were also not assessed in this study, because of the limited temporal scale. Larger scale channel adjustments occur at longer time scales than the scope of this study. Change in patterns of aggradation and degradation would likely be different after more high flows and years of study.

Beyond enhancing the size and the time of the study, it would be useful to add some form of hydraulic data. Having information on the hydraulics around the log structures during bankfull flows would allow one to link the flow patterns and sedimentation patterns and better explain some of the results.

CHAPTER VI

CONCLUSION

Overall, the log structures in both reaches remained relatively stable, which was the restoration intention. Two small structures completely washed out, and four larger structures endured minor changes. These sorts of changes were expected because not all logs were anchored and there was a very large flood in 2011. One large structure, RABE 10, was completely rearranged. Most of the structural logs were moved, four logs were washed away, and one log was recruited. This was more surprising, but there is still a structure remaining at the site, and although different, the structure is still enhancing channel complexity and maintaining a pool.

In the survey areas there was more aggradation overall than degradation in both reaches. RABE has higher volumes of aggradation per survey area than VIBR, and also less volume of degradation per survey area. Overall, RABE experienced more total change in topography, which is likely due to the generally larger structures in RABE. Most structures had 3 to 12 cm of change overall (volume of total sediment change divided by survey area), and there were a few structures that had over 15 cm of change.

Analysis showed that the volume of aggradation per survey area was related to both the porosity and the volume of the log structure. Very low and very high porosities, coupled with high log structure volumes, resulted in increased aggradation. At low porosity, aggradation occurred on the opposite side of the channel and at high porosity aggradation generally occurred under the structure and upstream and downstream. This suggests that the low porosity structures are acting as flow obstructions and are dissipating energy across the whole channel, but also flow is diverting under the structure leading to scour there. The high porosity structures are creating backwater effects by slowing the water, but still allowing it to flow through the structure and aggrade the channel under the structure as the flow loses more energy. This is coupled with volume differences, where log structures with large volumes also tended to have similar deposition patterns as the high porosity structures.

The area of change in each DoD that was aggradation is associated with porosity, but also with the proportion of logs within bankfull. High and low porosity showed more aggradation that intermediate porosity, and those patterns coupled with increasing proportion of bankfull logs resulted in larger areas of aggradation. The smaller proportion of logs in bankfull may have led to less obstructions in high flows and therefore less energy dissipation and aggradation.

One of the most important restoration goals was to increase fish habitat through creating and maintaining deep pools. I found that deep pools were being maintained at the log structures. The pools were over-dug during construction, so although most of the pools are shallowing, this does not imply that the log structures are not maintaining deep pools. A majority of the pools have decreased less than 20% their initial dug depth and 88% shallowed less than 30%. All of the structures still have pools with residual pool depths greater than 20cm.

Final residual pool depths and final pool volumes were found to be associated with the combination of volume of the log structures and channel obstruction. As log structure volume increases so does pool depth and volume, and as the proportion of channel obstruction decreases, pool depth and volume increase. Log structures with large volumes, spanned longer channel length and had more points of obstruction from individual logs within the structure along with the initial frontal area obstruction, resulting in larger pools. Structures with more channel obstruction lead to high amounts of aggradation and therefore smaller pool depths and volume.

Overall, the log structures appear to be meeting most of the restoration goals, even after the very high flow year in 2011. The structures are remaining stable, creating complex hydraulic habitat, and maintaining deep pools for fish refugia. Net aggradation is expected with flow obstructions, especially upstream and downstream of the structures, although aggradation is also seen on the opposite side of the channel in some cases, which appeared to be associated with very high and low porosities. Otherwise, degradation is occurring generally outboard of the structures, which was expected as flow is diverted around the structures.

More years of surveying will likely display more channel changes, which may help explain clear up some of the inconsistences associated with the results. More time will also give a clearer picture of the long term impacts of these structures beyond our limited 6 years of surveying. Much of the change shown in the surveys is likely the channel adjusting to the post-restoration conditions, so more years of survey would show how the channel changes once adjusted to the restoration and structures. In the future, understanding flow interaction with the log structures through the measurement of flow hydraulics, such as velocity at high flows, would help link the physical processes to the geomorphic results in a more concrete manner.

APPENDIX A

DEM OF DIFFERENCE AND DEMS FOR EACH LOG STRUCTURE

VIBR 1 DEM

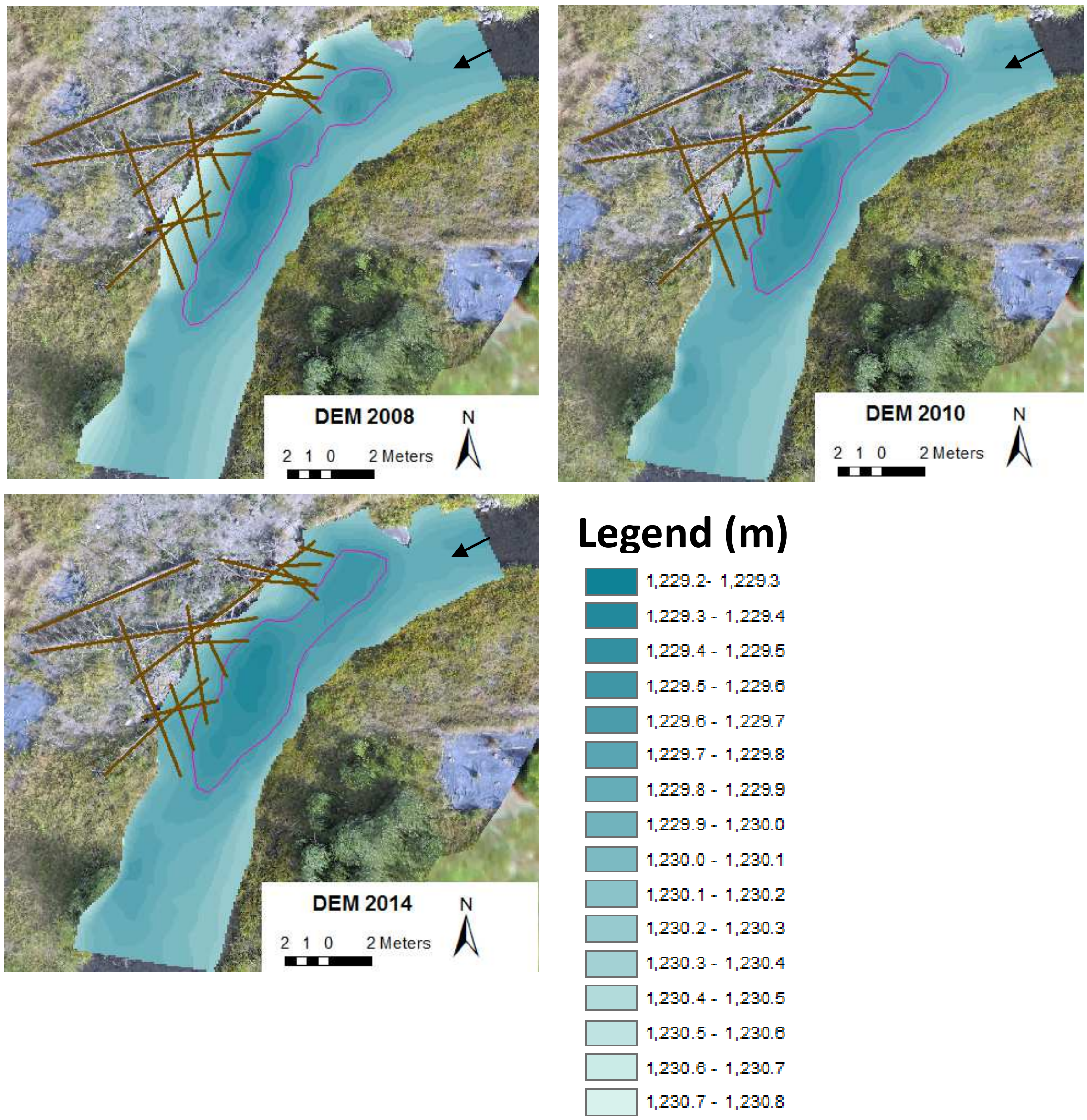
DEM 2008
N
2 1 0 2 Meters
DEM 2010
N
2 1 0 2 Meters
DEM 2014
N
2 1 0 2 Meters
Legend (m)
1,229.2- 1,229.3
1,229.3 - 1,229.4
1,229.4 - 1,229.5
1,229.5 - 1,229.6
1,229.6 - 1,229.7
1,229.7 - 1,229.8
1,229.8 - 1,229.9
1,229.9 - 1,230.0
1,230.0 - 1,230.1
1,230.1 - 1,230.2
1,230.2 - 1,230.3
1,230.3 - 1,230.4
1,230.4 - 1,230.5
1,230.5 - 1,230.6
1,230.6 - 1,230.7
1,230.7 - 1,230.8

VIBR 1 DoD

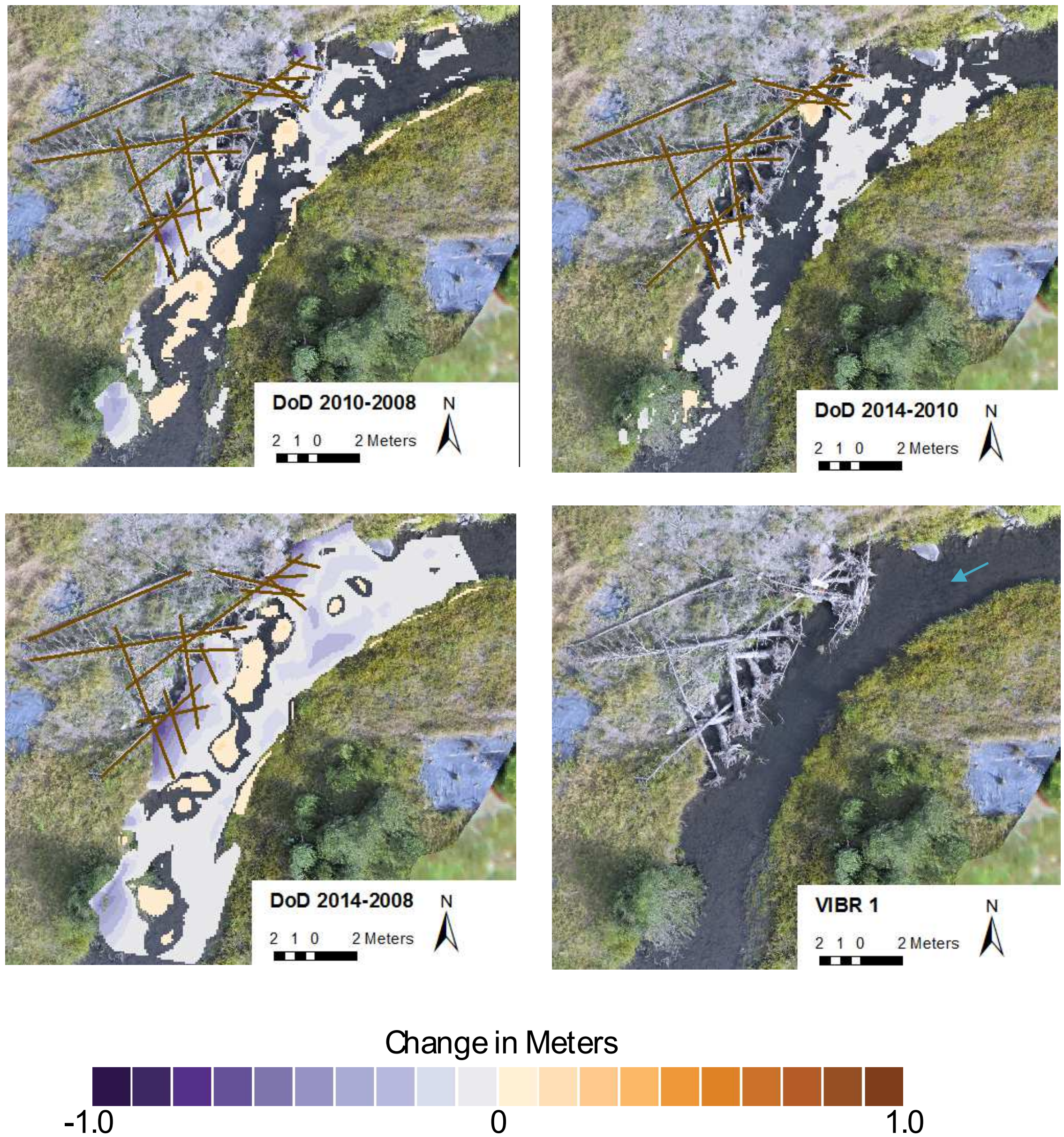
DoD 2010-2008
N
2 1 0 2 Meters
DoD 2014-2010
N
2 1 0 2 Meters
DoD 2014-2008
N
2 1 0 2 Meters
VIBR 1
N
2 1 0 2 Meters
Change in Meters
-1.0
0
1.0

VIBR 2 DEM

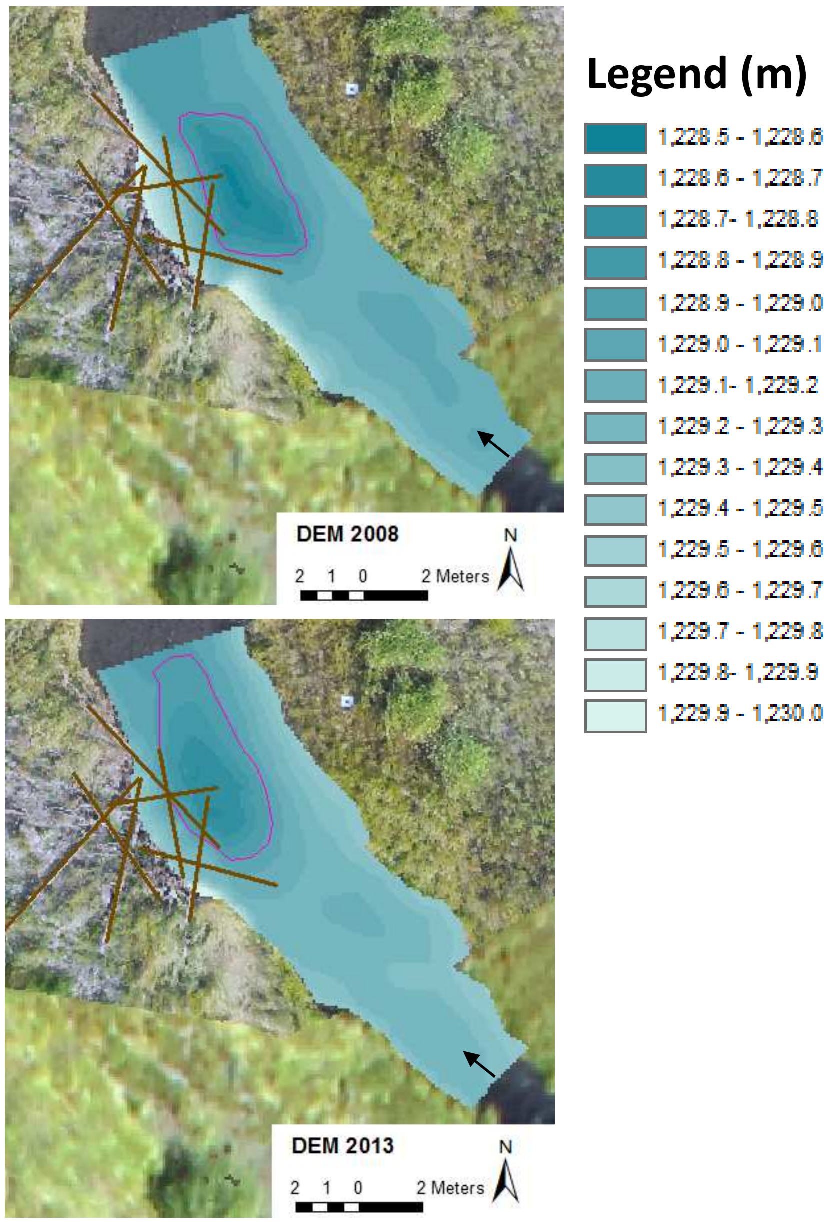

Legend (m)
1,228.5 - 1,228.6
1,228.6 - 1,228.7
1,228.7- 1,228.8
1,228.8 - 1,228.9
1,228.9 - 1,229.0
1,229.0 - 1,229.1
1,229.1- 1,229.2
1,229.2 - 1,229.3
1,229.3 - 1,229.4
1,229.4 - 1,229.5
1,229.5 - 1,229.6
1,229.6 - 1,229.7
1,229.7 - 1,229.8
1,229.8- 1,229.9
1,229.9 - 1,230.0
DEM 2008
2 1 0 2 Meters
N
DEM 2013
2 1 0 2 Meters
N

VIBR 2 DoD

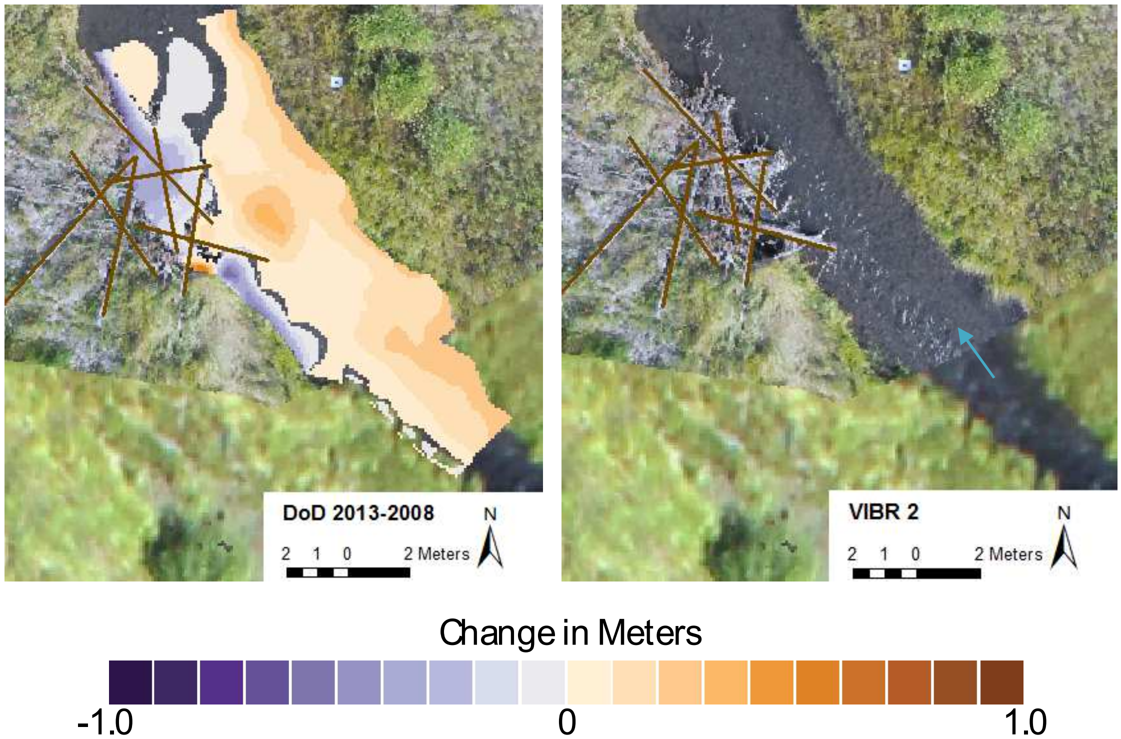
DoD 2013-2008
N
2 1 0 2 Meters
VIBR 2
N
2 1 0 2 Meters
Change in Meters
-1.0
0
1.0

VIBR 3 DEM

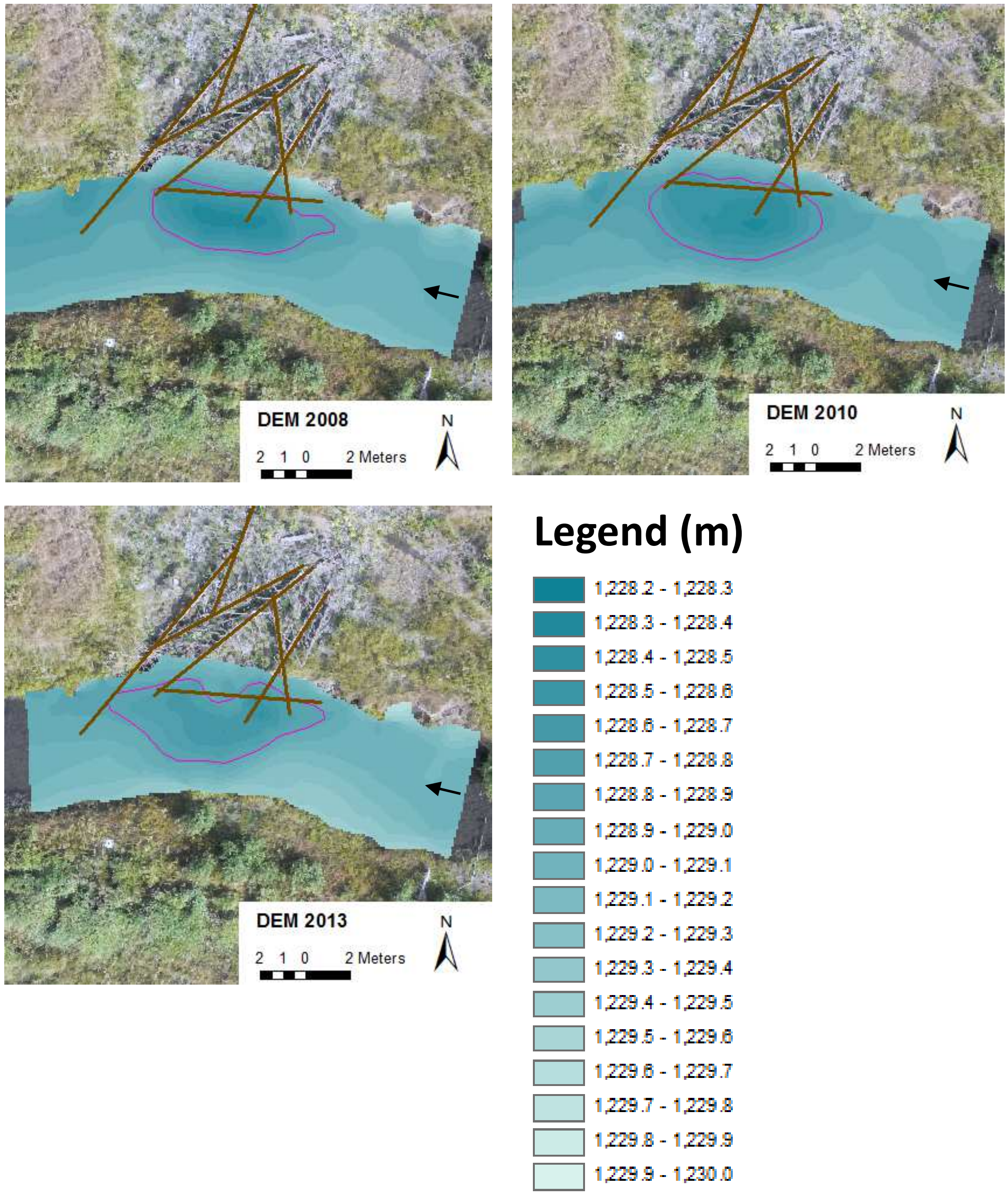
DEM 2008
N
2 1 0 2 Meters
DEM 2010
N
2 1 0 2 Meters
DEM 2013
N
2 1 0 2 Meters
Legend (m)
1,228.2 - 1,228.3
1,228.3 - 1,228.4
1,228.4 - 1,228.5
1,228.5 - 1,228.6
1,228.6 - 1,228.7
1,228.7 - 1,228.8
1,228.8 - 1,228.9
1,228.9 - 1,229.0
1,229.0 - 1,229.1
1,229.1 - 1,229.2
1,229.2 - 1,229.3
1,229.3 - 1,229.4
1,229.4 - 1,229.5
1,229.5 - 1,229.6
1,229.6 - 1,229.7
1,229.7 - 1,229.8
1,229.8 - 1,229.9
1,229.9 - 1,230.0

VIBR 3 DoD

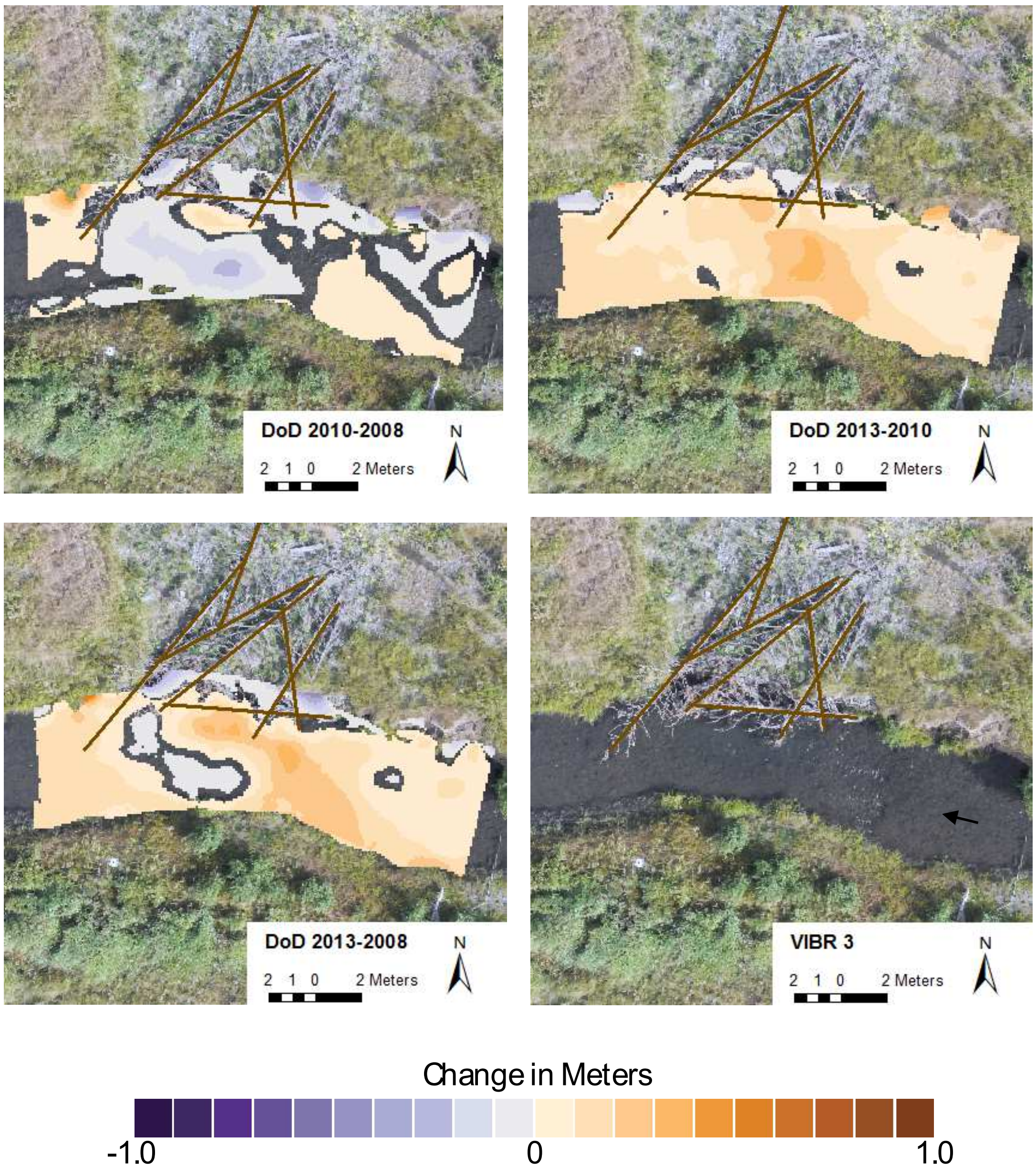
DoD 2010-2008
DoD 2013-2010
DoD 2013-2008
VIBR 3
N
2 1 0 2 Meters
Change in Meters
-1.0
0
1.0

VIBR 4 DEM

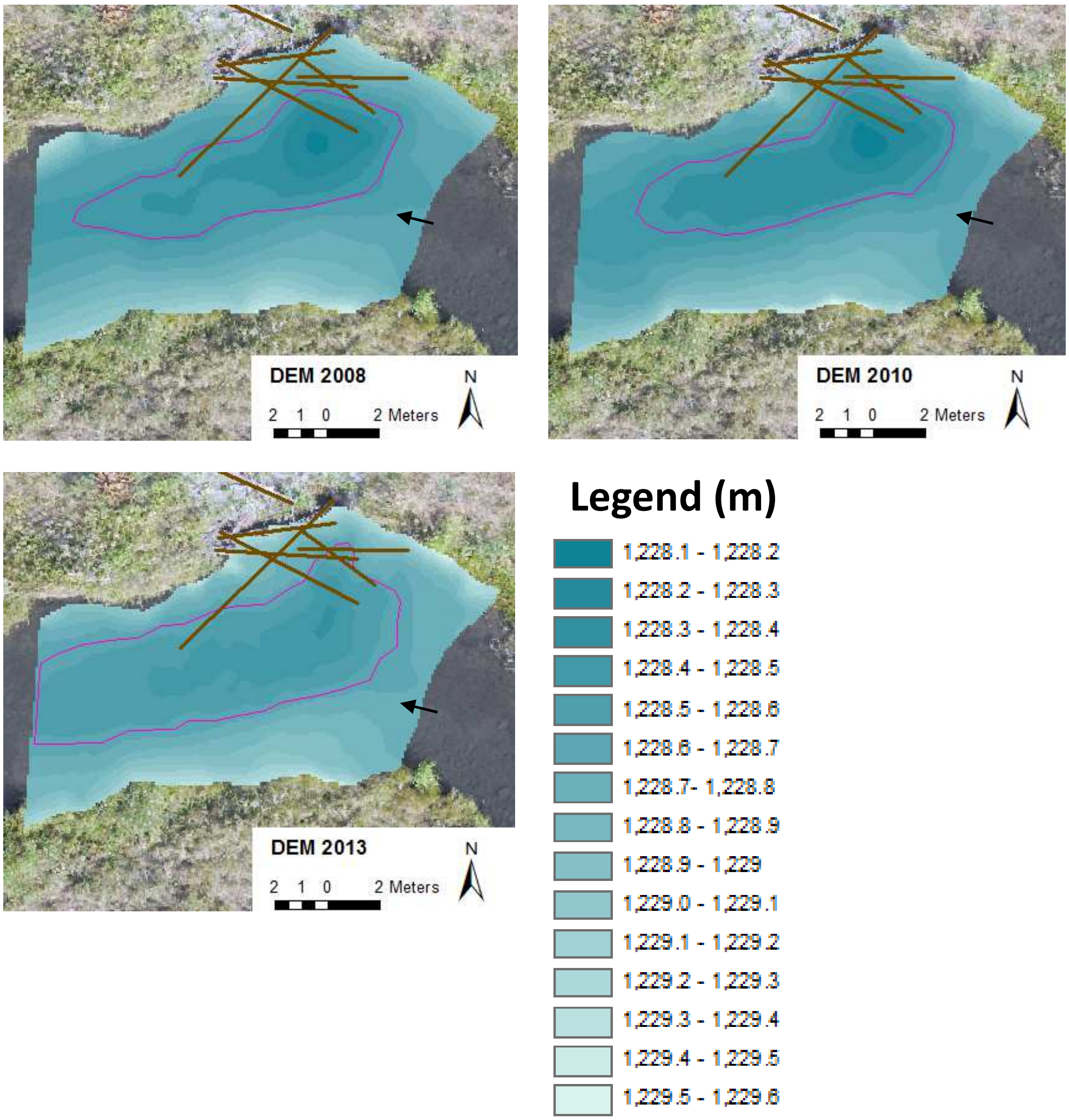
DEM 2008
N
2 1 0 2 Meters
DEM 2010
N
2 1 0 2 Meters
DEM 2013
N
2 1 0 2 Meters
Legend (m)
1,228.1 - 1,228.2
1,228.2 - 1,228.3
1,228.3 - 1,228.4
1,228.4 - 1,228.5
1,228.5 - 1,228.6
1,228.6 - 1,228.7
1,228.7- 1,228.8
1,228.8 - 1,228.9
1,228.9 - 1,229
1,229.0 - 1,229.1
1,229.1 - 1,229.2
1,229.2 - 1,229.3
1,229.3 - 1,229.4
1,229.4 - 1,229.5
1,229.5 - 1,229.6

VIBR 4 DoD

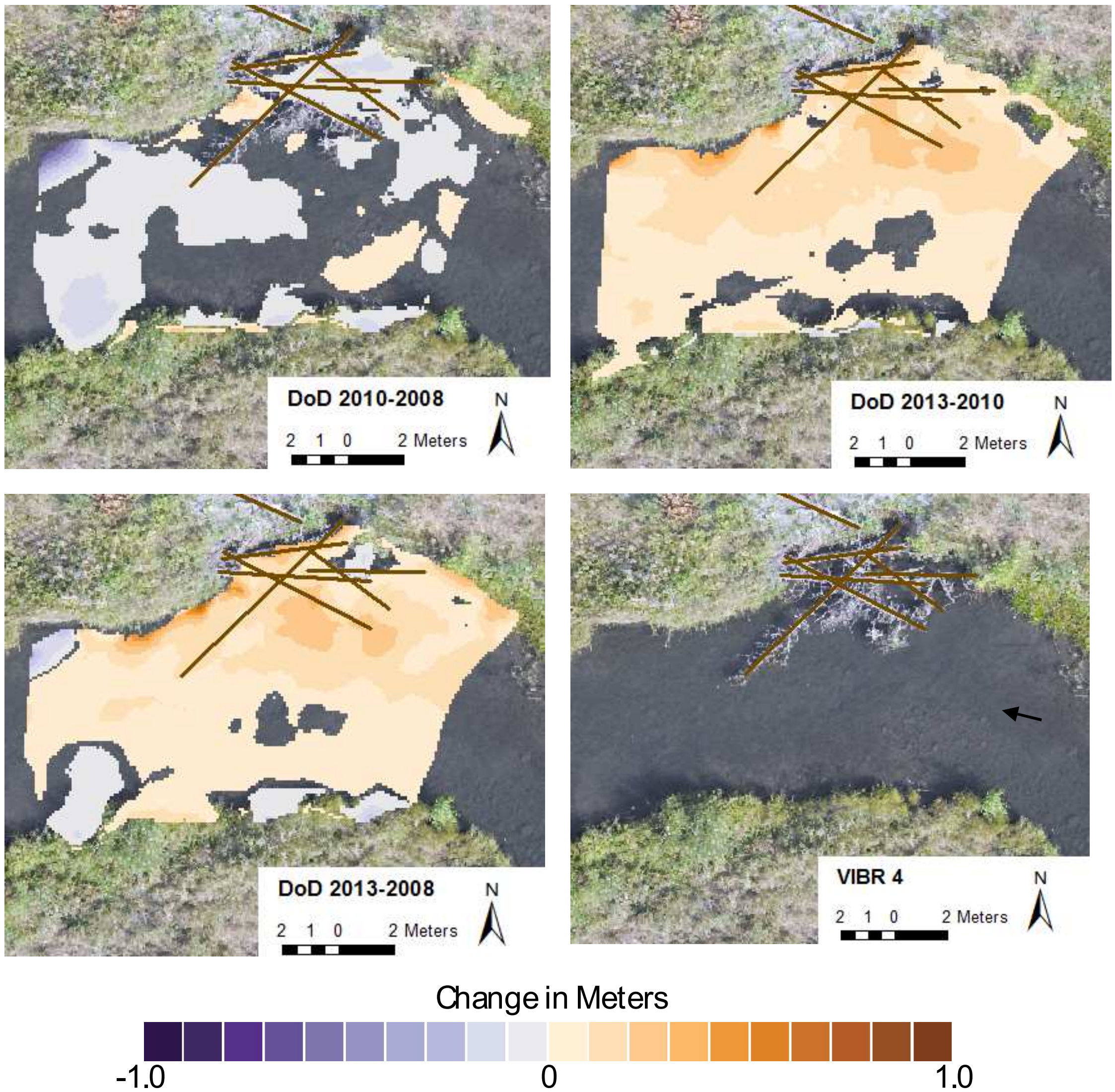
DoD 2010-2008
2 1 0 2 Meters
N
DoD 2013-2010
2 1 0 2 Meters
N
DoD 2013-2008
2 1 0 2 Meters
N
VIBR 4
2 1 0 2 Meters
N
Change in Meters
-1.0
0
1.0

VIBR 5 DEM

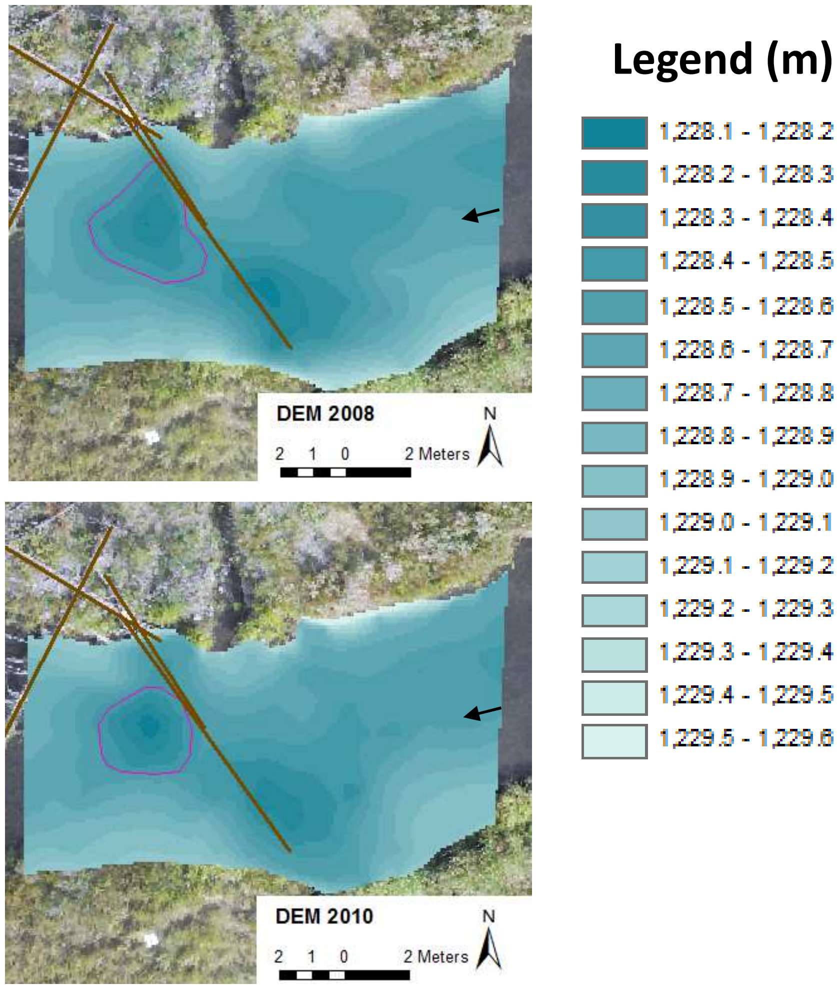
DEM 2008
2 1 0 2 Meters
N
DEM 2010
2 1 0 2 Meters
N
Legend (m)
1,228.1 - 1,228.2
1,228.2 - 1,228.3
1,228.3 - 1,228.4
1,228.4 - 1,228.5
1,228.5 - 1,228.6
1,228.6 - 1,228.7
1,228.7 - 1,228.8
1,228.8 - 1,228.9
1,228.9 - 1,229.0
1,229.0 - 1,229.1
1,229.1 - 1,229.2
1,229.2 - 1,229.3
1,229.3 - 1,229.4
1,229.4 - 1,229.5
1,229.5 - 1,229.6

VIBR 5 DoD

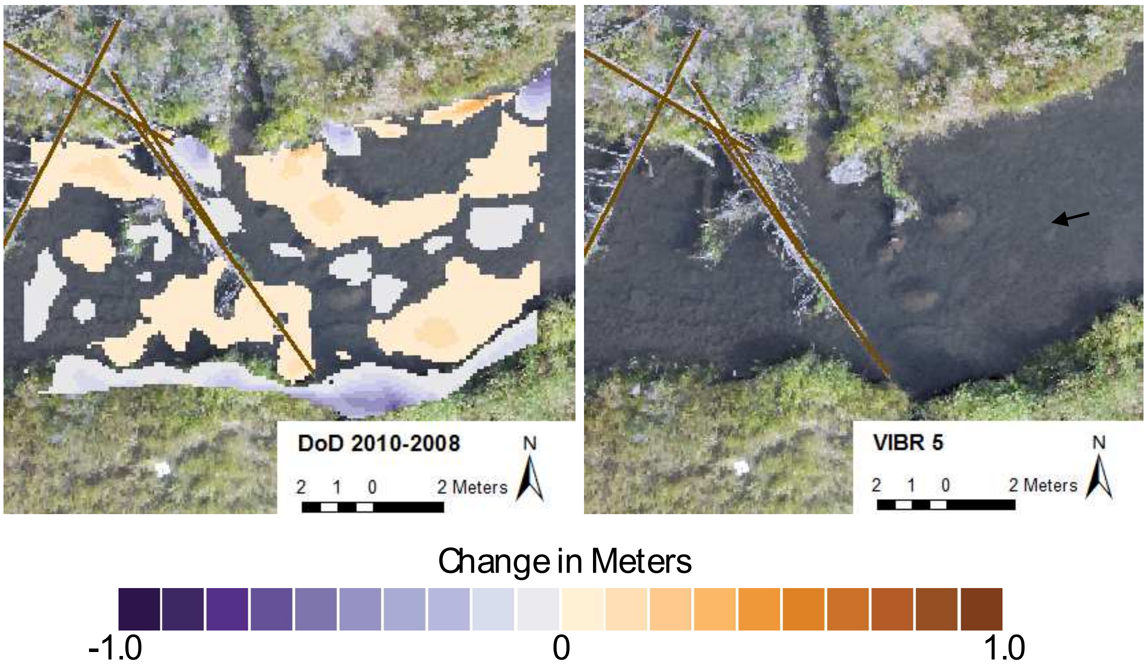
DoD 2010-2008
N
2 1 0 2 Meters
VIBR 5
N
2 1 0 2 Meters
Change in Meters
-1.0
0
1.0

VIBR 6 DEM

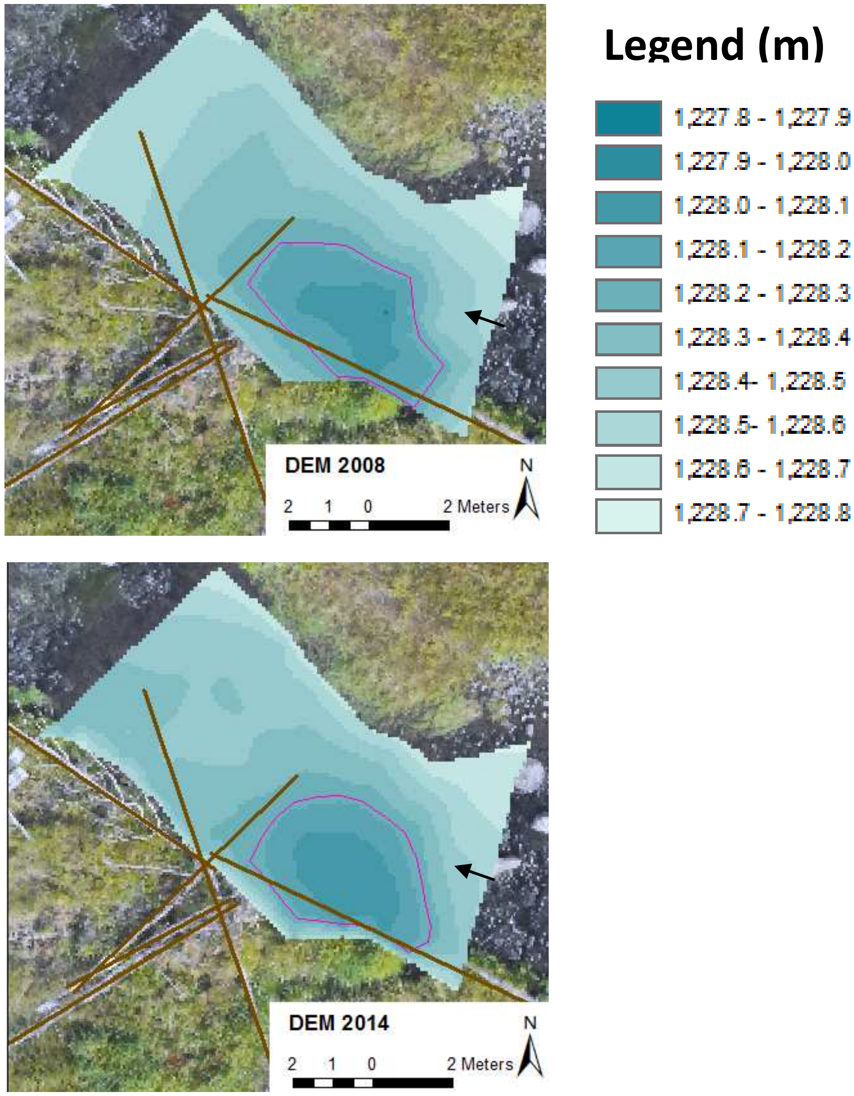

Legend (m)
1,227.8 - 1,227.9
1,227.9 - 1,228.0
1,228.0 - 1,228.1
1,228.1 - 1,228.2
1,228.2 - 1,228.3
1,228.3 - 1,228.4
1,228.4- 1,228.5
1,228.5- 1,228.6
1,228.6 - 1,228.7
1,228.7 - 1,228.8
DEM 2008
2 1 0 2 Meters
N
DEM 2014
2 1 0 2 Meters
N

VIBR 6 DoD

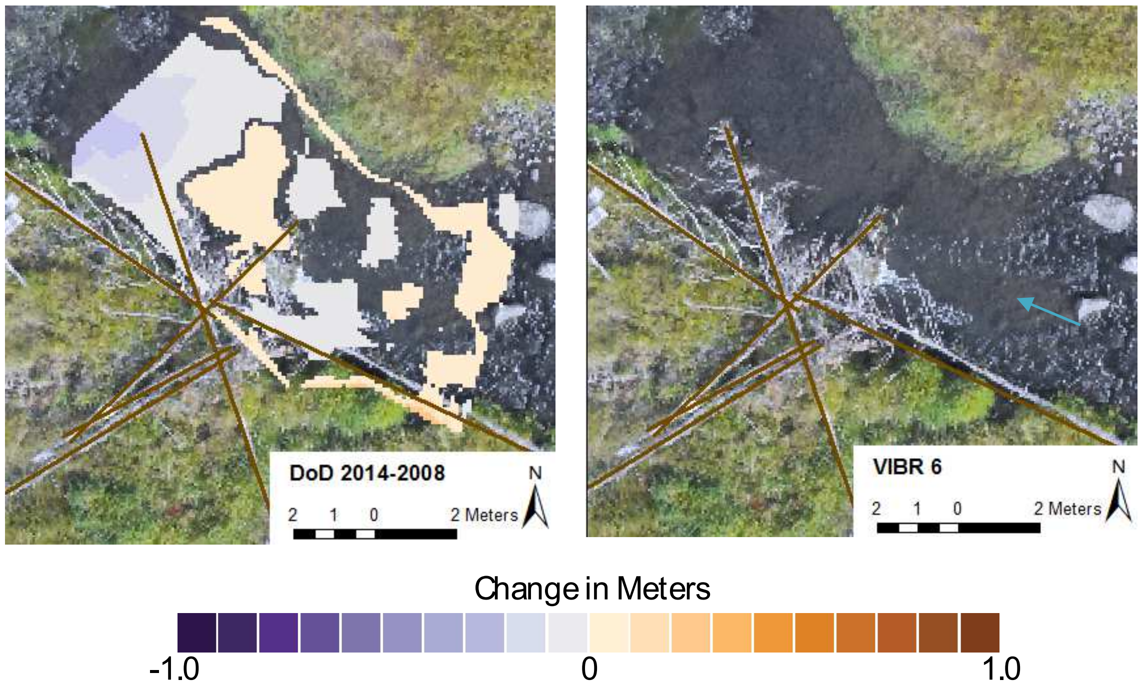

DoD 2014-2008
N
2 1 0 2 Meters
VIBR 6
N
2 1 0 2 Meters
Change in Meters
-1.0
0
1.0

VIBR 7 DEM

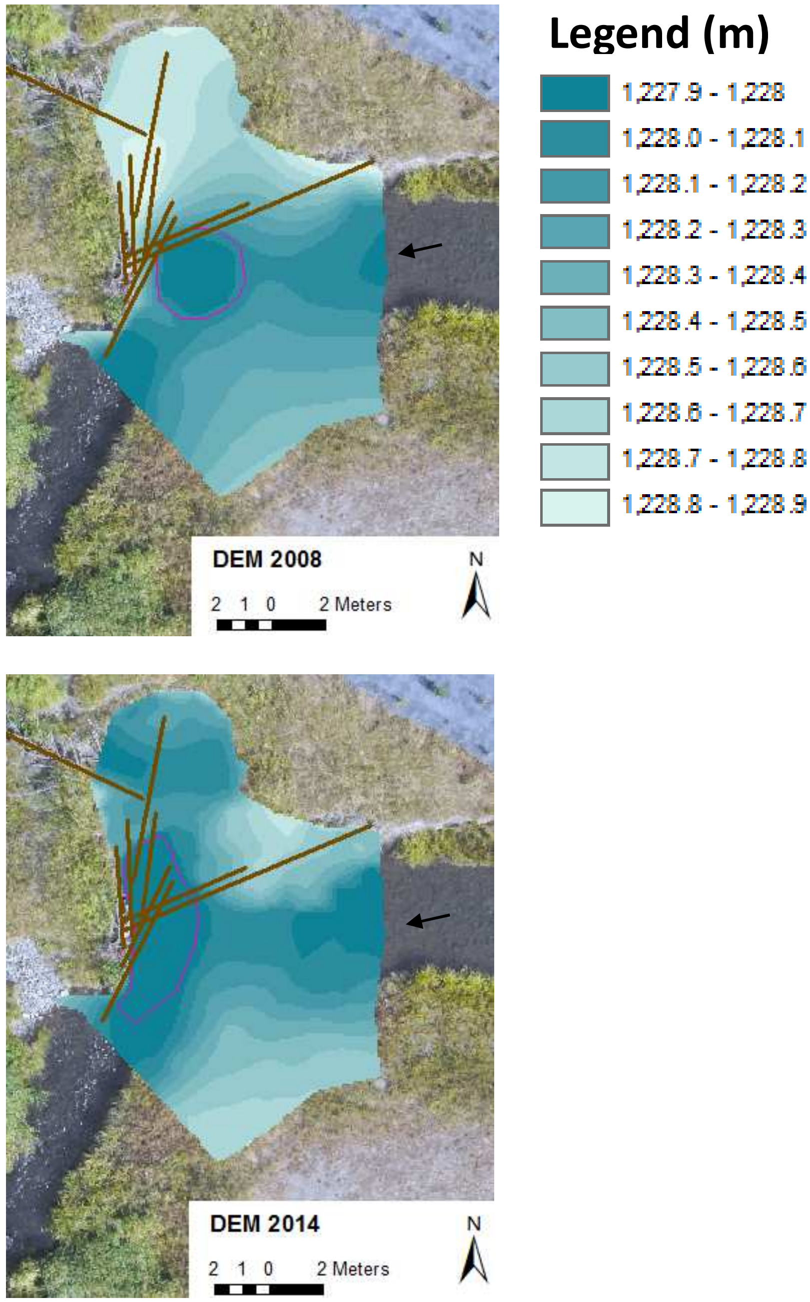

Legend (m)
1,227.9 - 1,228
1,228.0 - 1,228.1
1,228.1 - 1,228.2
1,228.2 - 1,228.3
1,228.3 - 1,228.4
1,228.4 - 1,228.5
1,228.5 - 1,228.6
1,228.6 - 1,228.7
1,228.7 - 1,228.8
1,228.8 - 1,228.9
DEM 2008
2 1 0 2 Meters
N
DEM 2014
2 1 0 2 Meters
N

VIBR 7 DoD

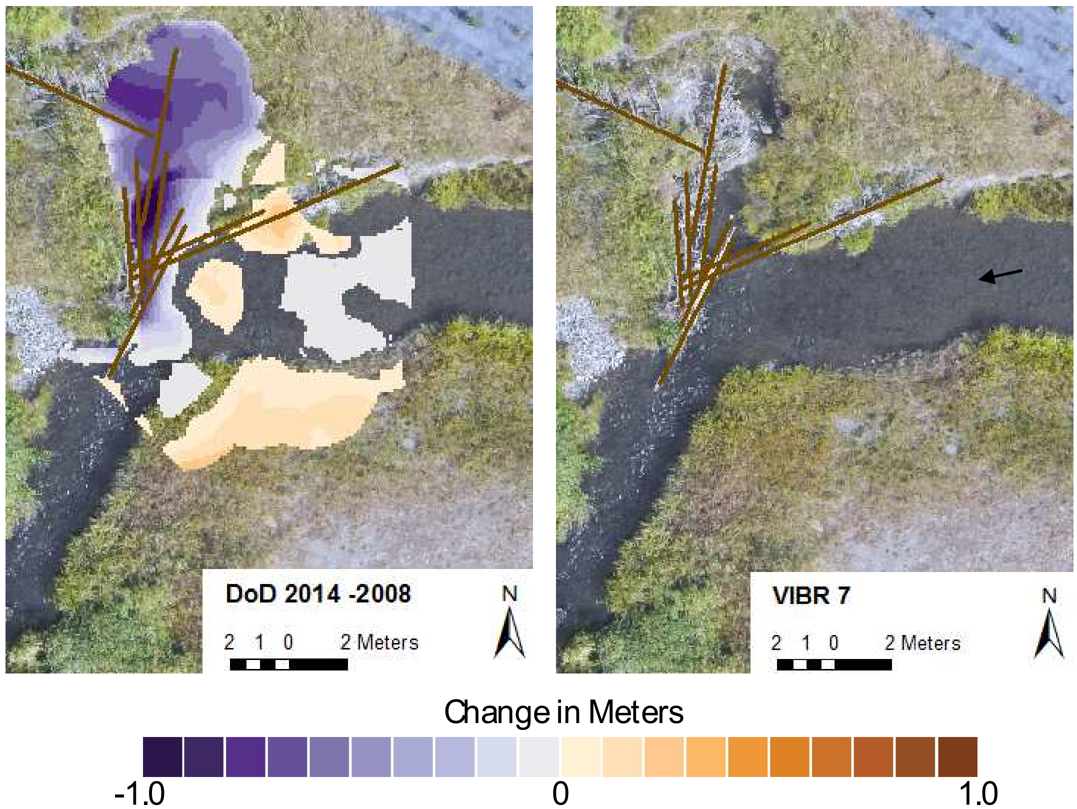
DoD 2014 -2008
2 1 0 2 Meters
N
VIBR 7
2 1 0 2 Meters
N
Change in Meters
-1.0
0
1.0

VIBR 8 DEM

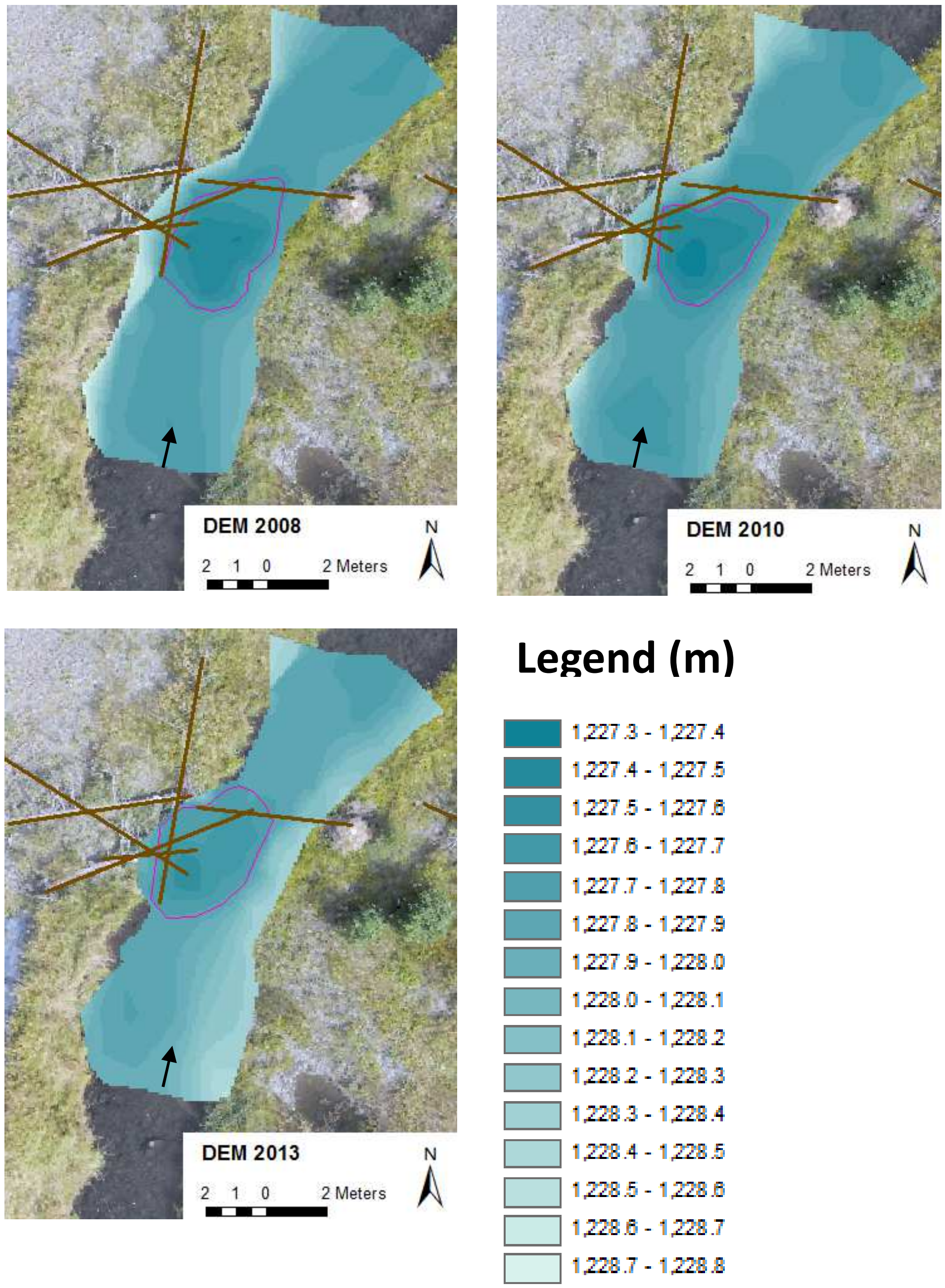
DEM 2008
2 1 0 2 Meters
N
DEM 2010
2 1 0 2 Meters
N
DEM 2013
2 1 0 2 Meters
N
Legend (m)
1,227.3 - 1,227.4
1,227.4 - 1,227.5
1,227.5 - 1,227.6
1,227.6 - 1,227.7
1,227.7 - 1,227.8
1,227.8 - 1,227.9
1,227.9 - 1,228.0
1,228.0 - 1,228.1
1,228.1 - 1,228.2
1,228.2 - 1,228.3
1,228.3 - 1,228.4
1,228.4 - 1,228.5
1,228.5 - 1,228.6
1,228.6 - 1,228.7
1,228.7 - 1,228.8

VIBR 8 DoD

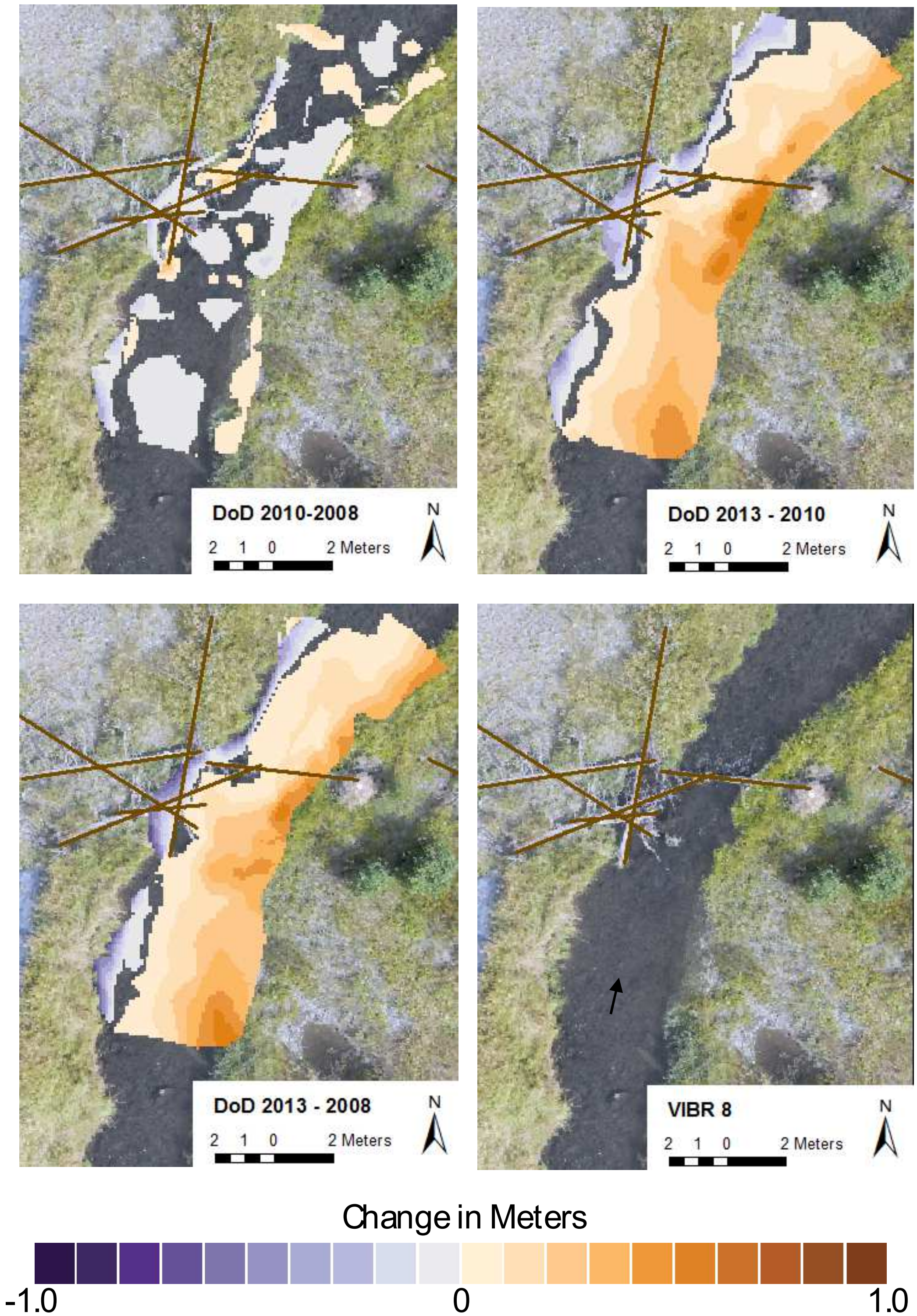

DoD 2010-2008
2 1 0 2 Meters
N
DoD 2013 - 2010
2 1 0 2 Meters
N
DoD 2013 - 2008
2 1 0 2 Meters
N
VIBR 8
2 1 0 2 Meters
N
Change in Meters
-1.0
0
1.0

VIBR 9 DEM

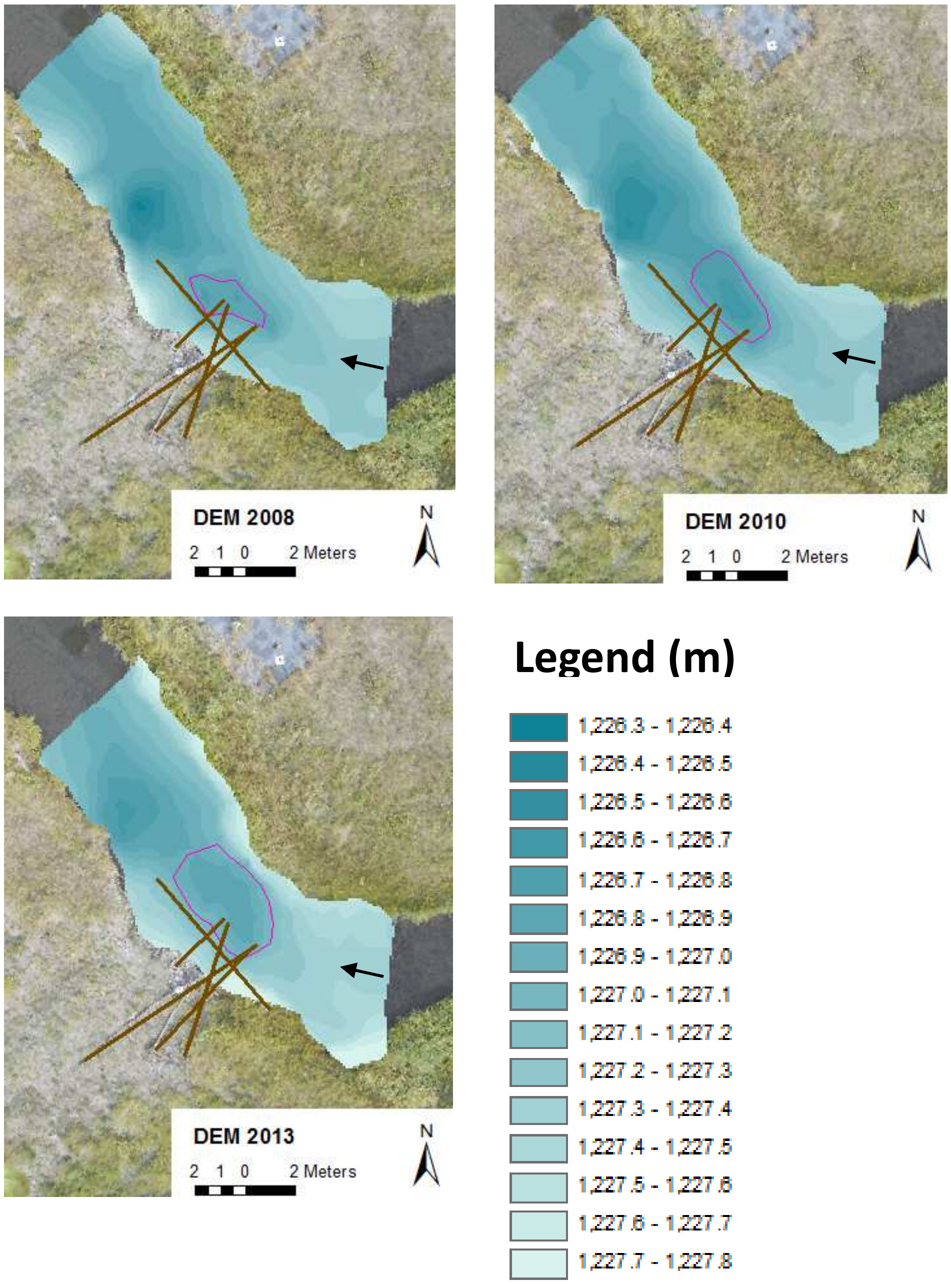
DEM 2008
2 1 0 2 Meters
N
DEM 2010
2 1 0 2 Meters
N
DEM 2013
2 1 0 2 Meters
N
Legend (m)
1,226.3 - 1,226.4
1,226.4 - 1,226.5
1,226.5 - 1,226.6
1,226.6 - 1,226.7
1,226.7 - 1,226.8
1,226.8 - 1,226.9
1,226.9 - 1,227.0
1,227.0 - 1,227.1
1,227.1 - 1,227.2
1,227.2 - 1,227.3
1,227.3 - 1,227.4
1,227.4 - 1,227.5
1,227.5 - 1,227.6
1,227.6 - 1,227.7
1,227.7 - 1,227.8

VIBR 9 DoD

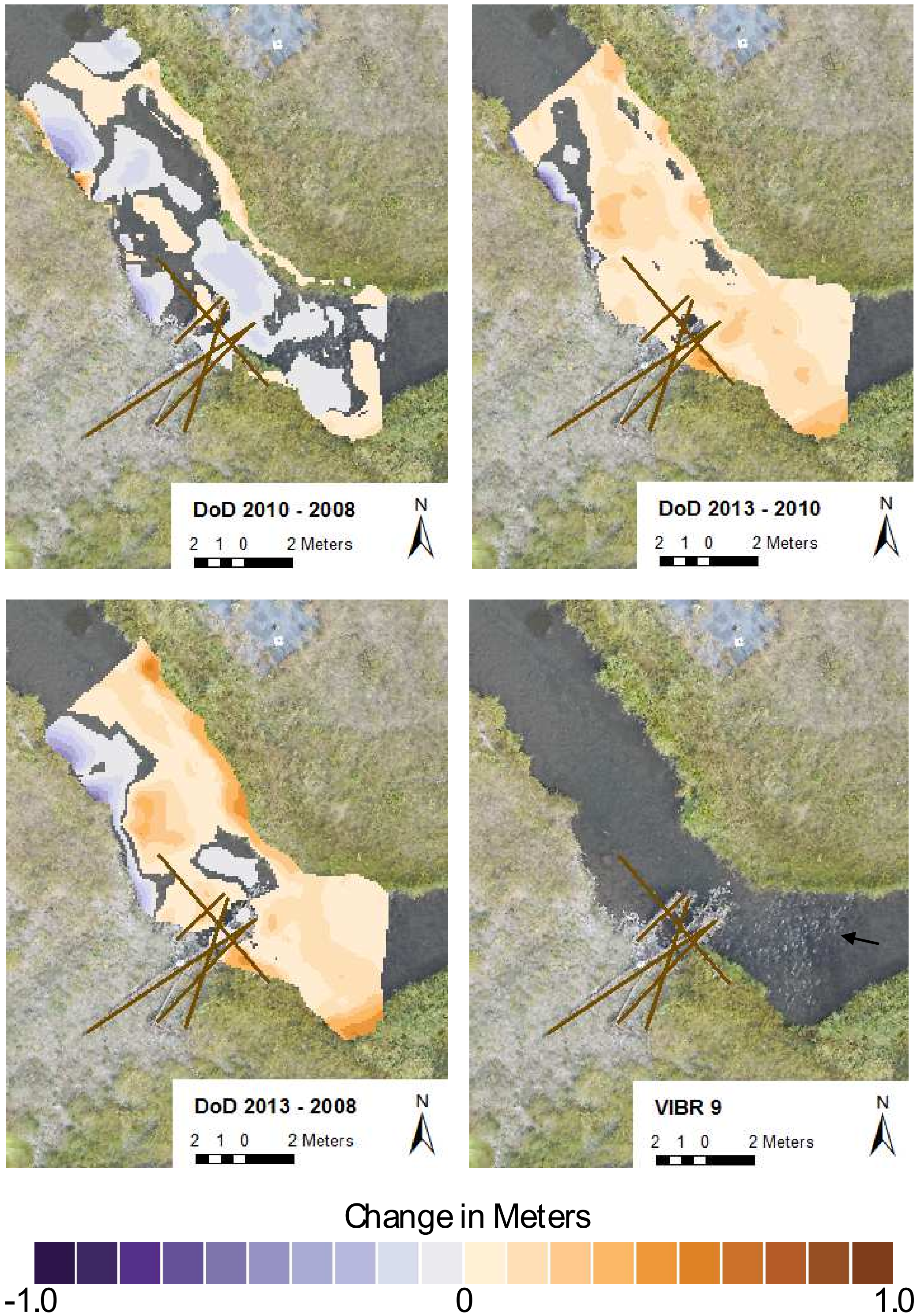
DoD 2010 - 2008
2 1 0 2 Meters
N
DoD 2013 - 2010
2 1 0 2 Meters
N
DoD 2013 - 2008
2 1 0 2 Meters
N
VIBR 9
2 1 0 2 Meters
N
Change in Meters
-1.0
0
1.0

VIBR 11 DEM

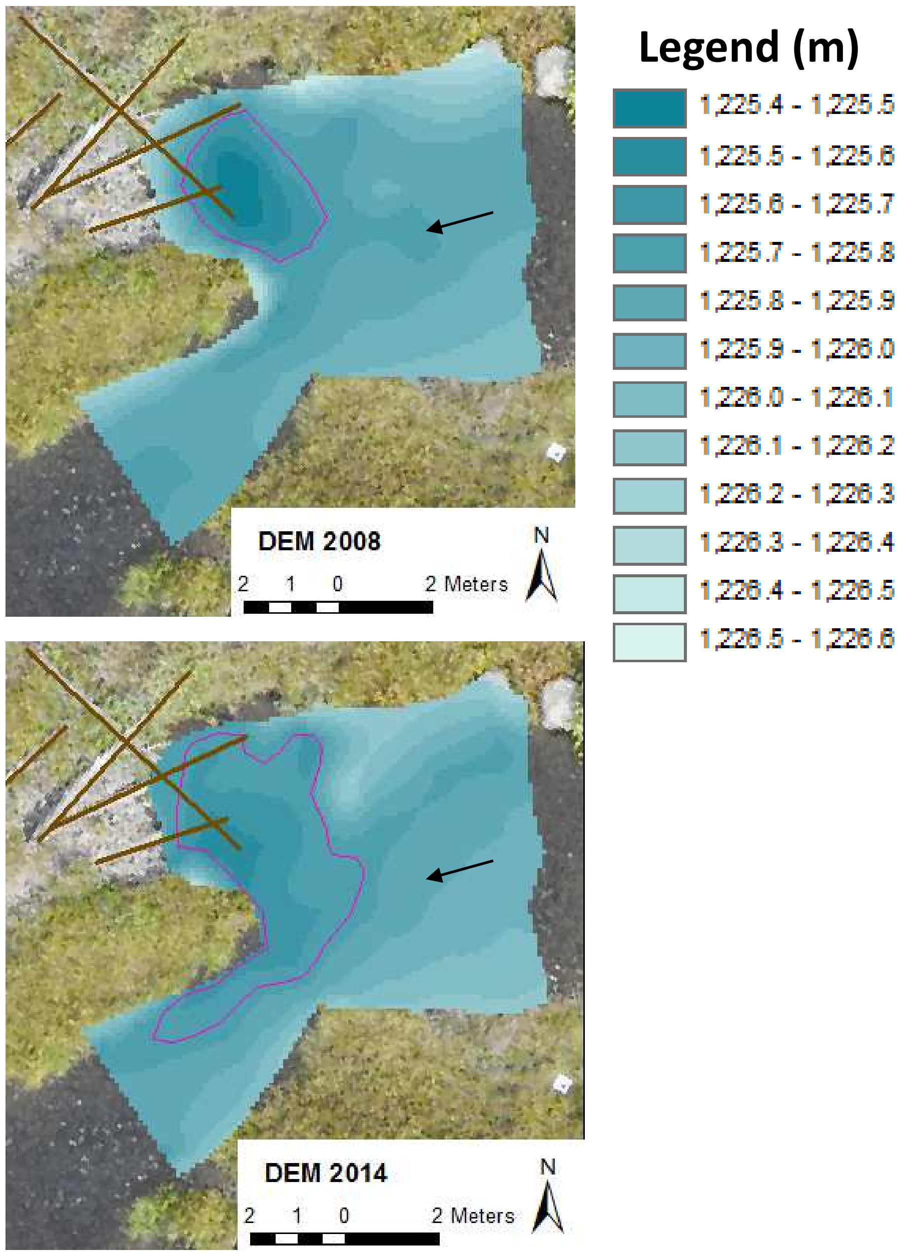
Legend (m)
1,225.4 - 1,225.5
1,225.5 - 1,225.6
1,225.6 - 1,225.7
1,225.7 - 1,225.8
1,225.8 - 1,225.9
1,225.9 - 1,226.0
1,226.0 - 1,226.1
1,226.1 - 1,226.2
1,226.2 - 1,226.3
1,226.3 - 1,226.4
1,226.4 - 1,226.5
1,226.5 - 1,226.6
DEM 2008
2 1 0 2 Meters
N
DEM 2014
2 1 0 2 Meters
N

VIBR 11 DoD

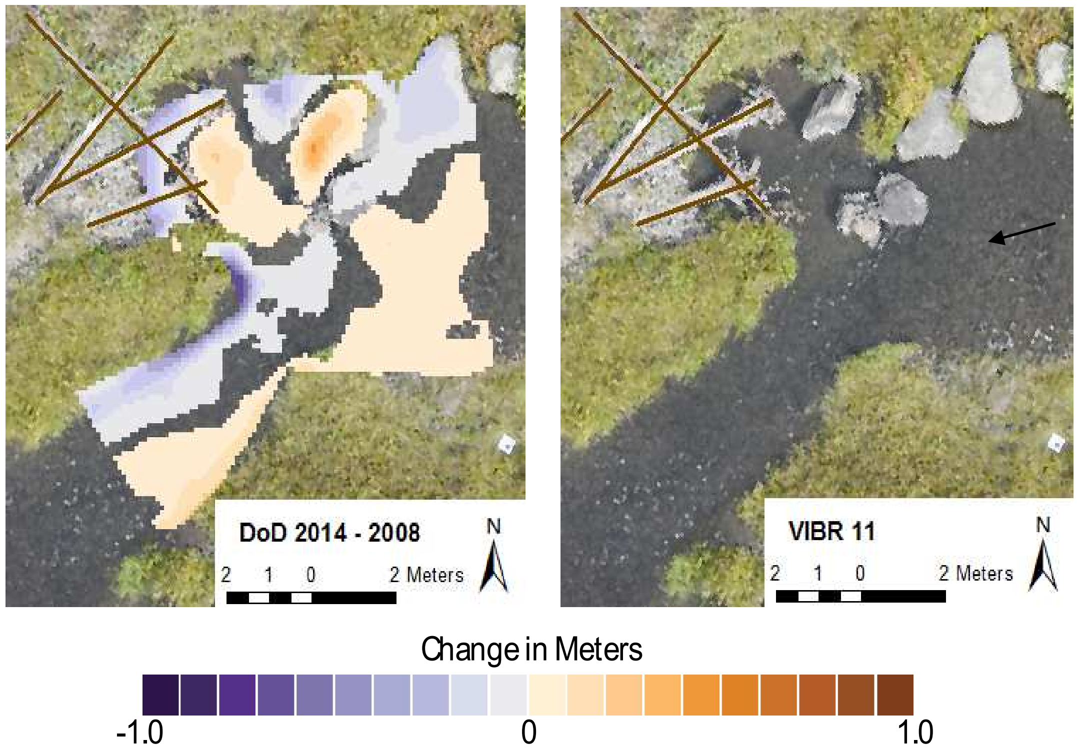
DoD 2014 - 2008
2 1 0 2 Meters
N
VIBR 11
2 1 0 2 Meters
N
Change in Meters
-1.0
0
1.0

VIBR 12 DEM

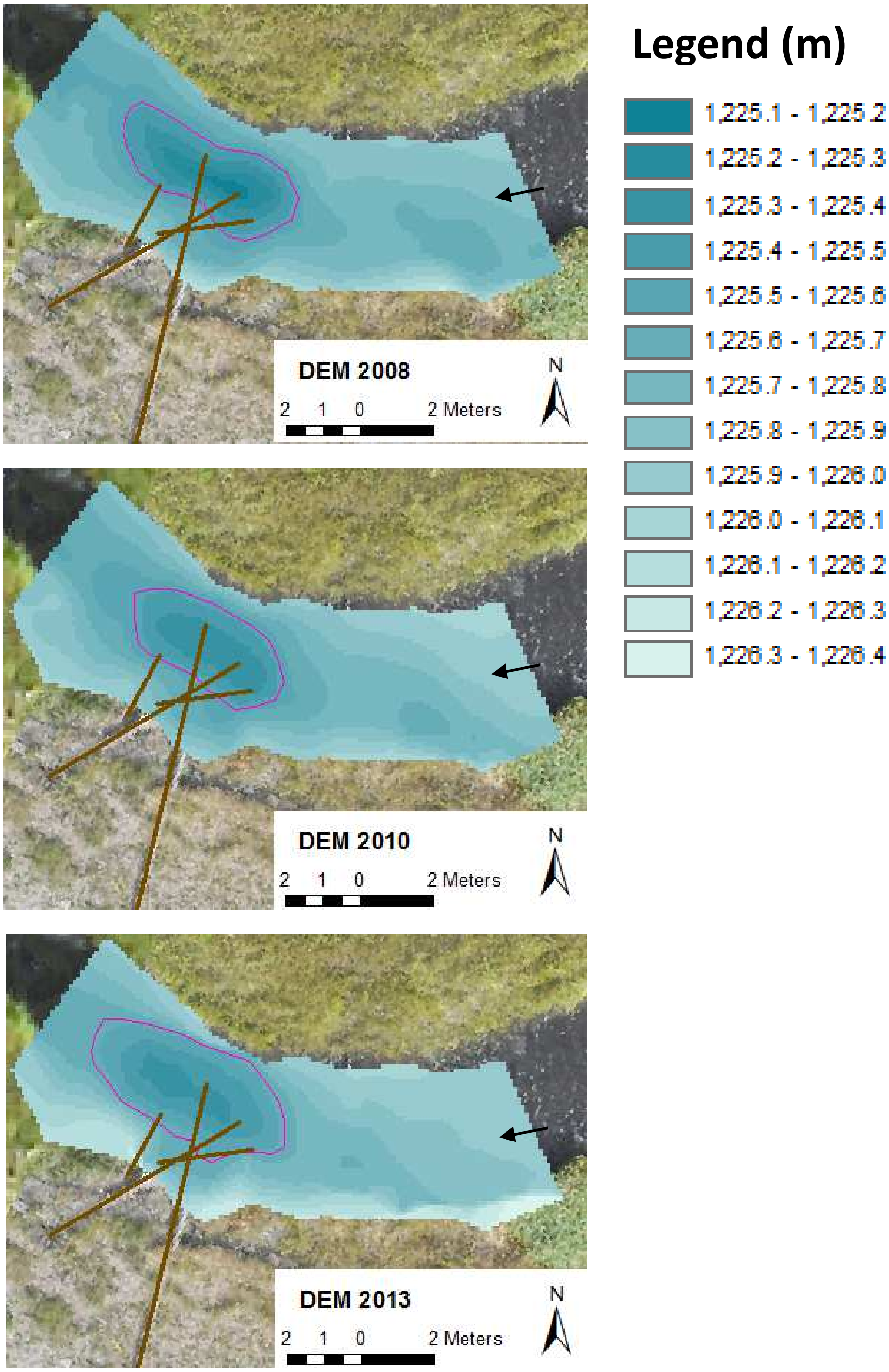

Legend (m)
1,225.1 - 1,225.2
1,225.2 - 1,225.3
1,225.3 - 1,225.4
1,225.4 - 1,225.5
1,225.5 - 1,225.6
1,225.6 - 1,225.7
1,225.7 - 1,225.8
1,225.8 - 1,225.9
1,225.9 - 1,226.0
1,226.0 - 1,226.1
1,226.1 - 1,226.2
1,226.2 - 1,226.3
1,226.3 - 1,226.4
DEM 2008
2 1 0 2 Meters
N
DEM 2010
2 1 0 2 Meters
N
DEM 2013
2 1 0 2 Meters
N

VIBR 12 DoD

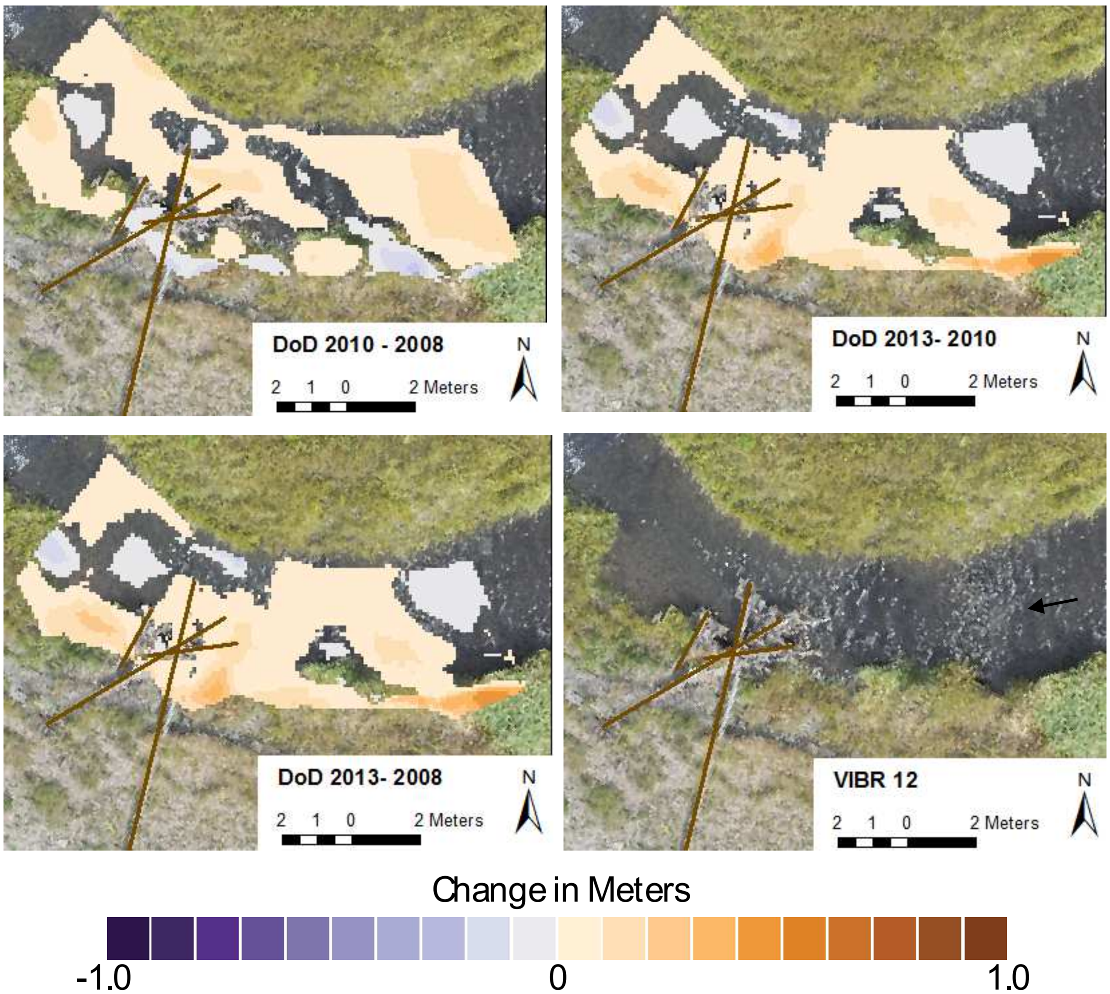
DoD 2010 - 2008
DoD 2013- 2010
DoD 2013- 2008
VIBR 12
N
2 1 0 2 Meters
Change in Meters
-1.0
0
1.0

VIBR 13 DEM

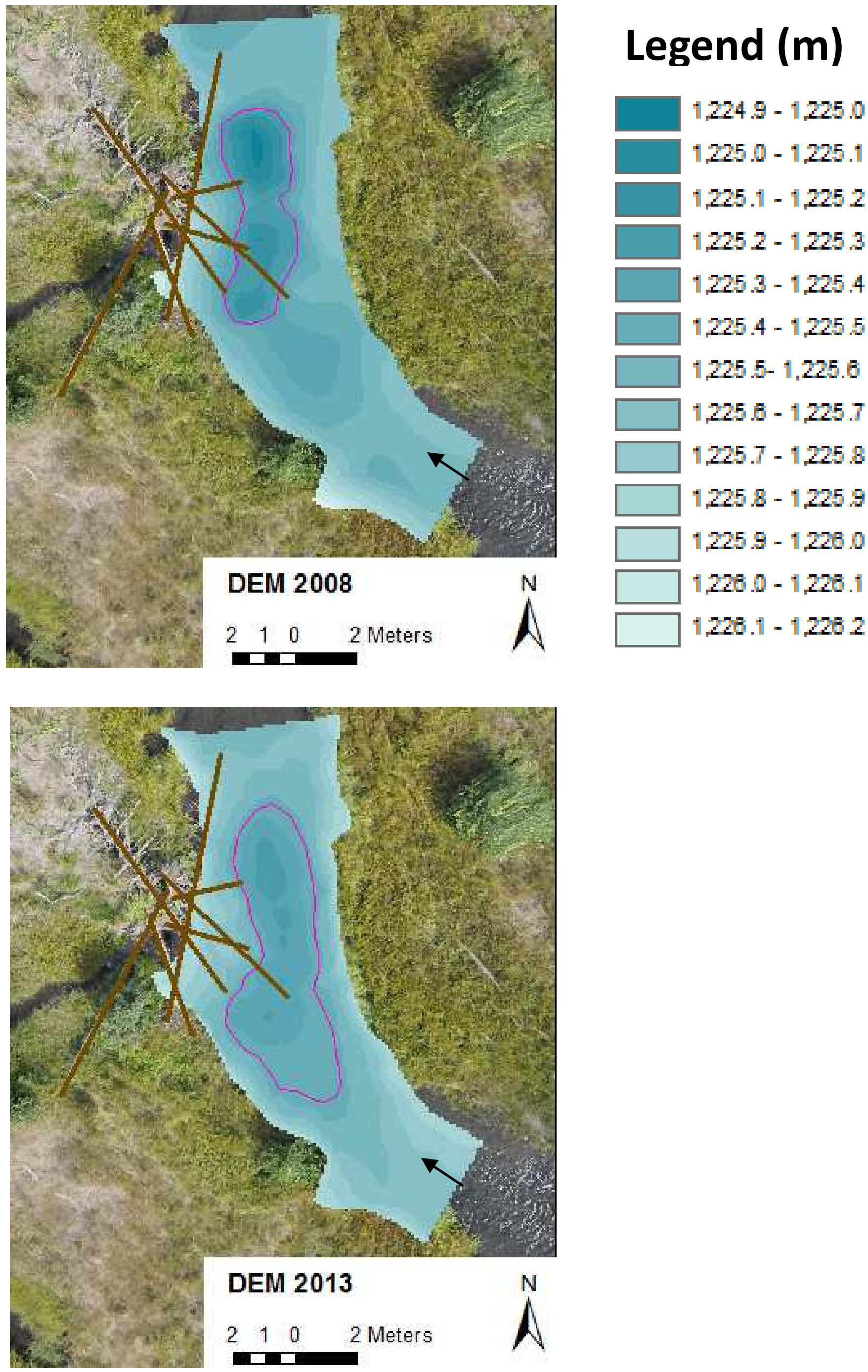

Legend (m)
1,224.9 - 1,225.0
1,225.0 - 1,225.1
1,225.1 - 1,225.2
1,225.2 - 1,225.3
1,225.3 - 1,225.4
1,225.4 - 1,225.5
1,225.5- 1,225.6
1,225.6 - 1,225.7
1,225.7 - 1,225.8
1,225.8 - 1,225.9
1,225.9 - 1,226.0
1,226.0 - 1,226.1
1,226.1 - 1,226.2
DEM 2008
2 1 0 2 Meters
N
DEM 2013
2 1 0 2 Meters
N

VIBR 13 DoD

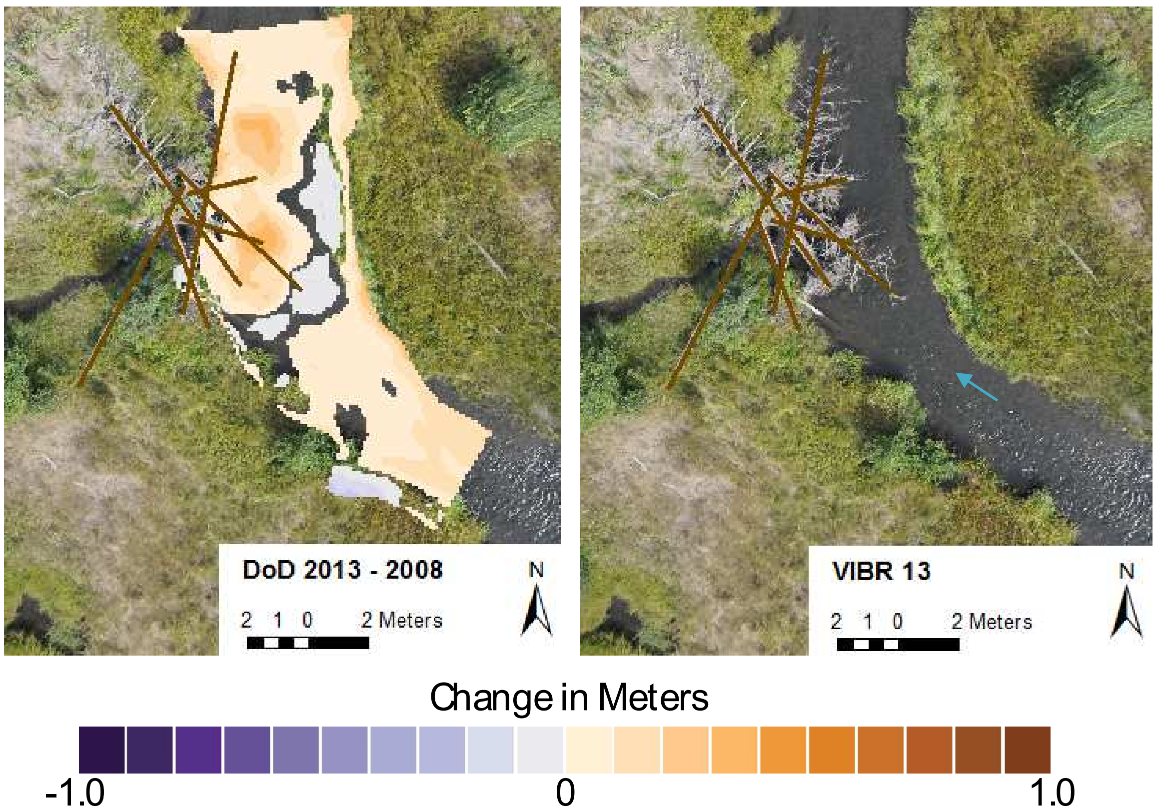
DoD 2013 - 2008
2 1 0 2 Meters
N
VIBR 13
2 1 0 2 Meters
N
Change in Meters
-1.0
0
1.0

VIBR 14 DEM

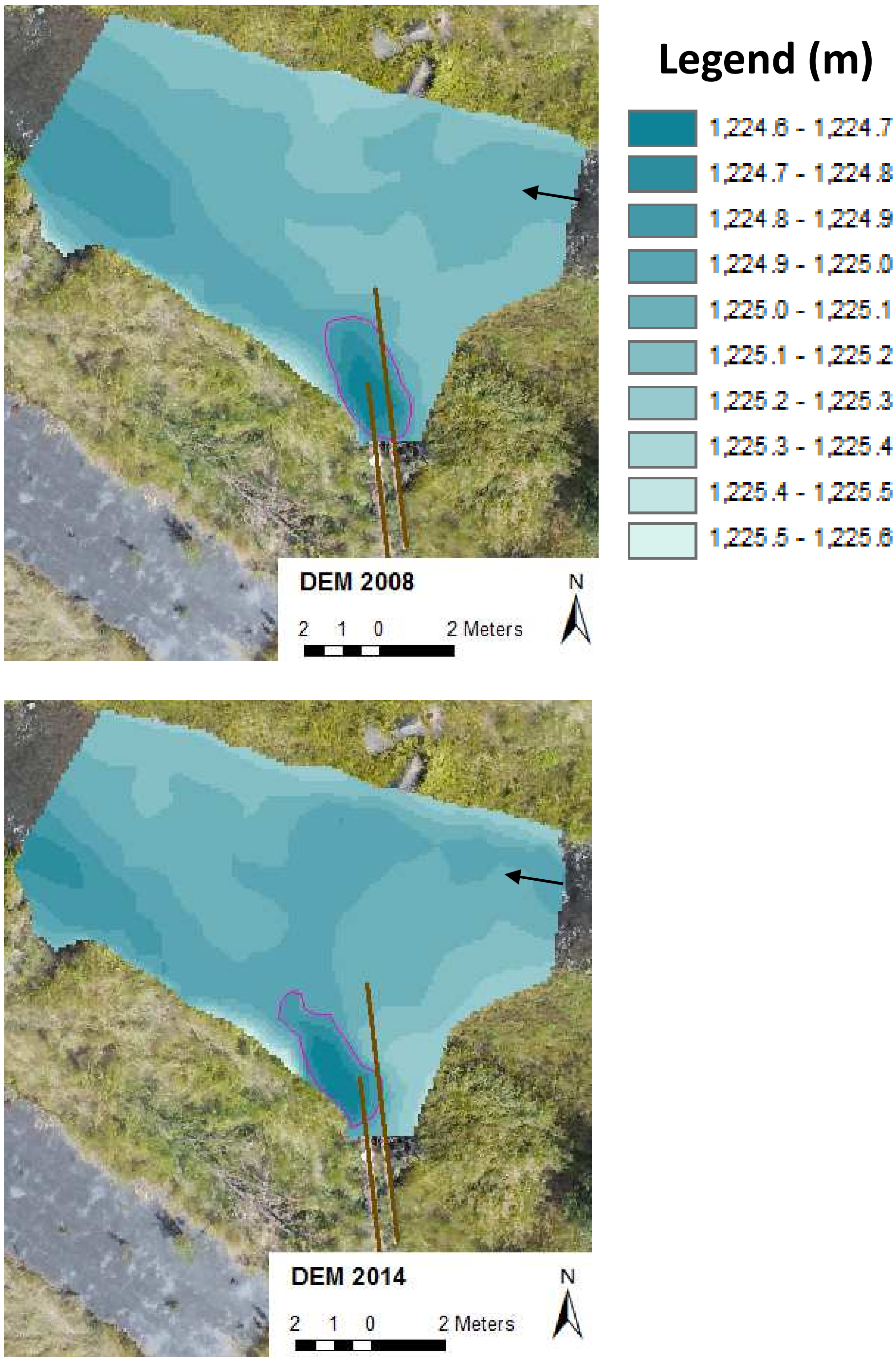
Legend (m)
1,224.6 - 1,224.7
1,224.7 - 1,224.8
1,224.8 - 1,224.9
1,224.9 - 1,225.0
1,225.0 - 1,225.1
1,225.1 - 1,225.2
1,225.2 - 1,225.3
1,225.3 - 1,225.4
1,225.4 - 1,225.5
1,225.5 - 1,225.6
DEM 2008
2 1 0 2 Meters
N
DEM 2014
2 1 0 2 Meters
N

VIBR 14 DoD

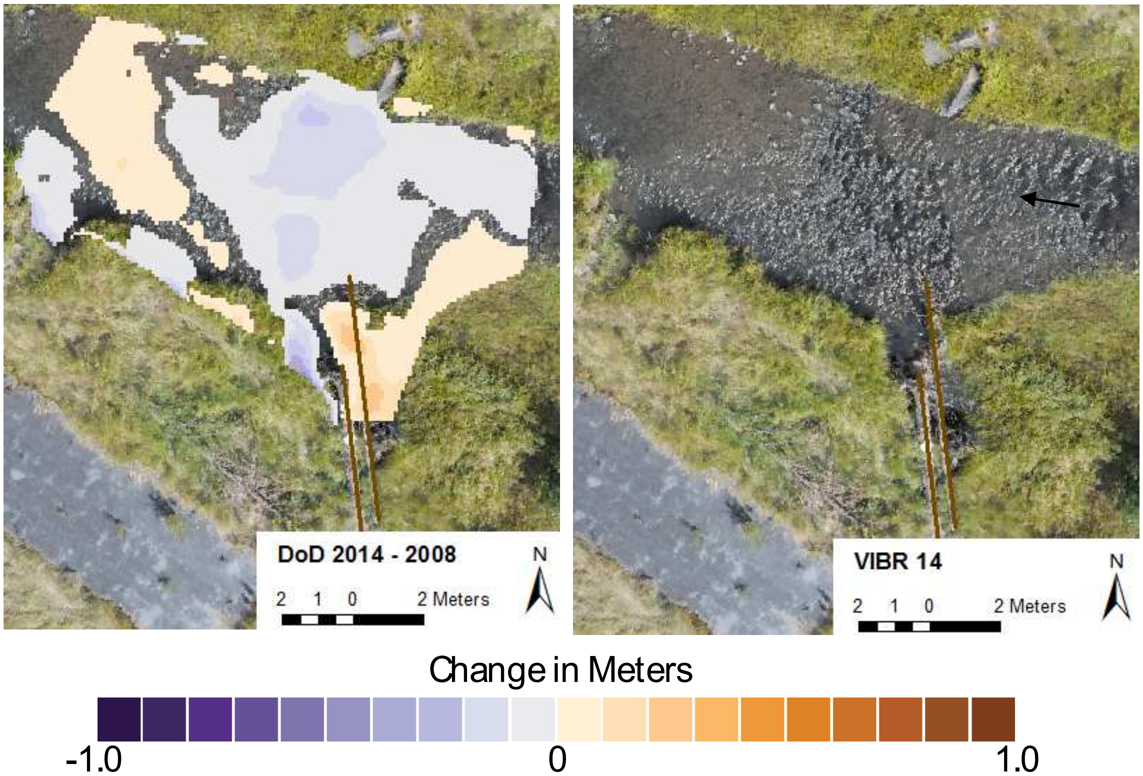
DoD 2014 - 2008
2 1 0 2 Meters
N
VIBR 14
2 1 0 2 Meters
N
Change in Meters
-1.0
0
1.0

VIBR 15 DEM

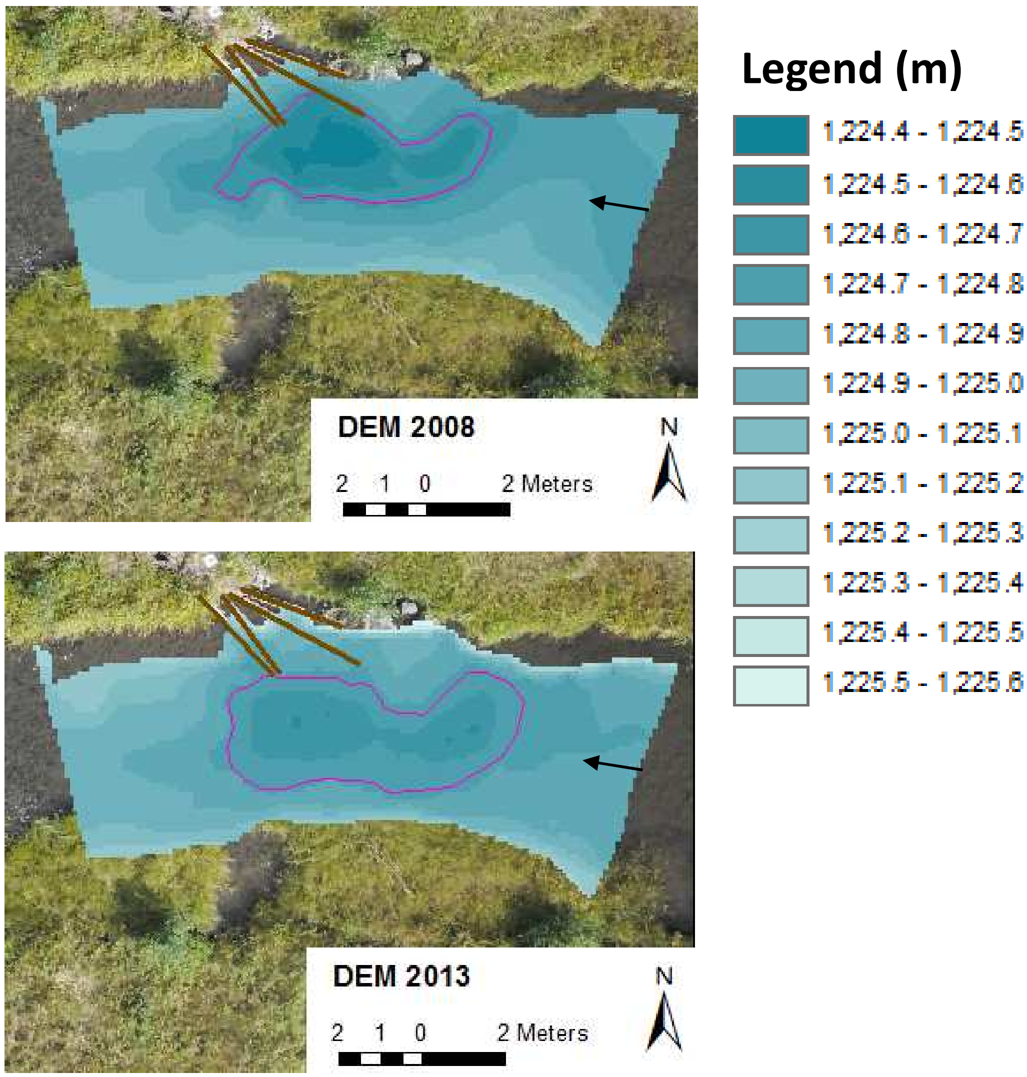

DEM 2008
2 1 0 2 Meters
N
DEM 2013
2 1 0 2 Meters
N
Legend (m)
1,224.4 - 1,224.5
1,224.5 - 1,224.6
1,224.6 - 1,224.7
1,224.7 - 1,224.8
1,224.8 - 1,224.9
1,224.9 - 1,225.0
1,225.0 - 1,225.1
1,225.1 - 1,225.2
1,225.2 - 1,225.3
1,225.3 - 1,225.4
1,225.4 - 1,225.5
1,225.5 - 1,225.6

VIBR 15 DoD

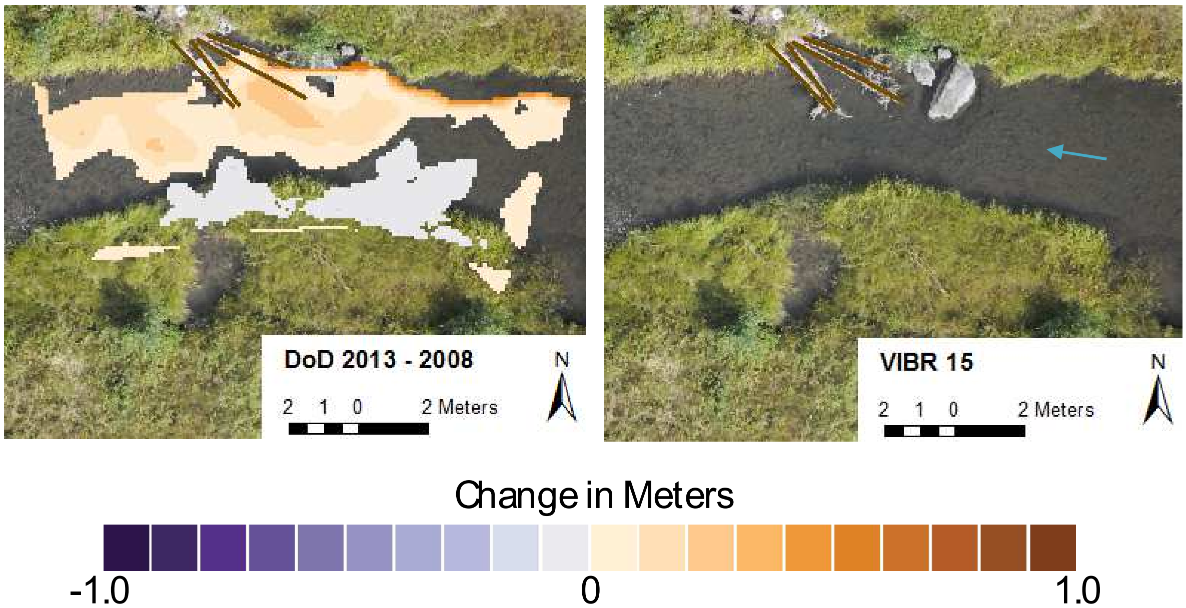
DoD 2013 - 2008
2 1 0 2 Meters
N
VIBR 15
2 1 0 2 Meters
N
Change in Meters
-1.0
0
1.0

VIBR 16 DEM

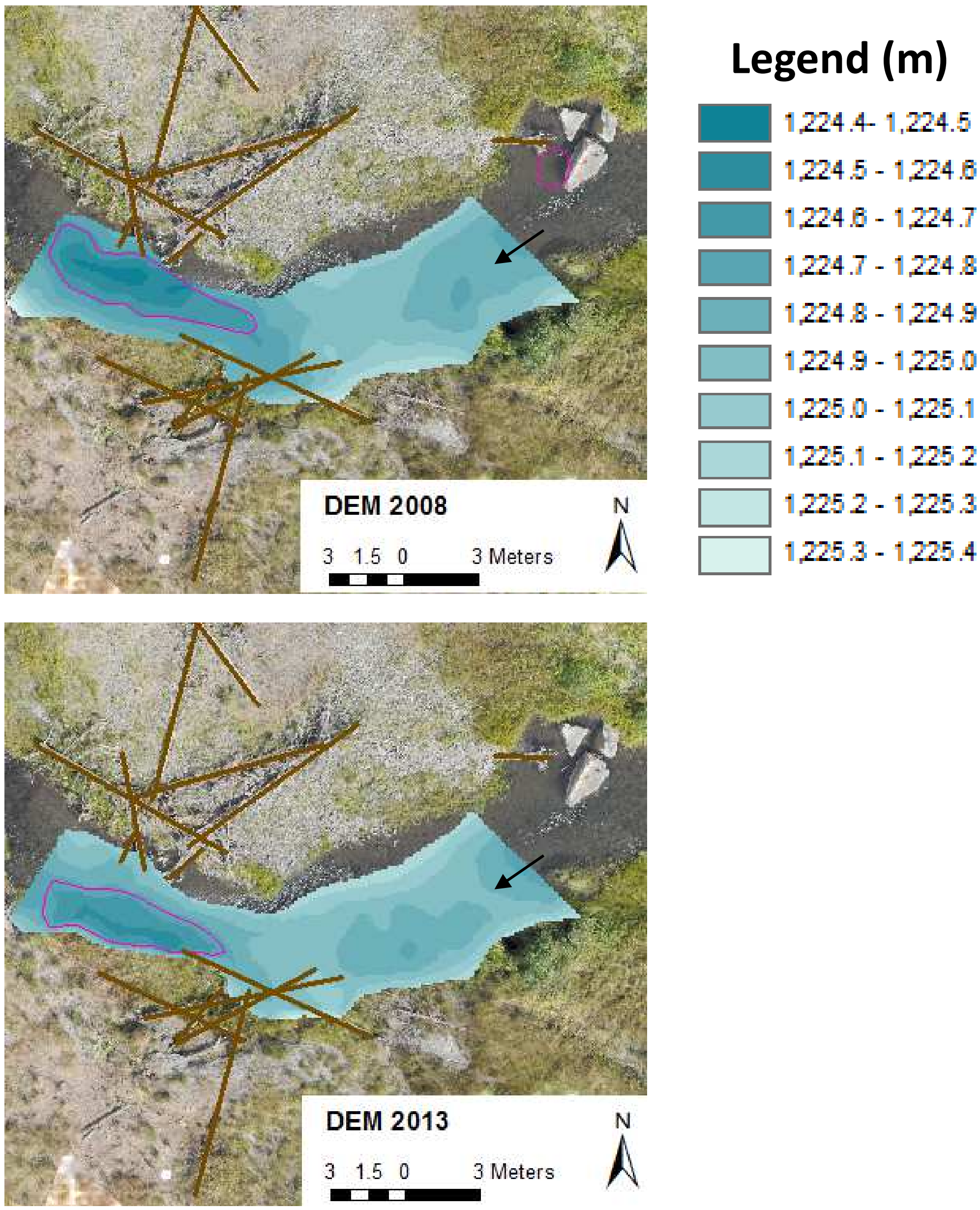

Legend (m)
1,224.4- 1,224.5
1,224.5 - 1,224.6
1,224.6 - 1,224.7
1,224.7 - 1,224.8
1,224.8 - 1,224.9
1,224.9 - 1,225.0
1,225.0 - 1,225.1
1,225.1 - 1,225.2
1,225.2 - 1,225.3
1,225.3 - 1,225.4
DEM 2008
3 1.5 0 3 Meters
N
DEM 2013
3 1.5 0 3 Meters
N

VIBR 16 DoD

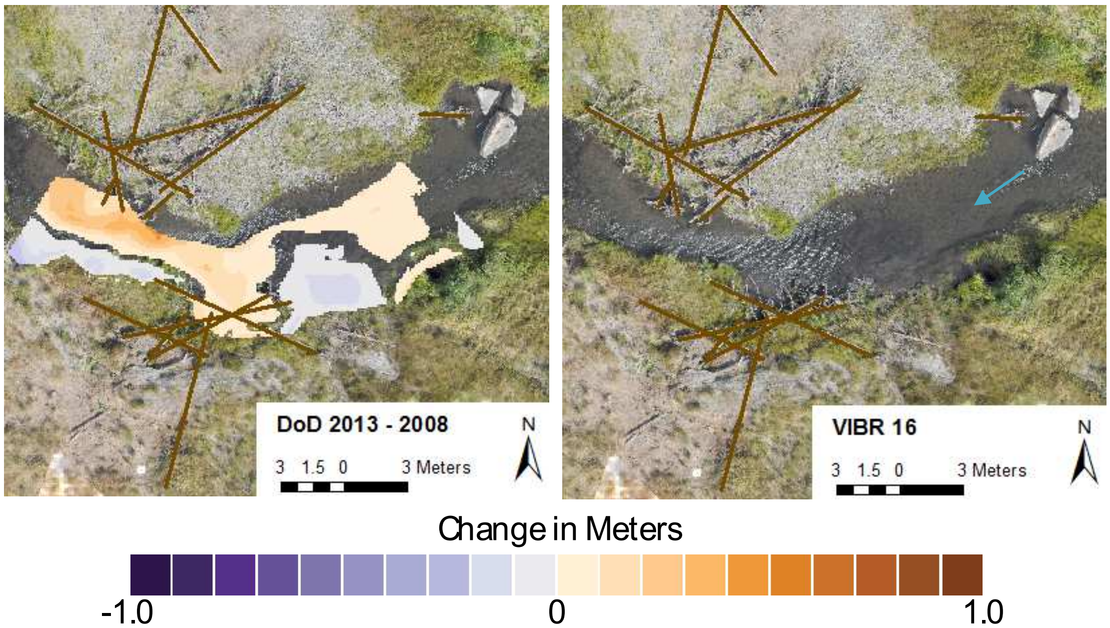
DoD 2013 - 2008
3 1.5 0 3 Meters
N
VIBR 16
3 1.5 0 3 Meters
N
Change in Meters
-1.0
0
1.0

VIBR 17 DEM

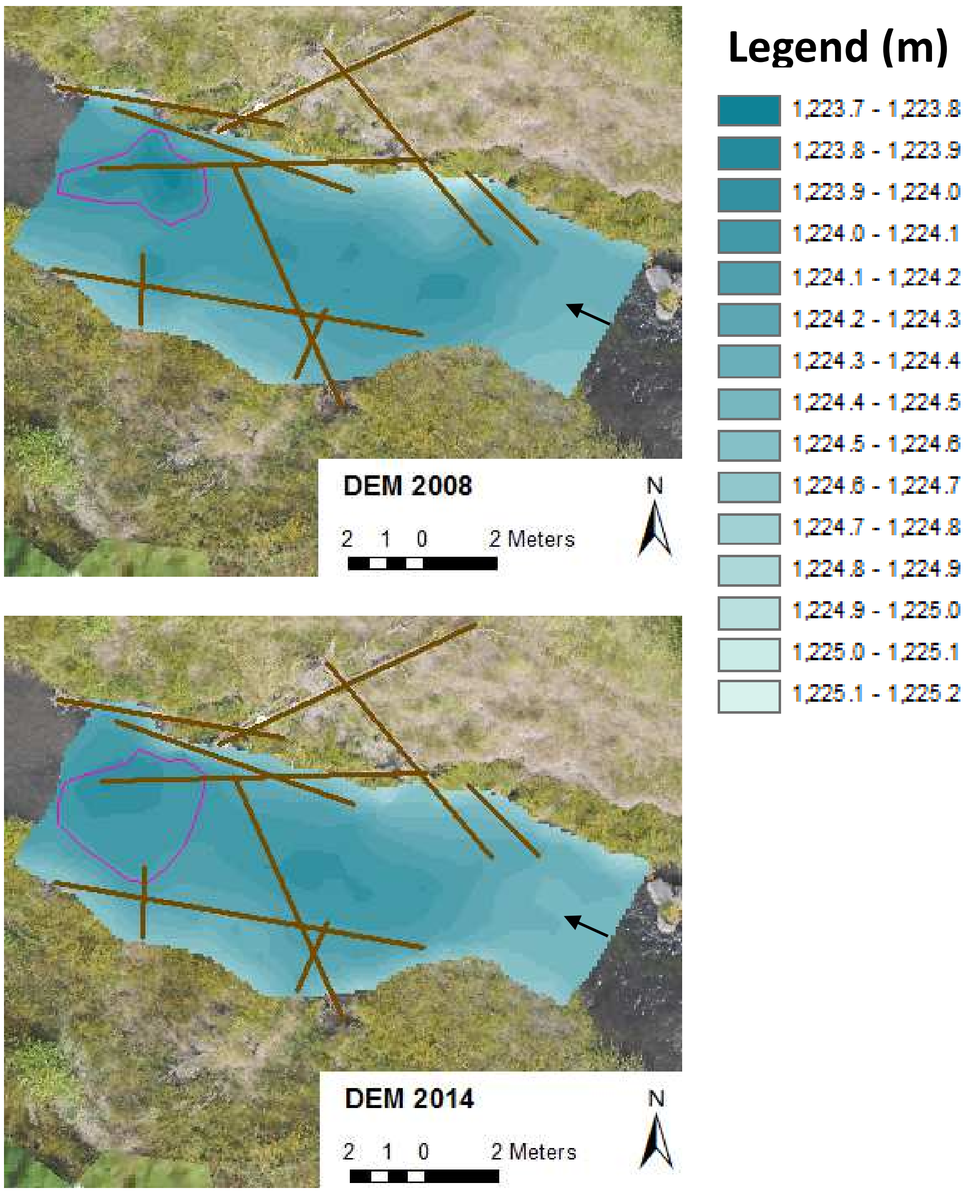

DEM 2008
2 1 0 2 Meters
N
DEM 2014
2 1 0 2 Meters
N
Legend (m)
1,223.7 - 1,223.8
1,223.8 - 1,223.9
1,223.9 - 1,224.0
1,224.0 - 1,224.1
1,224.1 - 1,224.2
1,224.2 - 1,224.3
1,224.3 - 1,224.4
1,224.4 - 1,224.5
1,224.5 - 1,224.6
1,224.6 - 1,224.7
1,224.7 - 1,224.8
1,224.8 - 1,224.9
1,224.9 - 1,225.0
1,225.0 - 1,225.1
1,225.1 - 1,225.2

VIBR 17 DoD

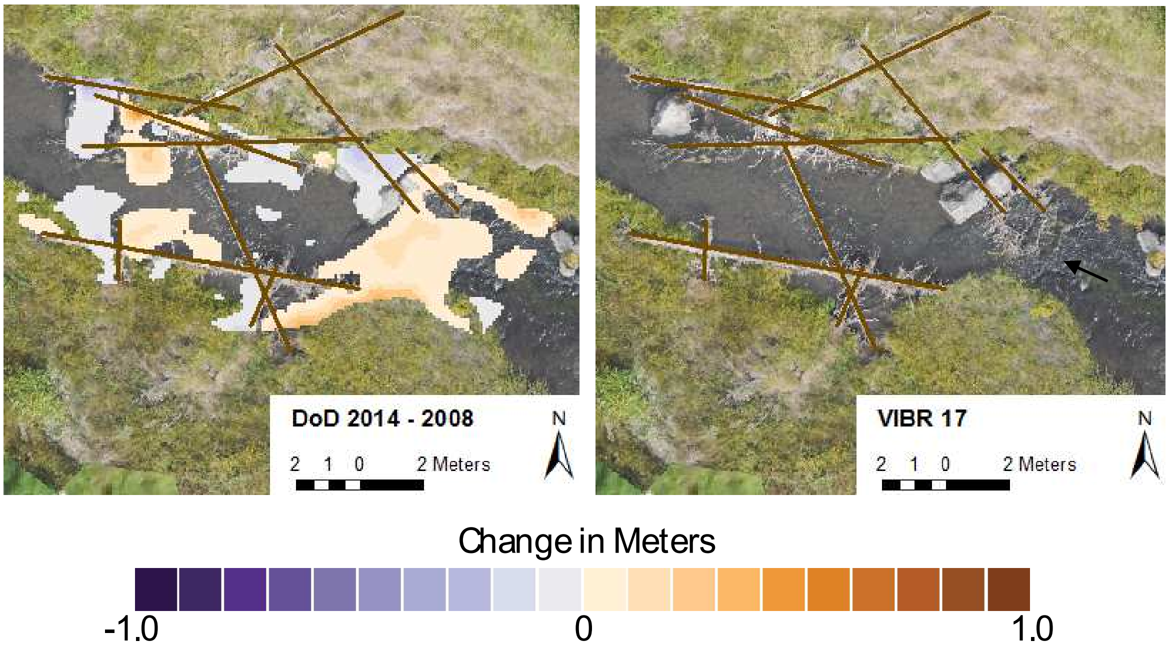
DoD 2014 - 2008
2 1 0 2 Meters
N
VIBR 17
2 1 0 2 Meters
N
Change in Meters
-1.0
0
1.0

RABE 1 DEM

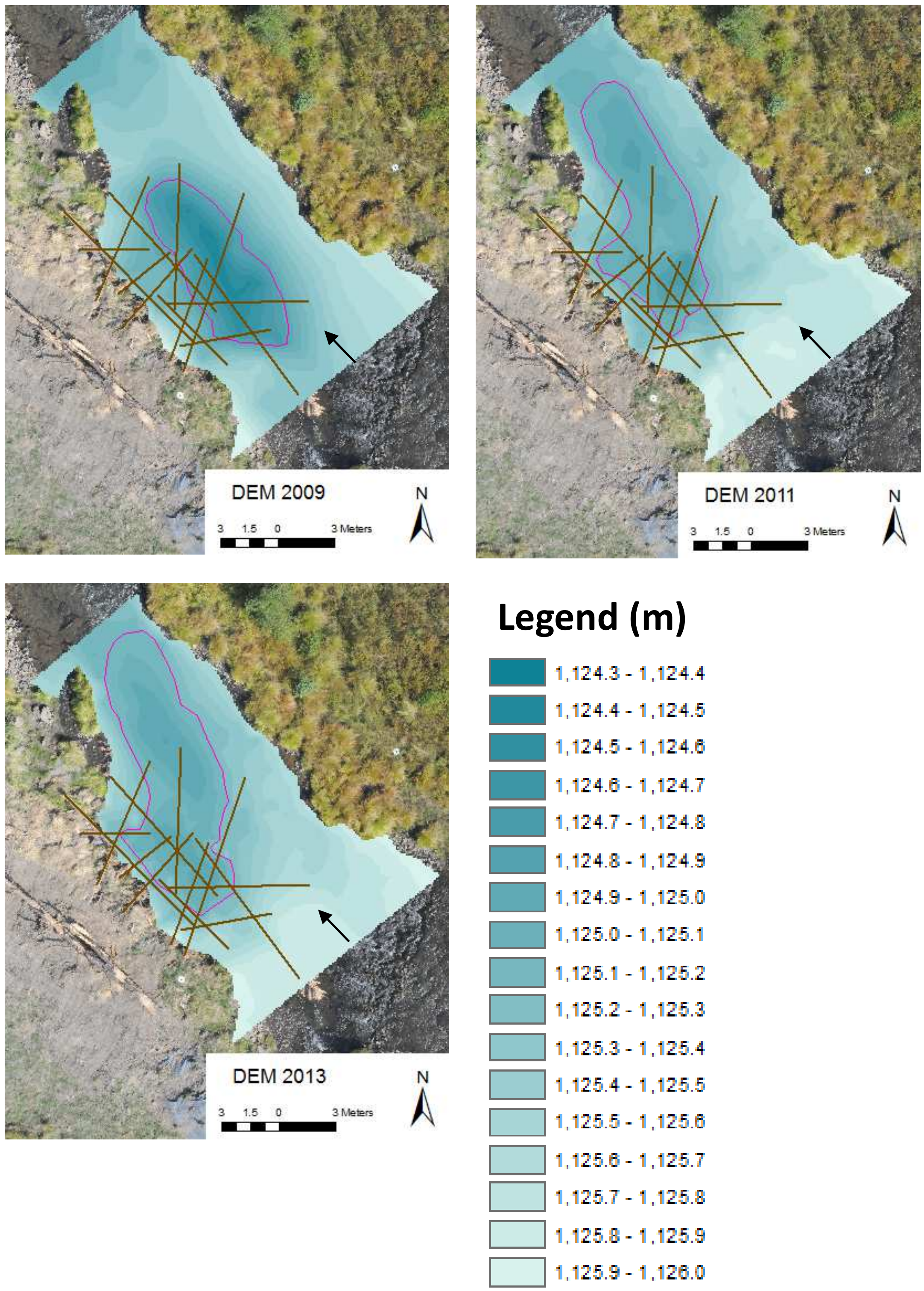
DEM 2009
N
3 1.5 0 3 Meters
DEM 2011
N
3 1.5 0 3 Meters
DEM 2013
N
3 1.5 0 3 Meters
Legend (m)
1,124.3 - 1,124.4
1,124.4 - 1,124.5
1,124.5 - 1,124.6
1,124.6 - 1,124.7
1,124.7 - 1,124.8
1,124.8 - 1,124.9
1,124.9 - 1,125.0
1,125.0 - 1,125.1
1,125.1 - 1,125.2
1,125.2 - 1,125.3
1,125.3 - 1,125.4
1,125.4 - 1,125.5
1,125.5 - 1,125.6
1,125.6 - 1,125.7
1,125.7 - 1,125.8
1,125.8 - 1,125.9
1,125.9 - 1,126.0

RABE 1 DoD

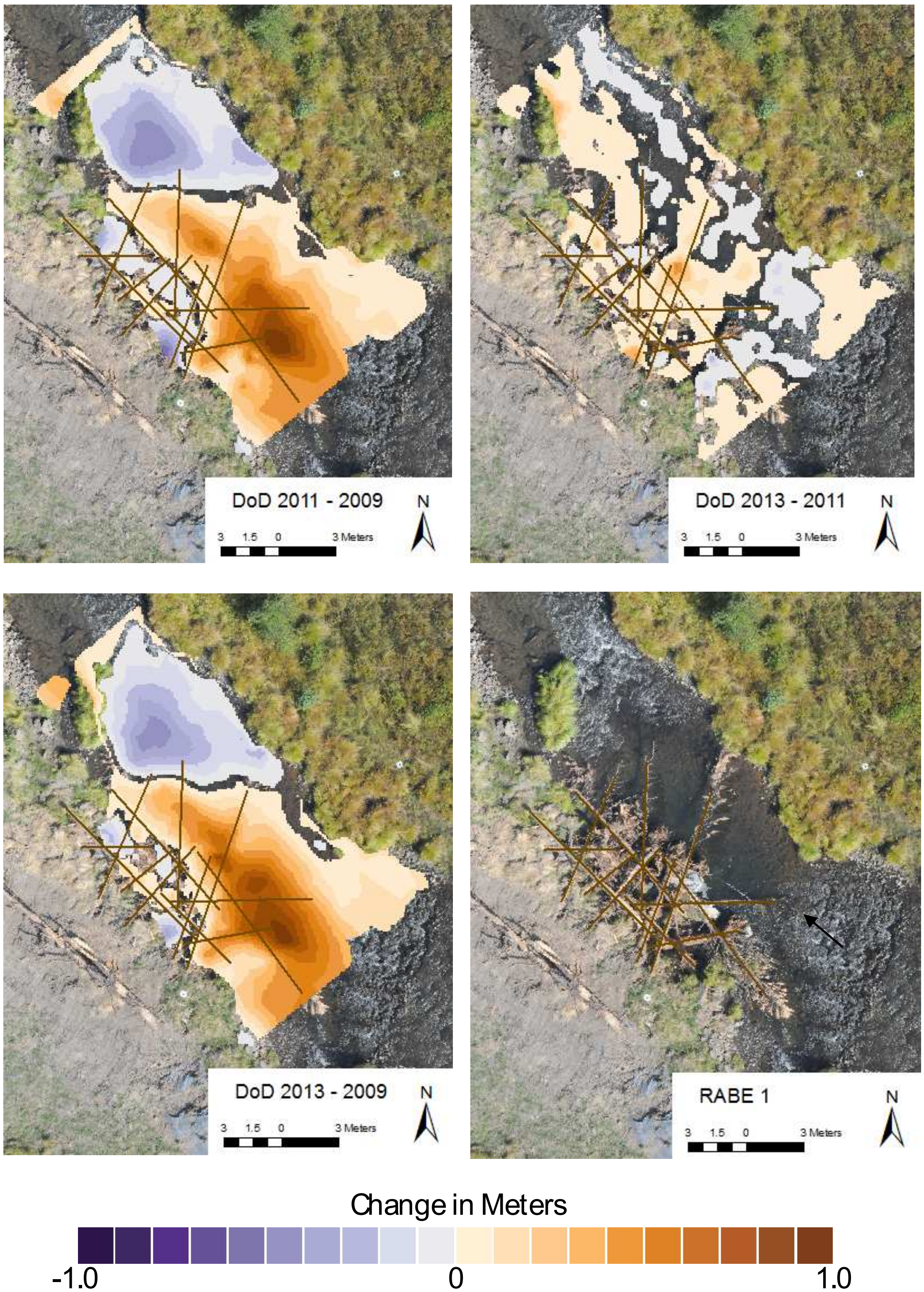
DoD 2011 - 2009
3 1.5 0 3 Meters
N
DoD 2013 - 2011
3 1.5 0 3 Meters
N
DoD 2013 - 2009
3 1.5 0 3 Meters
N
RABE 1
3 1.5 0 3 Meters
N
Change in Meters
-1.0
0
1.0

RABE 2 DEM

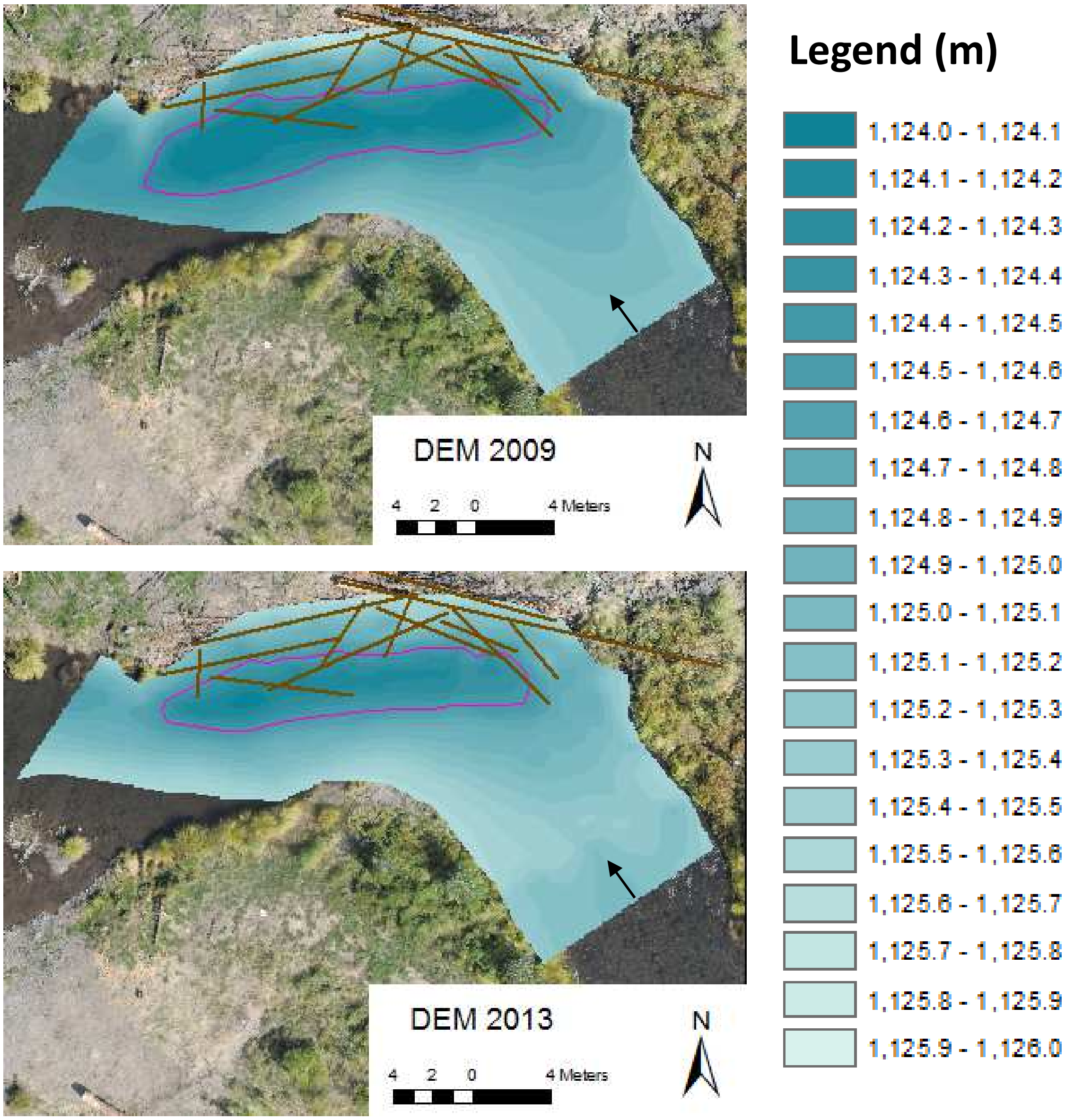
Legend (m)
1,124.0 - 1,124.1
1,124.1 - 1,124.2
1,124.2 - 1,124.3
1,124.3 - 1,124.4
1,124.4 - 1,124.5
1,124.5 - 1,124.6
1,124.6 - 1,124.7
1,124.7 - 1,124.8
1,124.8 - 1,124.9
1,124.9 - 1,125.0
1,125.0 - 1,125.1
1,125.1 - 1,125.2
1,125.2 - 1,125.3
1,125.3 - 1,125.4
1,125.4 - 1,125.5
1,125.5 - 1,125.6
1,125.6 - 1,125.7
1,125.7 - 1,125.8
1,125.8 - 1,125.9
1,125.9 - 1,126.0
DEM 2009
4 2 0 4 Meters
N
DEM 2013
4 2 0 4 Meters
N

RABE 2 DoD

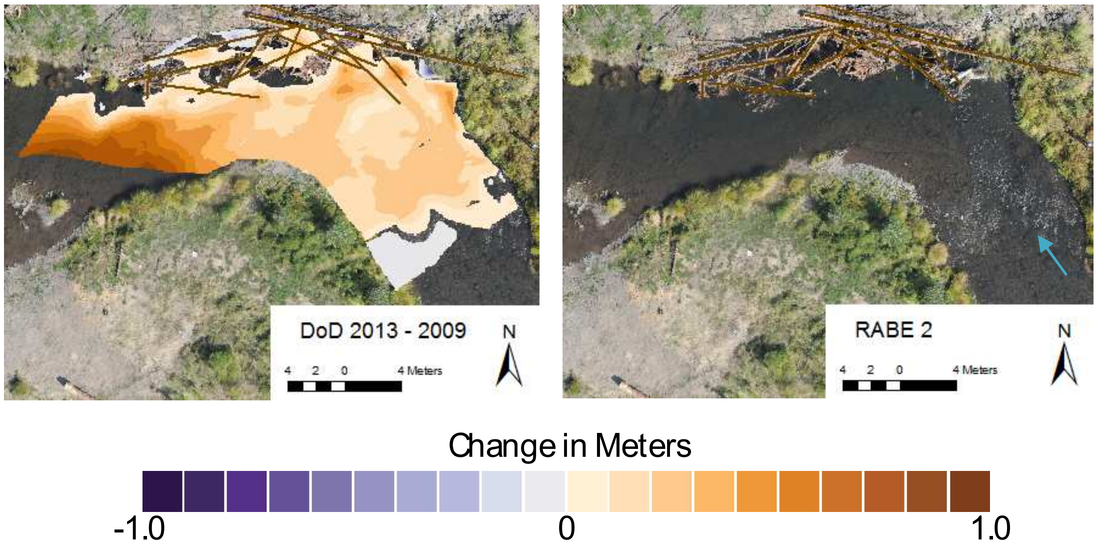

DoD 2013 - 2009
4 2 0 4 Meters
N
RABE 2
4 2 0 4 Meters
N
Change in Meters
-1.0
0
1.0

RABE 4 DEM

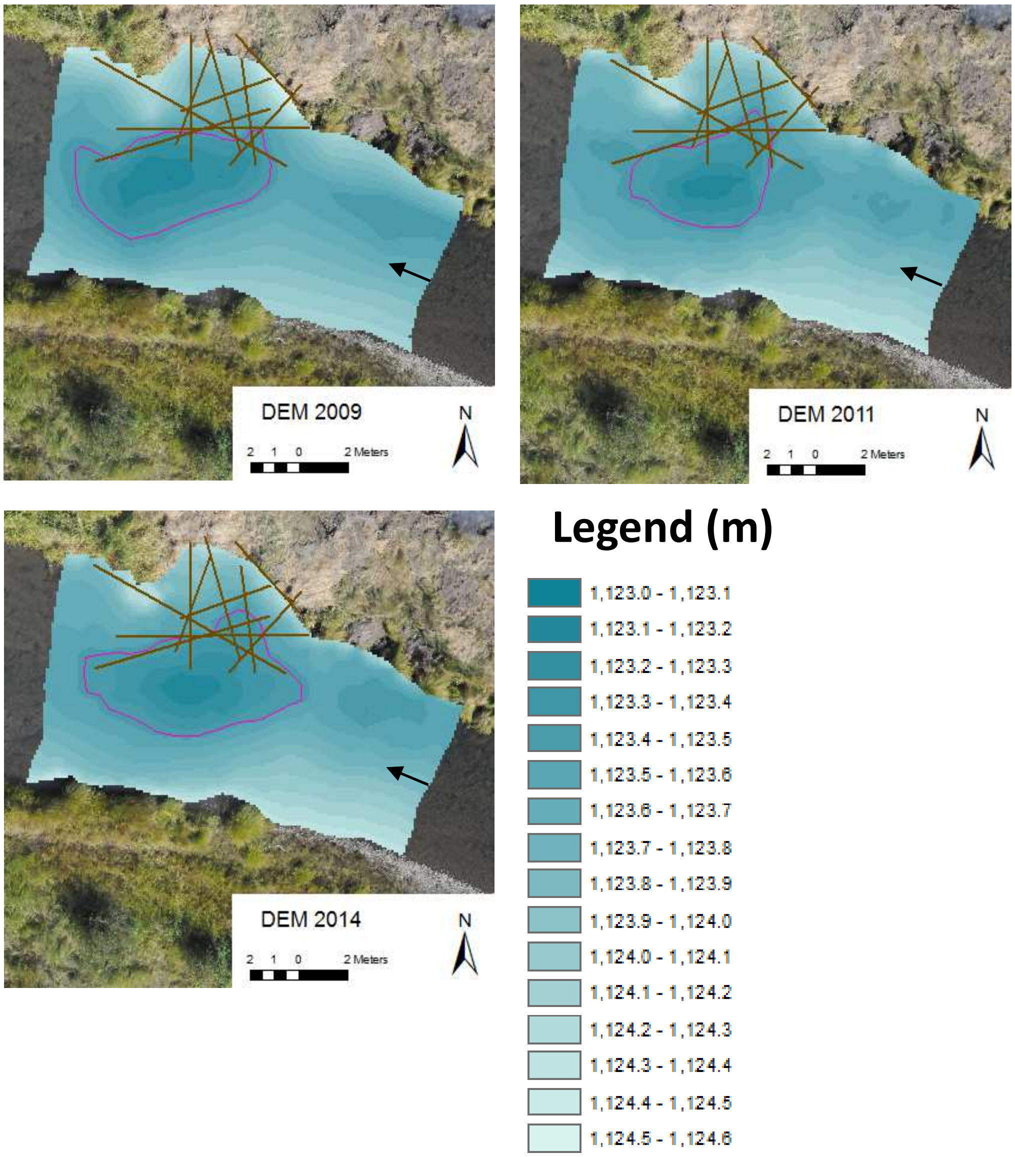
DEM 2009
2 1 0 2 Meters
N
DEM 2011
2 1 0 2 Meters
N
DEM 2014
2 1 0 2 Meters
N
Legend (m)
1,123.0 - 1,123.1
1,123.1 - 1,123.2
1,123.2 - 1,123.3
1,123.3 - 1,123.4
1,123.4 - 1,123.5
1,123.5 - 1,123.6
1,123.6 - 1,123.7
1,123.7 - 1,123.8
1,123.8 - 1,123.9
1,123.9 - 1,124.0
1,124.0 - 1,124.1
1,124.1 - 1,124.2
1,124.2 - 1,124.3
1,124.3 - 1,124.4
1,124.4 - 1,124.5
1,124.5 - 1,124.6

RABE 4 DoD

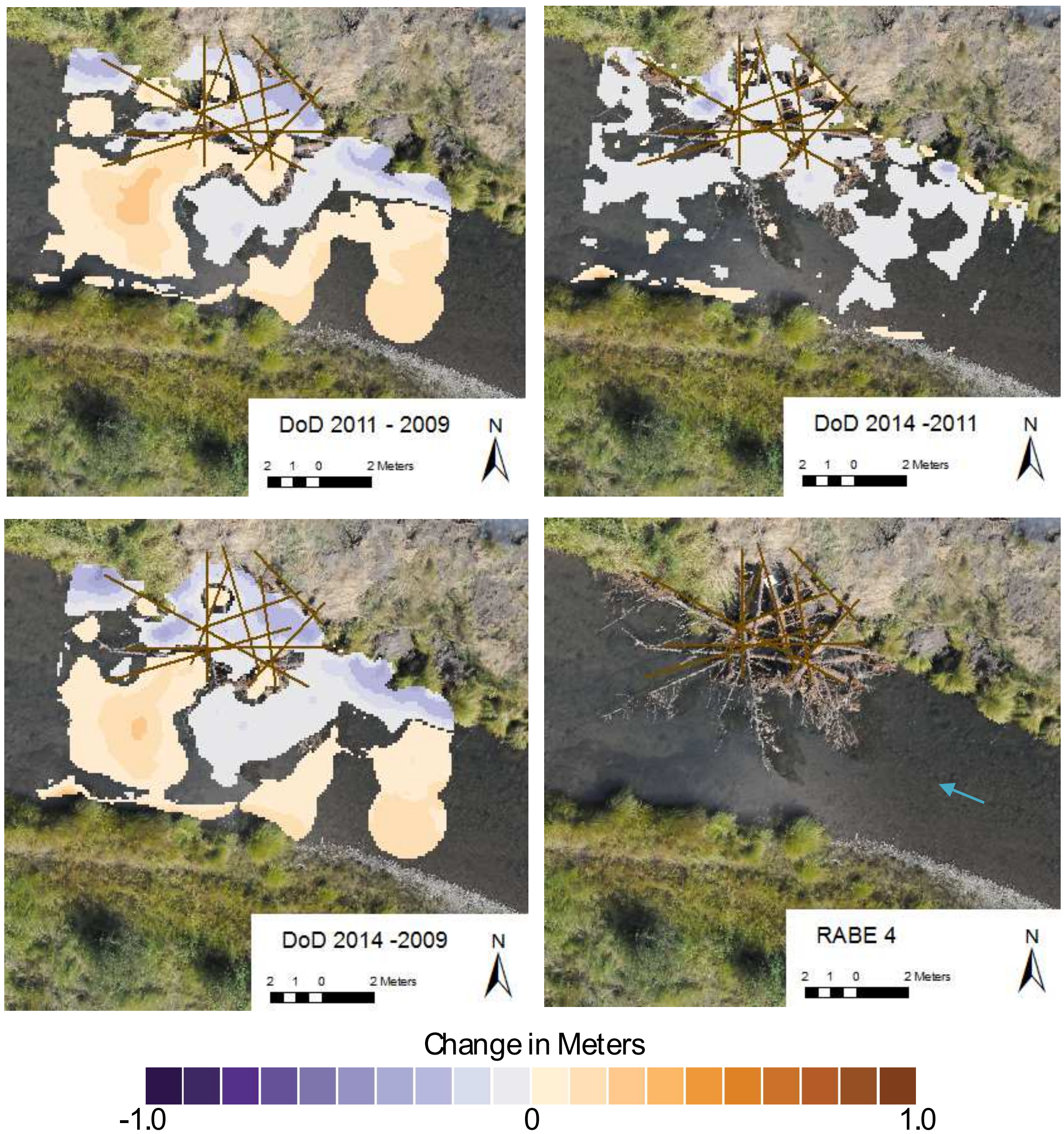
DoD 2011 - 2009
2 1 0 2 Meters
N
DoD 2014 -2011
2 1 0 2 Meters
N
DoD 2014 -2009
2 1 0 2 Meters
N
RABE 4
2 1 0 2 Meters
N
Change in Meters
-1.0
0
1.0

RABE 6 DEM

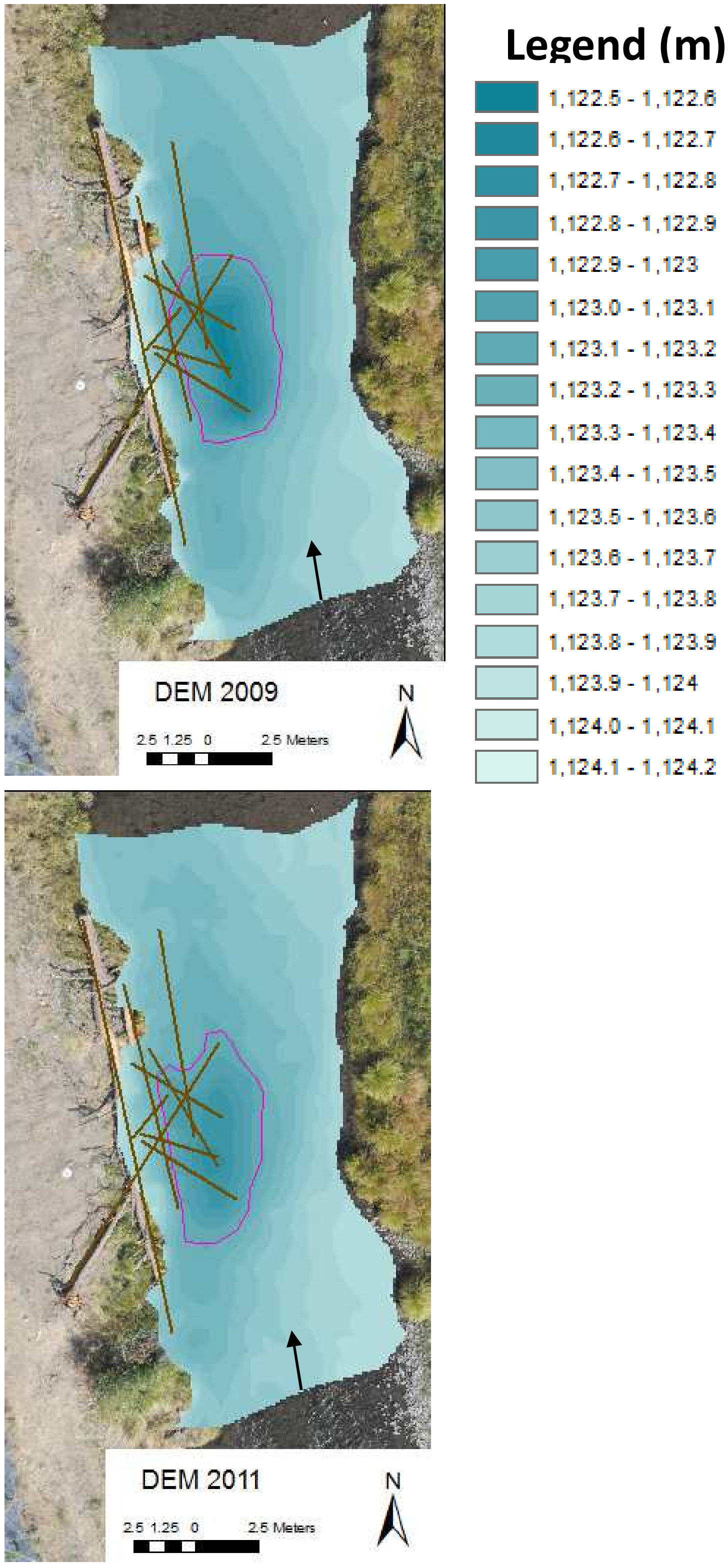
Legend (m)
1,122.5 - 1,122.6
1,122.6 - 1,122.7
1,122.7 - 1,122.8
1,122.8 - 1,122.9
1,122.9 - 1,123
1,123.0 - 1,123.1
1,123.1 - 1,123.2
1,123.2 - 1,123.3
1,123.3 - 1,123.4
1,123.4 - 1,123.5
1,123.5 - 1,123.6
1,123.6 - 1,123.7
1,123.7 - 1,123.8
1,123.8 - 1,123.9
1,123.9 - 1,124
1,124.0 - 1,124.1
1,124.1 - 1,124.2
DEM 2009
2.5 1.25 0 2.5 Meters
N
DEM 2011
2.5 1.25 0 2.5 Meters
N

RABE 6 DoD

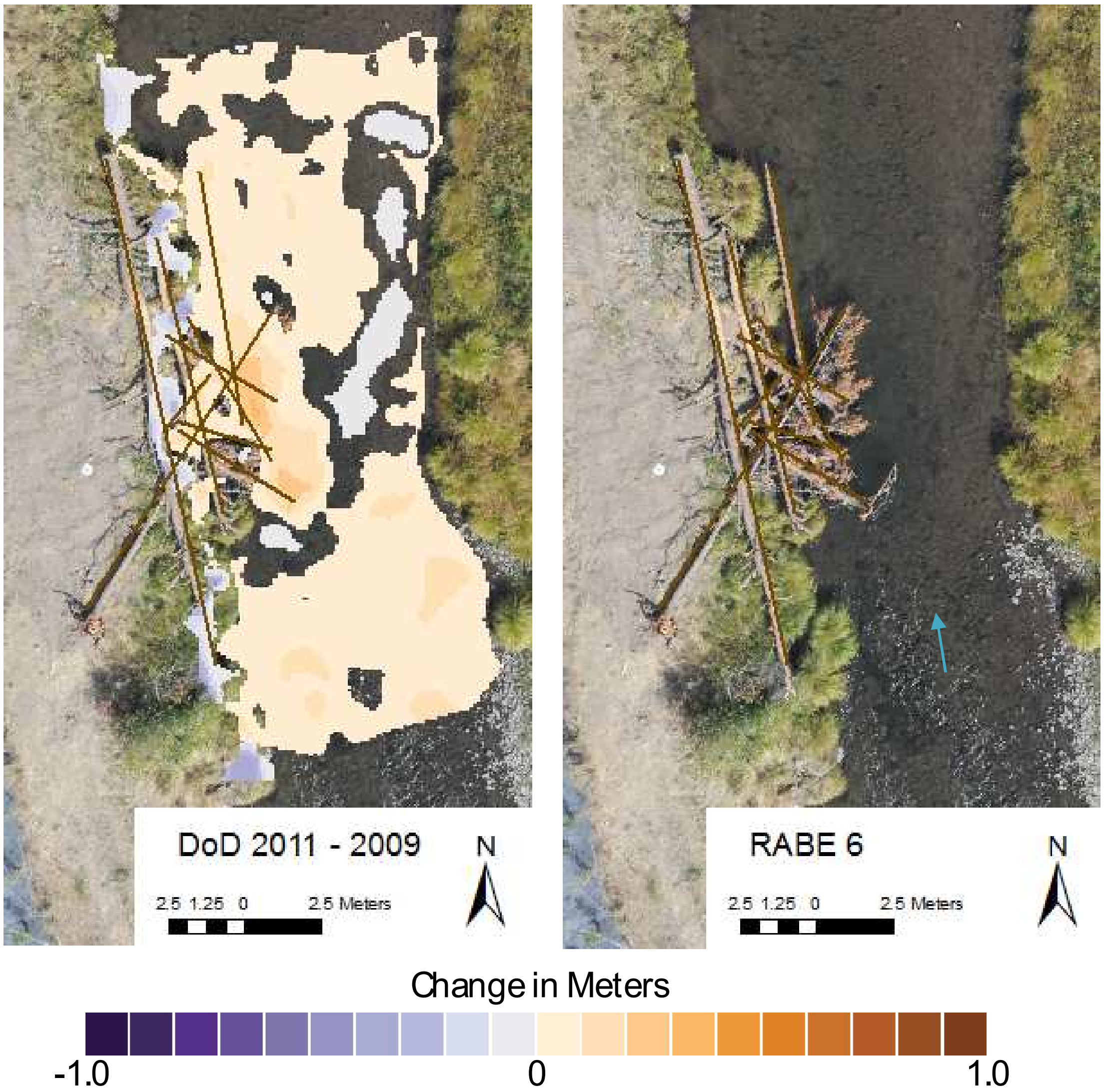

DoD 2011 - 2009
N
2.5 1.25 0 2.5 Meters
RABE 6
N
2.5 1.25 0 2.5 Meters
Change in Meters
-1.0
0
1.0

RABE 7 DEM

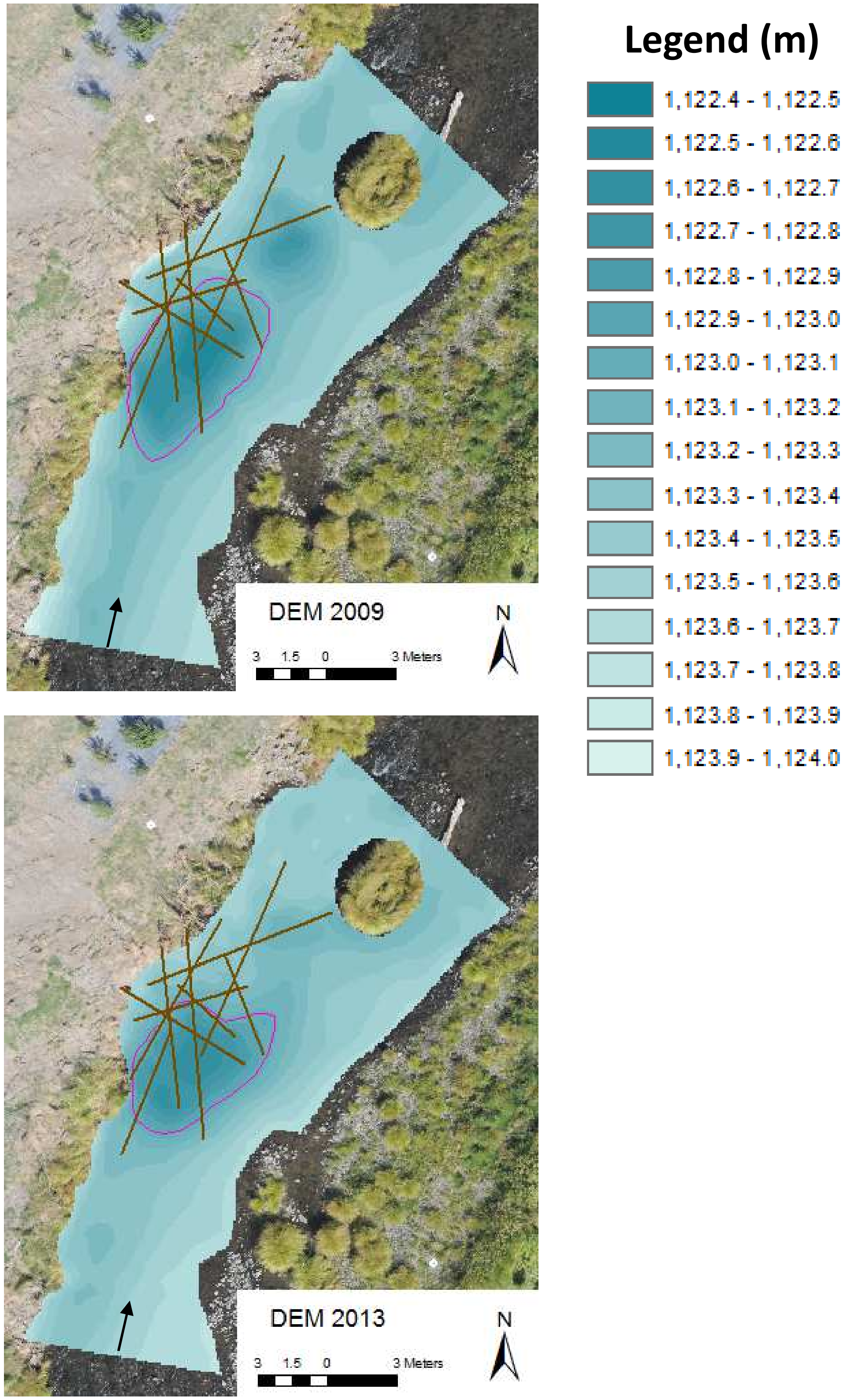
DEM 2009
3 1.5 0 3 Meters
N
DEM 2013
3 1.5 0 3 Meters
N
Legend (m)
1,122.4 - 1,122.5
1,122.5 - 1,122.6
1,122.6 - 1,122.7
1,122.7 - 1,122.8
1,122.8 - 1,122.9
1,122.9 - 1,123.0
1,123.0 - 1,123.1
1,123.1 - 1,123.2
1,123.2 - 1,123.3
1,123.3 - 1,123.4
1,123.4 - 1,123.5
1,123.5 - 1,123.6
1,123.6 - 1,123.7
1,123.7 - 1,123.8
1,123.8 - 1,123.9
1,123.9 - 1,124.0

RABE 7 DoD

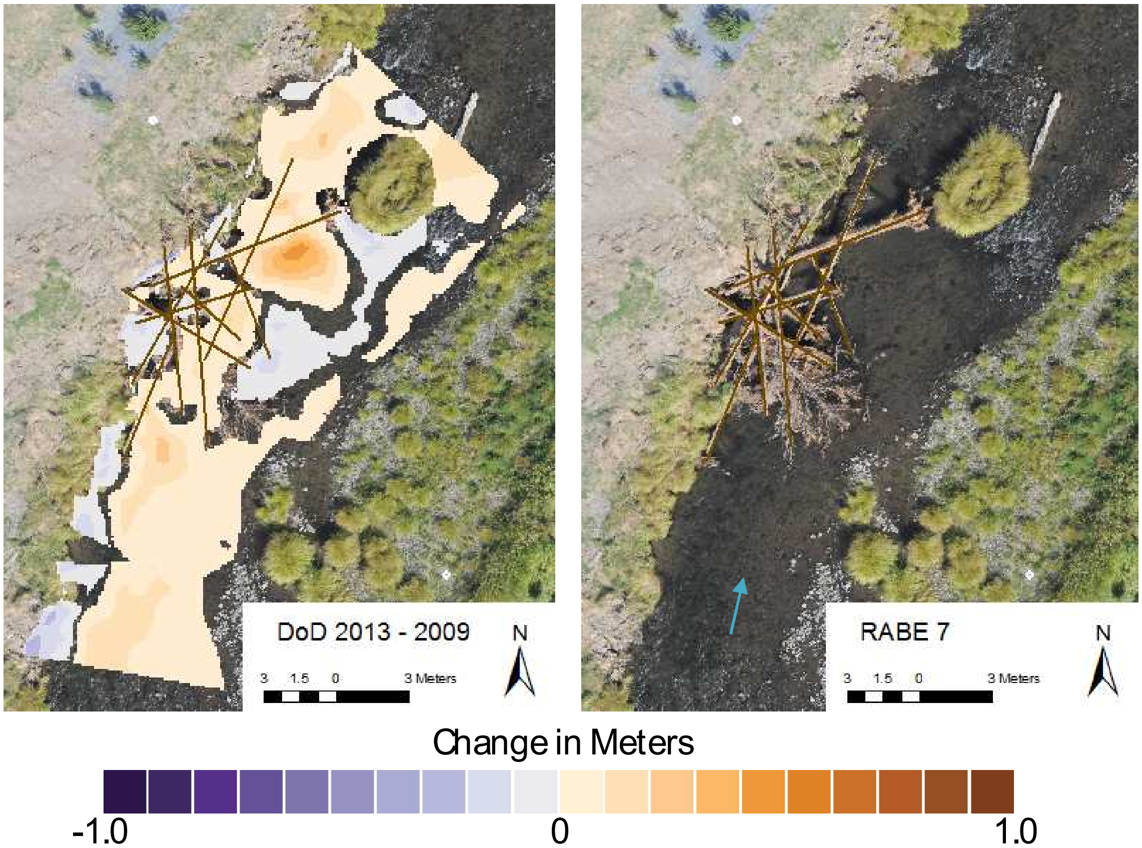
DoD 2013 - 2009
3 1.5 0 3 Meters
N
RABE 7
3 1.5 0 3 Meters
N
Change in Meters
-1.0
0
1.0

RABE 8 DEM

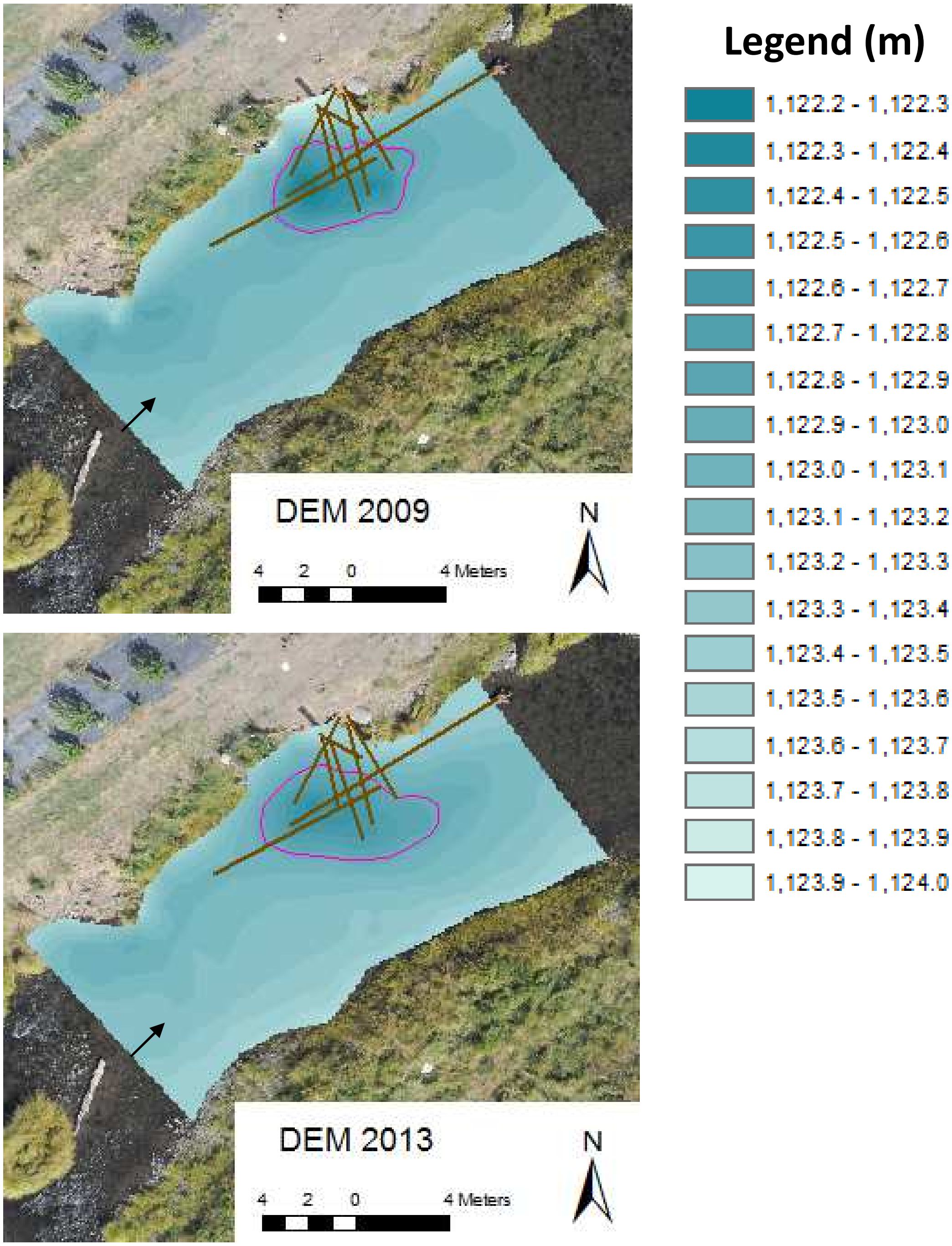
DEM 2009
4 2 0 4 Meters
N
DEM 2013
4 2 0 4 Meters
N
Legend (m)
1,122.2 - 1,122.3
1,122.3 - 1,122.4
1,122.4 - 1,122.5
1,122.5 - 1,122.6
1,122.6 - 1,122.7
1,122.7 - 1,122.8
1,122.8 - 1,122.9
1,122.9 - 1,123.0
1,123.0 - 1,123.1
1,123.1 - 1,123.2
1,123.2 - 1,123.3
1,123.3 - 1,123.4
1,123.4 - 1,123.5
1,123.5 - 1,123.6
1,123.6 - 1,123.7
1,123.7 - 1,123.8
1,123.8 - 1,123.9
1,123.9 - 1,124.0

RABE 8 DoD

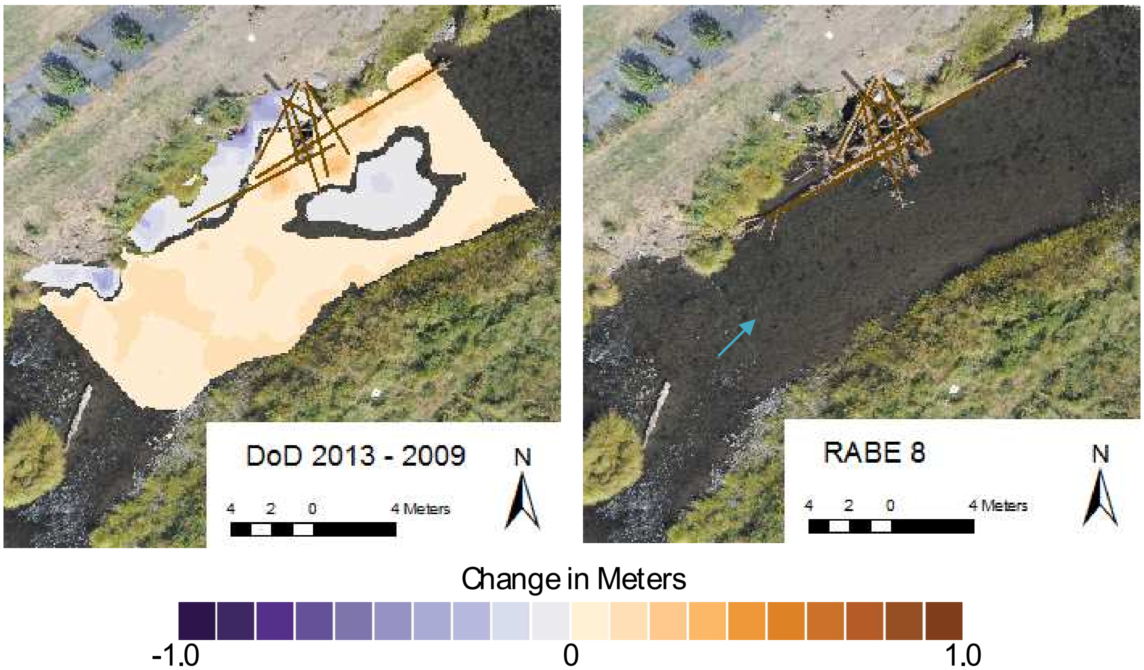
DoD 2013 - 2009
4 2 0 4 Meters
N
RABE 8
4 2 0 4 Meters
N
Change in Meters
-1.0
0
1.0

RABE 9 DEM

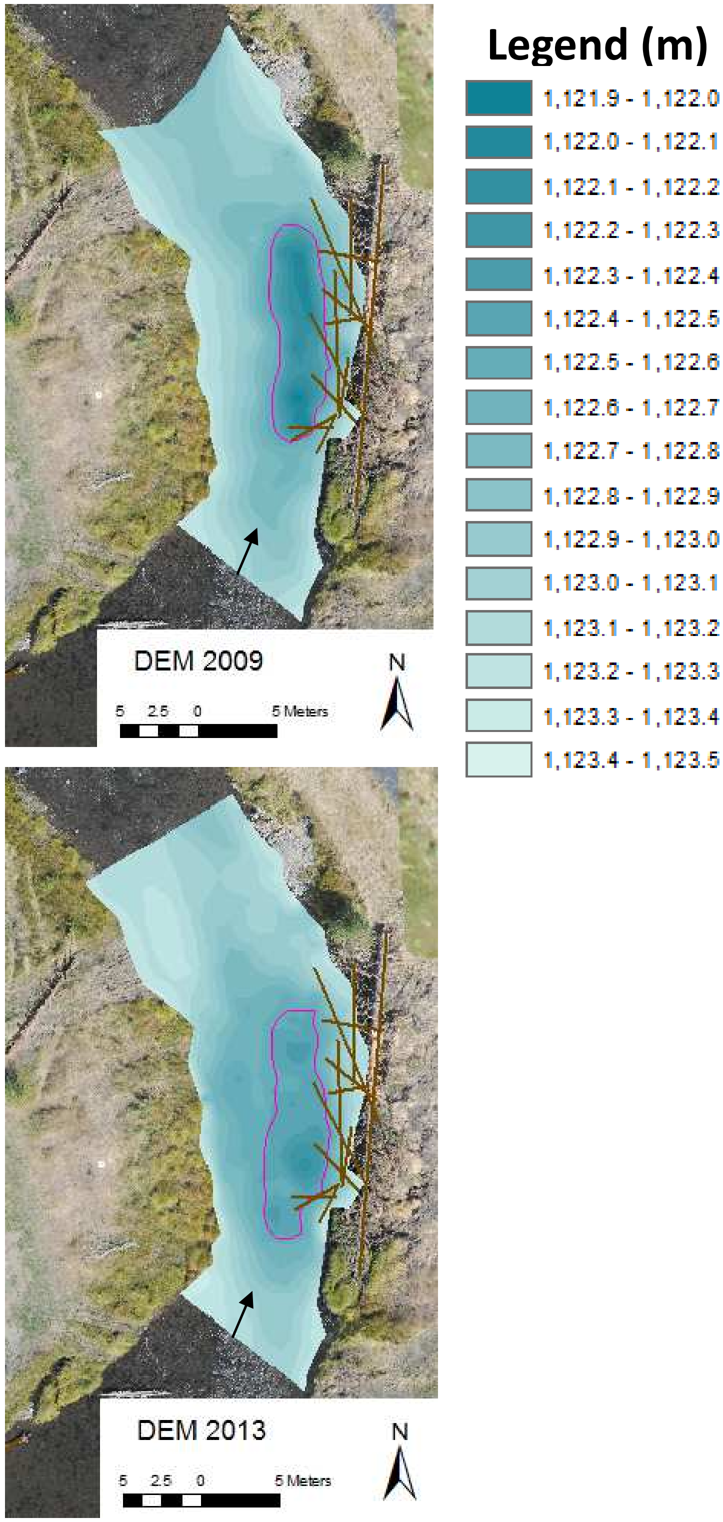

Legend (m)
1,121.9 - 1,122.0
1,122.0 - 1,122.1
1,122.1 - 1,122.2
1,122.2 - 1,122.3
1,122.3 - 1,122.4
1,122.4 - 1,122.5
1,122.5 - 1,122.6
1,122.6 - 1,122.7
1,122.7 - 1,122.8
1,122.8 - 1,122.9
1,122.9 - 1,123.0
1,123.0 - 1,123.1
1,123.1 - 1,123.2
1,123.2 - 1,123.3
1,123.3 - 1,123.4
1,123.4 - 1,123.5
DEM 2009
5 2.5 0 5 Meters
N
DEM 2013
5 2.5 0 5 Meters
N

RABE 9 DoD

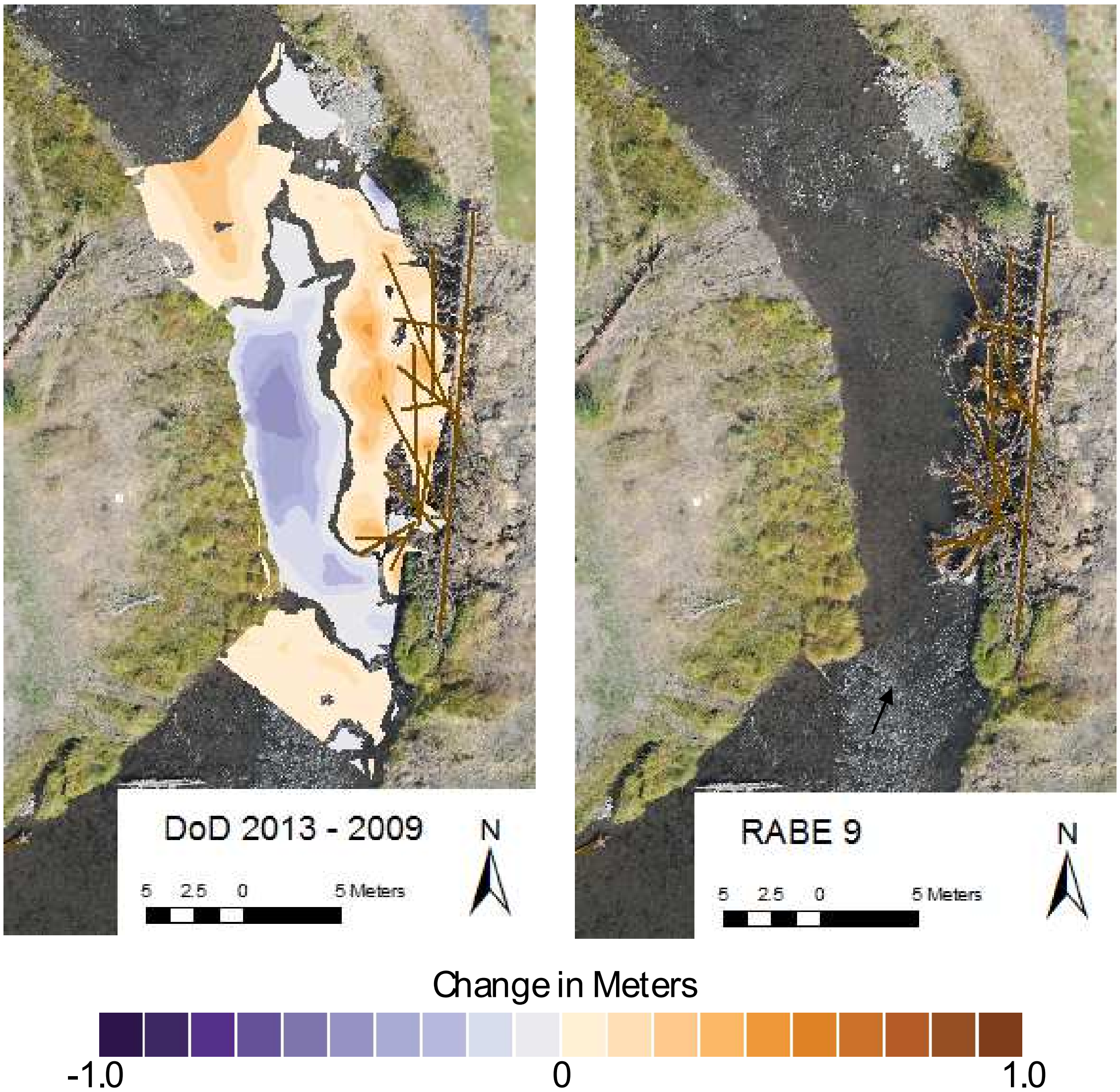
DoD 2013 - 2009
N
5 2.5 0 5 Meters
RABE 9
N
5 2.5 0 5 Meters
Change in Meters
-1.0
0
1.0

RABE 10 DEM

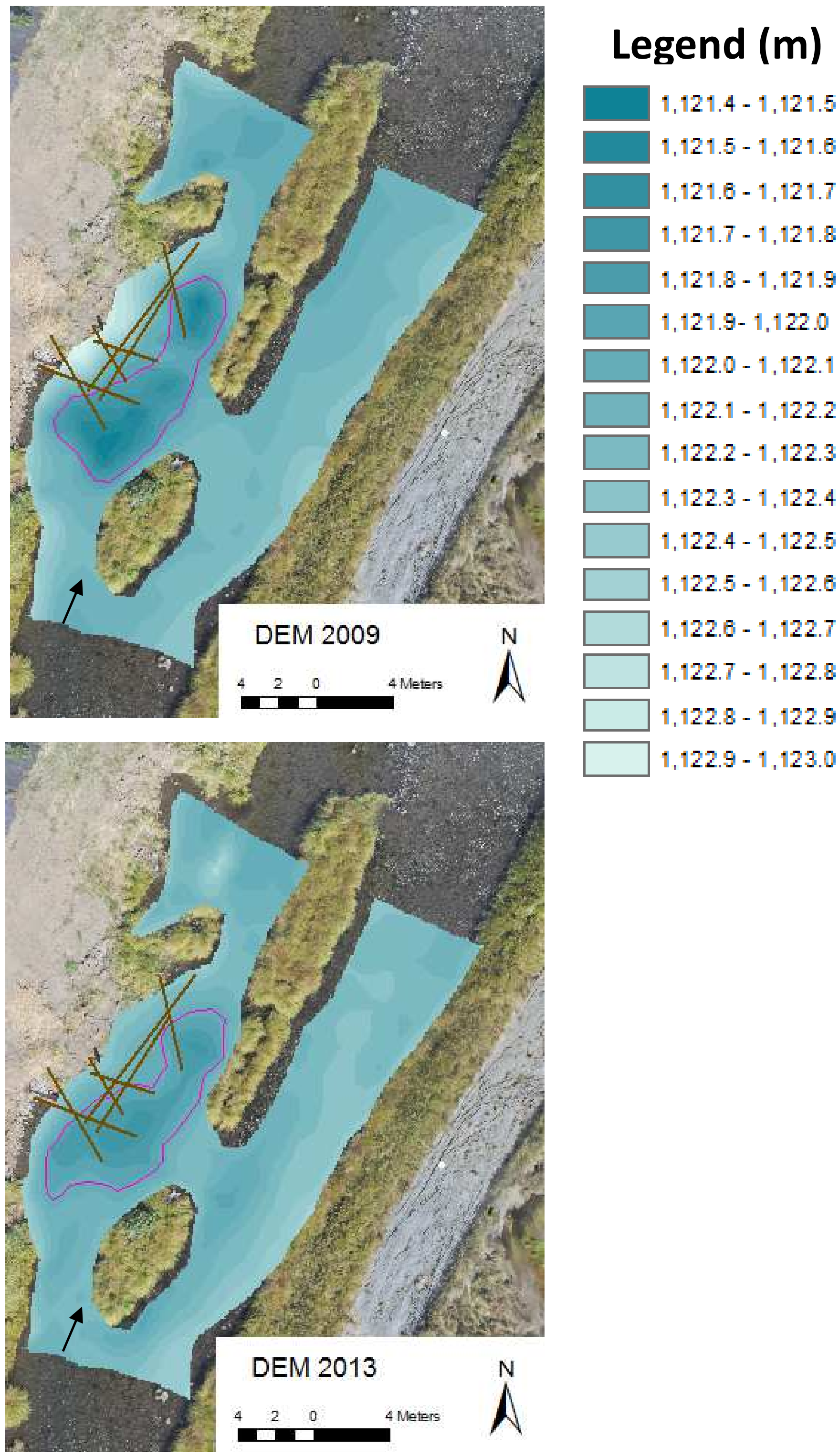
Legend (m)
1,121.4 - 1,121.5
1,121.5 - 1,121.6
1,121.6 - 1,121.7
1,121.7 - 1,121.8
1,121.8 - 1,121.9
1,121.9- 1,122.0
1,122.0 - 1,122.1
1,122.1 - 1,122.2
1,122.2 - 1,122.3
1,122.3 - 1,122.4
1,122.4 - 1,122.5
1,122.5 - 1,122.6
1,122.6 - 1,122.7
1,122.7 - 1,122.8
1,122.8 - 1,122.9
1,122.9 - 1,123.0
DEM 2009
N
4 2 0 4 Meters
DEM 2013
N
4 2 0 4 Meters

RABE 10 DoD

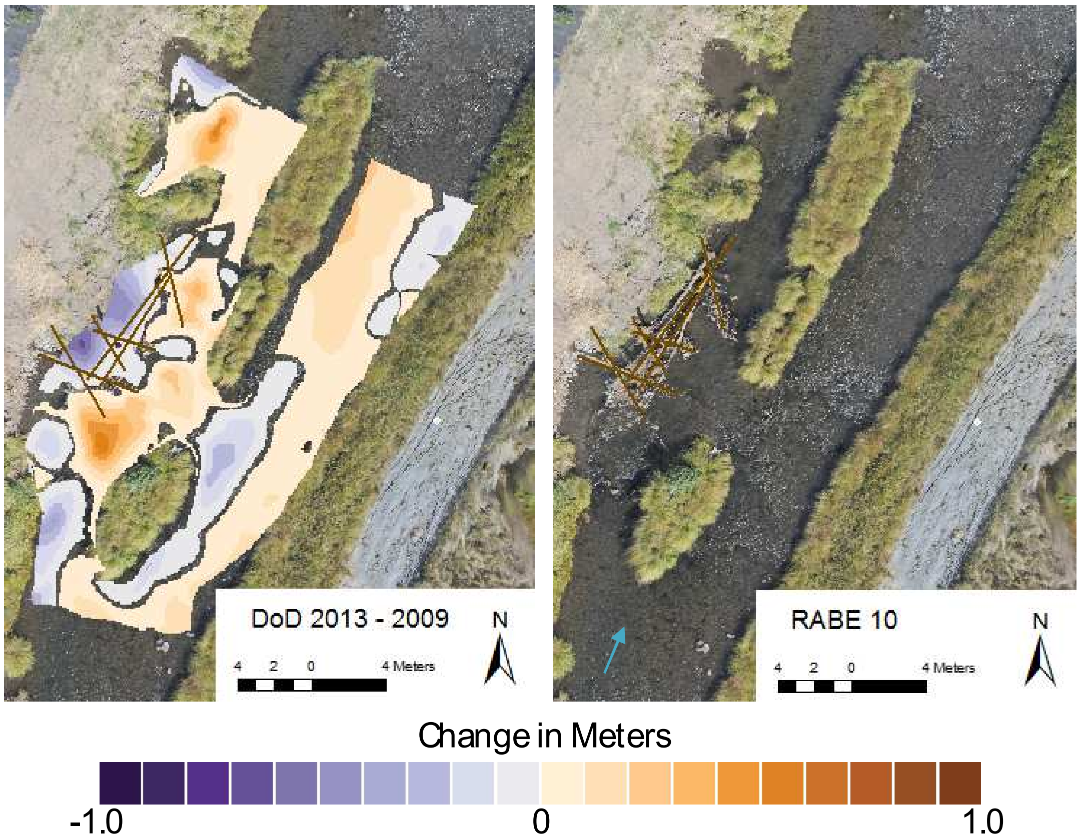
DoD 2013 - 2009
4 2 0 4 Meters
N
RABE 10
4 2 0 4 Meters
N
Change in Meters
-1.0
0
1.0

RABE 11 DEM

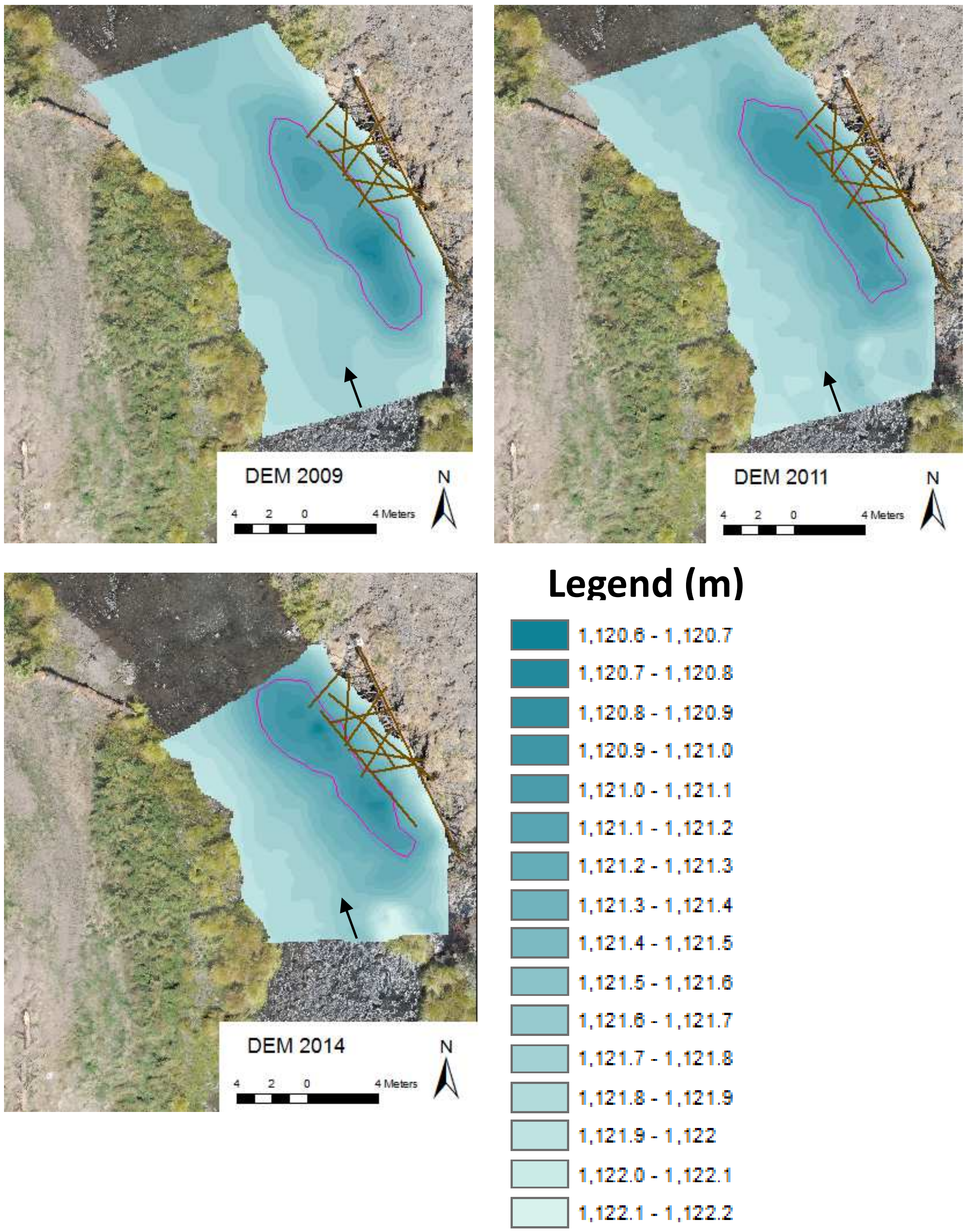
DEM 2009
N
4 2 0 4 Meters
DEM 2011
N
4 2 0 4 Meters
DEM 2014
N
4 2 0 4 Meters
Legend (m)
1,120.6 - 1,120.7
1,120.7 - 1,120.8
1,120.8 - 1,120.9
1,120.9 - 1,121.0
1,121.0 - 1,121.1
1,121.1 - 1,121.2
1,121.2 - 1,121.3
1,121.3 - 1,121.4
1,121.4 - 1,121.5
1,121.5 - 1,121.6
1,121.6 - 1,121.7
1,121.7 - 1,121.8
1,121.8 - 1,121.9
1,121.9 - 1,122
1,122.0 - 1,122.1
1,122.1 - 1,122.2

RABE 11 DoD

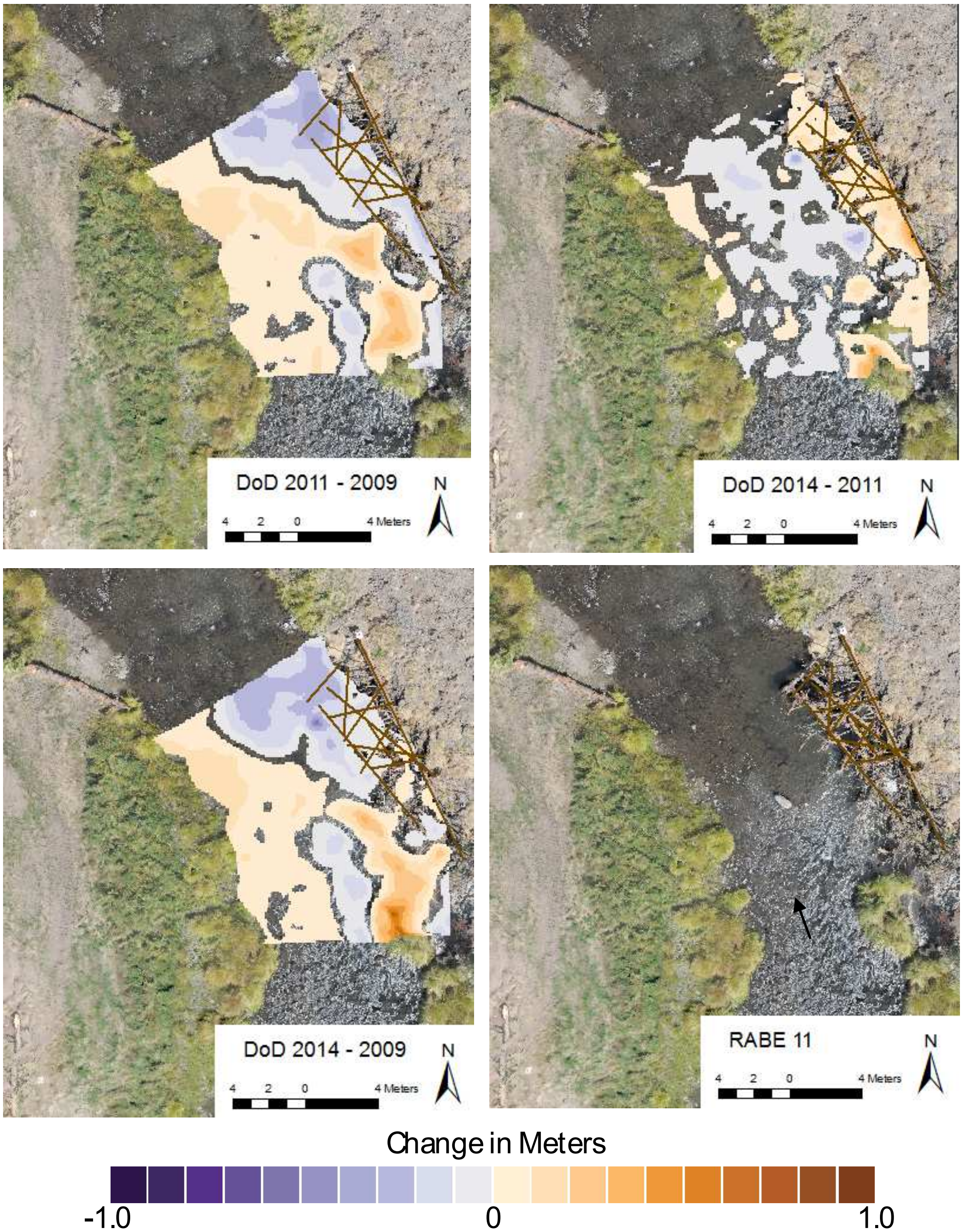
DoD 2011 - 2009
N
4 2 0 4 Meters
DoD 2014 - 2011
N
4 2 0 4 Meters
DoD 2014 - 2009
N
4 2 0 4 Meters
RABE 11
N
4 2 0 4 Meters
Change in Meters
-1.0
0
1.0

RABE 12 DEM

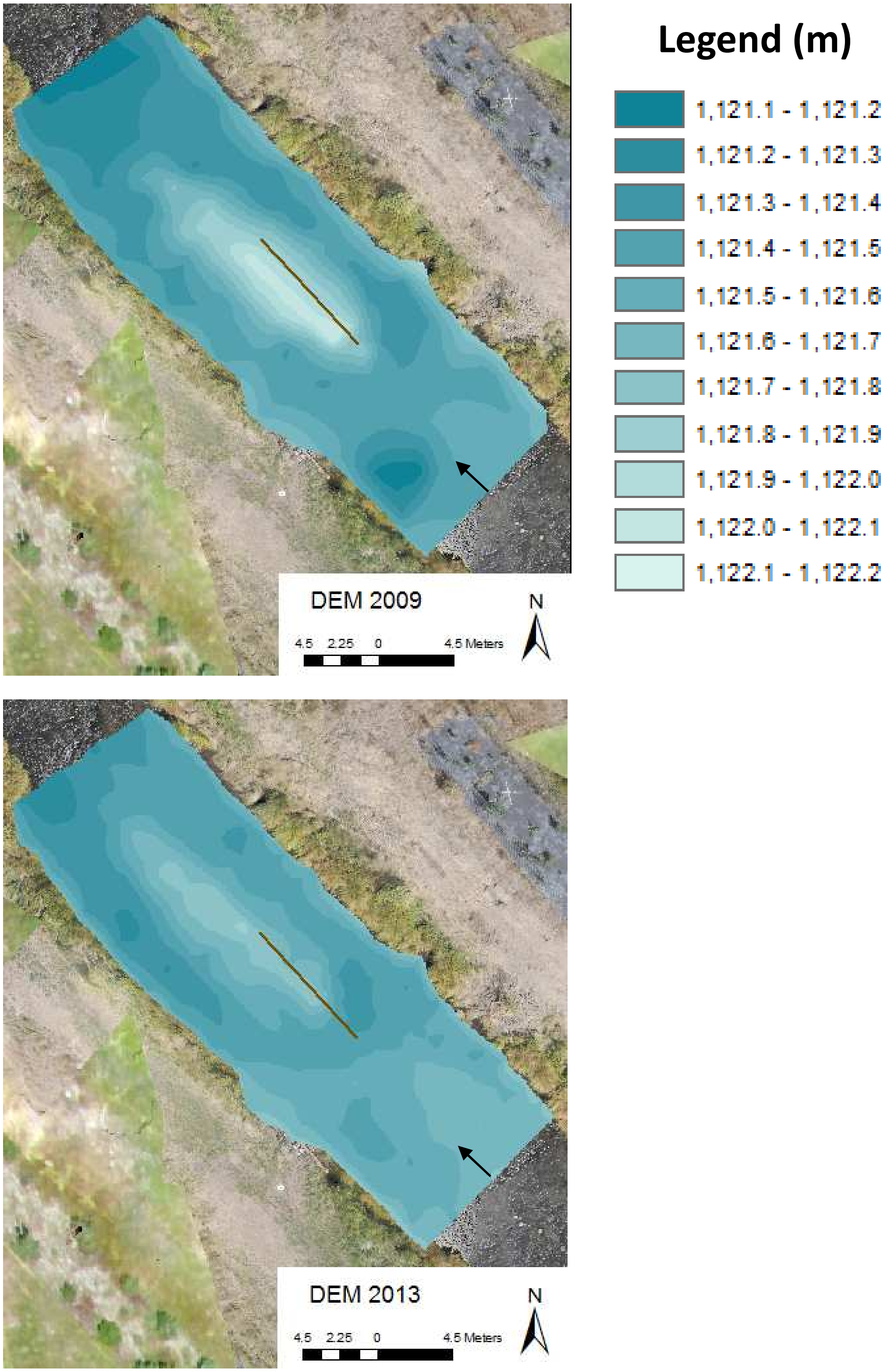
Legend (m)
1,121.1 - 1,121.2
1,121.2 - 1,121.3
1,121.3 - 1,121.4
1,121.4 - 1,121.5
1,121.5 - 1,121.6
1,121.6 - 1,121.7
1,121.7 - 1,121.8
1,121.8 - 1,121.9
1,121.9 - 1,122.0
1,122.0 - 1,122.1
1,122.1 - 1,122.2
DEM 2009
4.5 2.25 0 4.5 Meters
N
DEM 2013
4.5 2.25 0 4.5 Meters
N

RABE 12 DoD

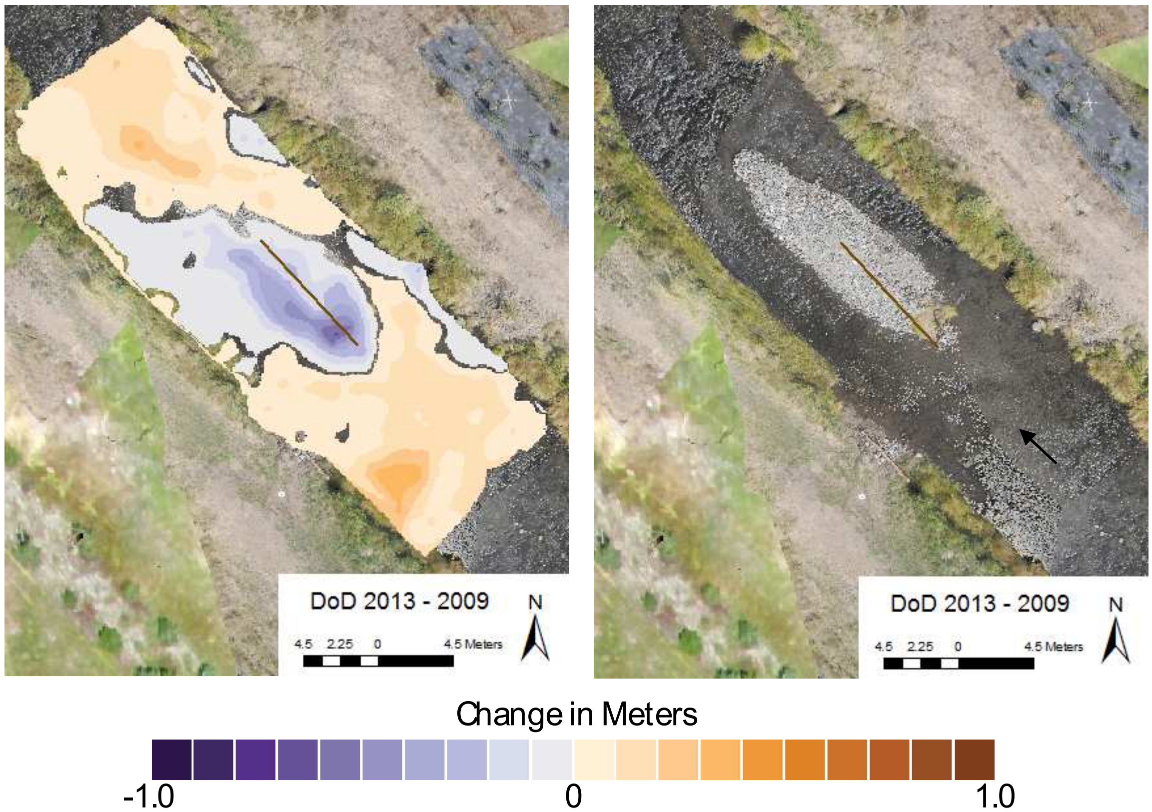
DoD 2013 - 2009
N
4.5 2.25 0 4.5 Meters
DoD 2013 - 2009
N
4.5 2.25 0 4.5 Meters
Change in Meters
-1.0
0
1.0

RABE 16 DEM

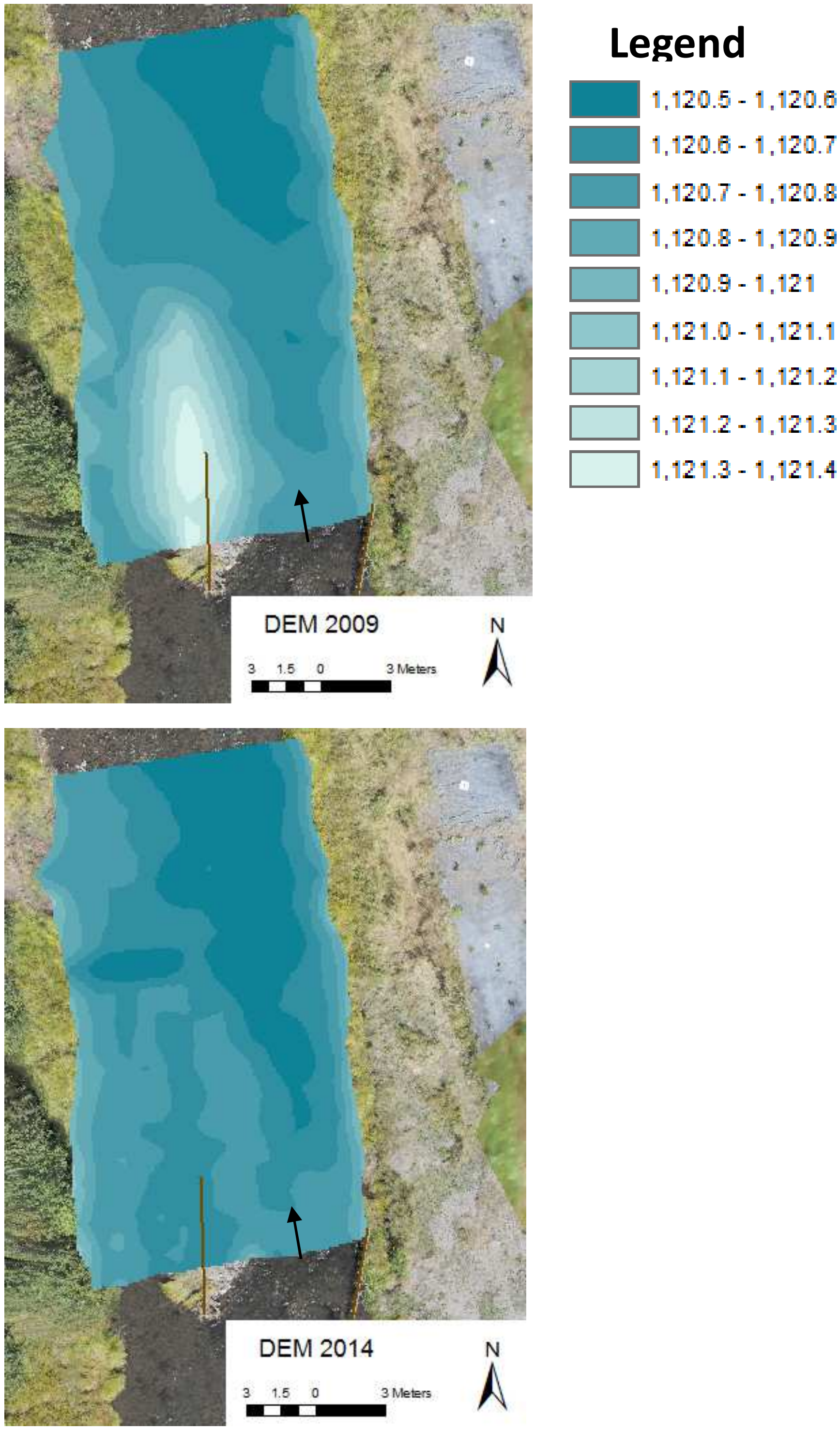
Legend
1,120.5 - 1,120.6
1,120.6 - 1,120.7
1,120.7 - 1,120.8
1,120.8 - 1,120.9
1,120.9 - 1,121
1,121.0 - 1,121.1
1,121.1 - 1,121.2
1,121.2 - 1,121.3
1,121.3 - 1,121.4
DEM 2009
N
3 1.5 0 3 Meters
DEM 2014
N
3 1.5 0 3 Meters

RABE 16 DoD

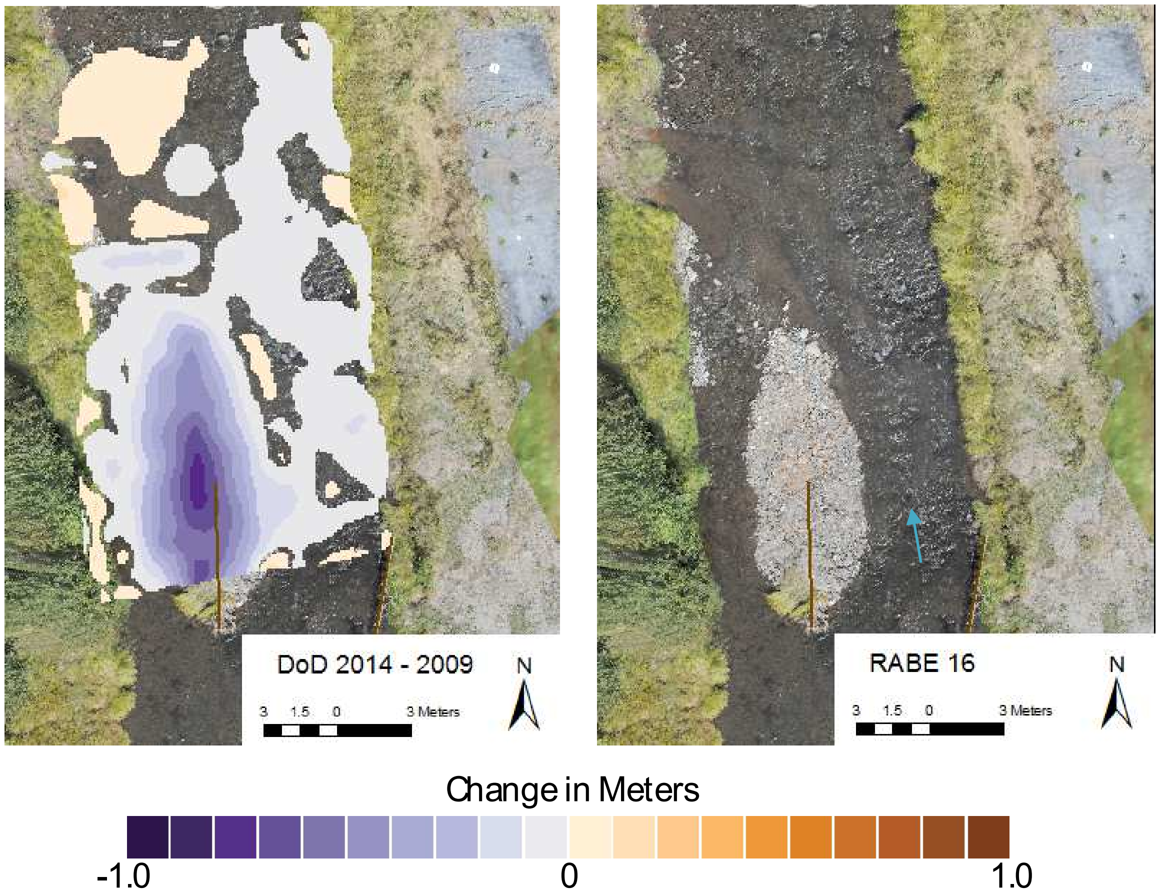

DoD 2014 - 2009
N
3 1.5 0 3 Meters
RABE 16
N
3 1.5 0 3 Meters
Change in Meters
-1.0
0
1.0

APPENDIX B

DESCRIPTION OF VARIABLES IN STUDY

Variables	Units	Description of Variable	Method
Total logs BF	Count	Total number of logs within bankfull and logs within bankfull that extend into the floodplain	Field
Total logs not BF	Count	Total number of logs in the structure outside of bankfull	Field
Anchored BF	Count	Number of logs that are buried into the bank or floodplain within bankfull and logs that are within bankfull and extend into floodplain	Field
Anchored not BF	Count	Number of logs that are buried into the bank or floodplain outside of bankfull	Field
Woven BF	Count	Number of logs that are woven in between other logs within bankfull and logs that are within bankfull and extend into floodplain	Field
Woven not BF	Count	Number of logs that are woven in between other logs into structure outside of bankfull	Field
Loose BF	Count	Number of logs that are not anchored or under other logs within bankfull and logs that are within bankfull and extend into floodplain	Field
Loose not BF	Count	Number of logs that are not anchored or under other logs outside of bankfull	Field
Perpend. BF	Count	Number of logs that are perpendicular (~80-100 degrees) to flow direction with in bankfull	Field
Perpend not BF	Count	Number of logs that are perpendicular (~80-100 degrees) to flow direction outside of bankfull	Field
Rootwads BF	Count	Number of rootwads that are part of the structure within bankfull	Field
Rootwads not BF	Count	Number of rootwads that are part of the structure outside of bankfull	Field
Bed Contact	Count	Number of logs in contact with the channel bed	Field
Body Length	m	Length (along the bank) of the main part of the structure encompassing where the majority of the logs are, but excluding any single logs extending far passed the rest of the structure	ArcGIS
Body Width	m	Width (protruding into the channel) of the main part of the structure encompassing where the majority of the logs are, but excluding single logs extending far passed the rest of the structure	ArcGIS
Body Height	cm	Height from the base of the lowest log to the top of the main part of the structure encompassing where the majority of the logs are	Stadia Rod
Height bed to log	cm	Height from the bed of the channel to the base of the lowest log	Stadia

Variables	**Units**	**Description of Variable**	**Method**
Total logs BF	Count	Total number of logs within bankfull and logs within bankfull that extend into the floodplain	Field
Total logs not BF	Count	Total number of logs in the structure outside of bankfull	Field
Anchored BF	Count	Number of logs that are buried into the bank or floodplain within bankfull and logs that are within bankfull and extend into floodplain	Field
			Rod
Volume LS	m^3	Length * width * height	Calculated
Area of survey	m^2	Area of the DoD survey for each log structure	ArcGIS
Volume fill	m^3	Total volume of aggraded material in DoD	ArcGIS
Volume fill/area	m	Volume of aggraded material divided by the total survey area for each DoD survey	Calculated
Volume scour	m^3	Total volume of scoured material in DoD	ArcGIS
Volume scour/area	m	Calculated volume scour/ total survey area for each LS DoD survey	Calculated
Radius curvature	m	Radius of the circle arc centered around each log structure that connects points 1.5 bankfull upstream and downstream of the structure	ArcGIS & Calculated

APPENDIX C

CORRELATION MATRIX FOR EXPLANATORY AND RESPONSE VARIABLES

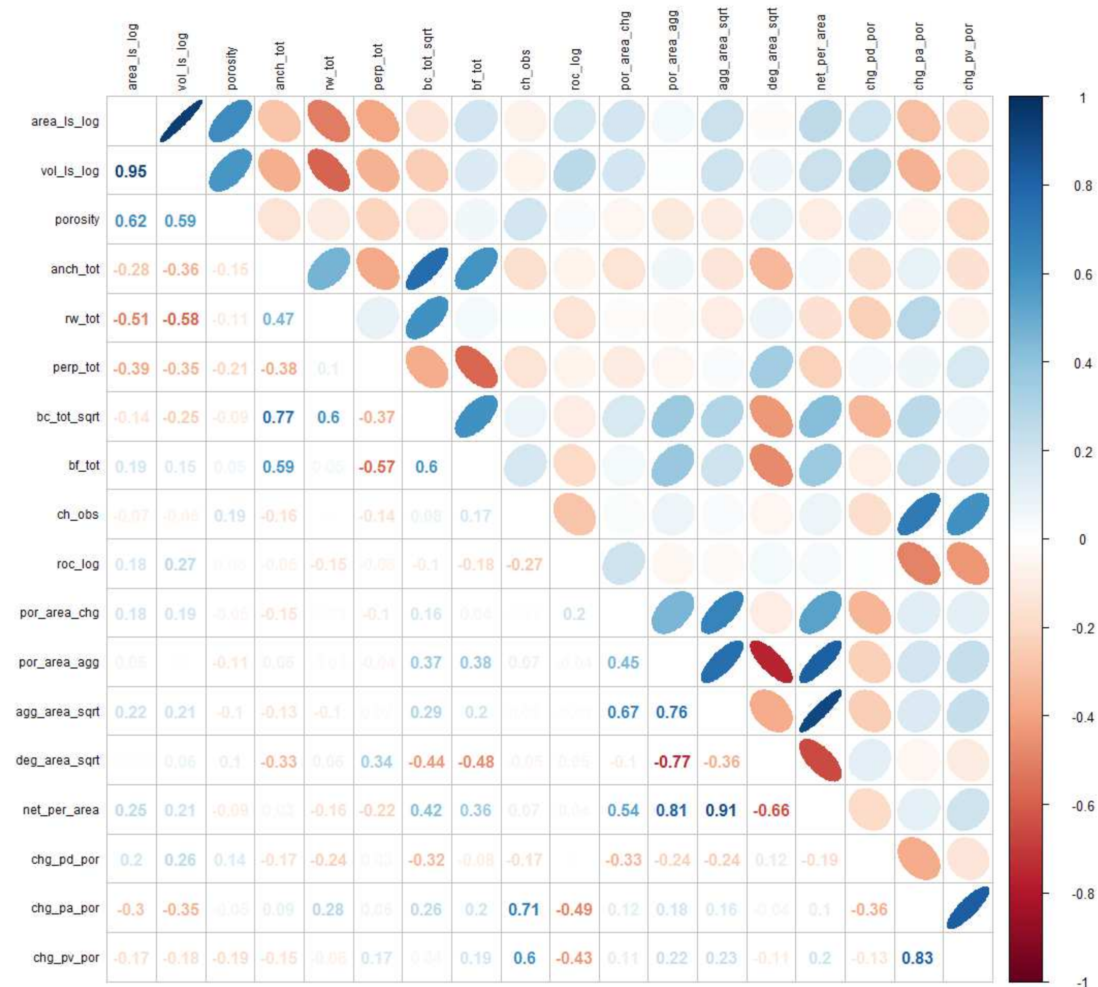

The upper half of the correlation matrix shows the direction and magnitude of the correlation. Blue ovals are positive correlation and red are negative correlations. Wider ovals are less correlated and narrower are highly correlated. The lower half of the matric shows the correlation values for each of these variable combinations. The shown correlations with transformed data. Variable descriptions are shown in Table 3 of the text.

APPENDIX D

LOG STRUCTURE STRUCTURAL CHANGES

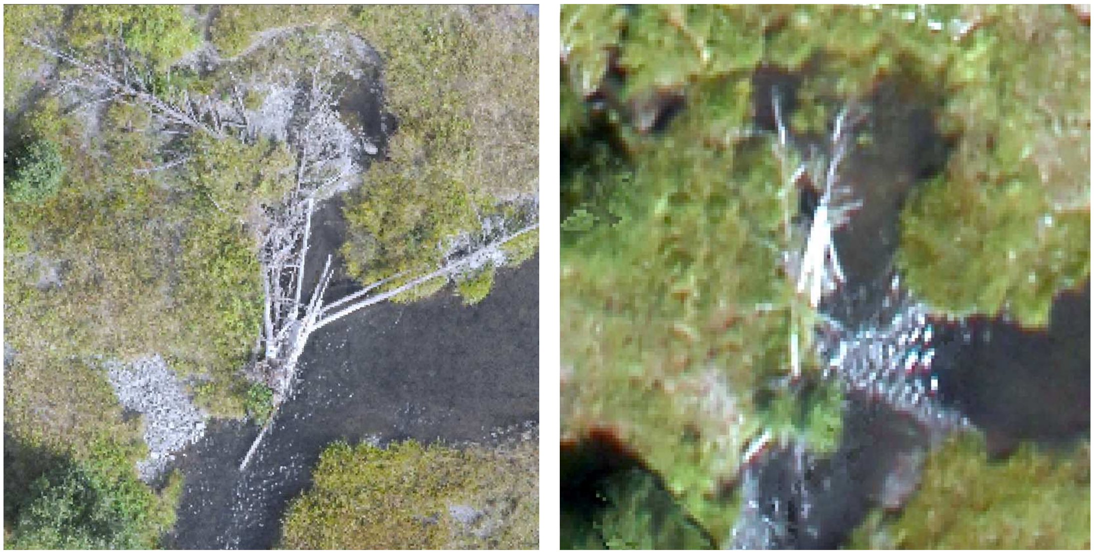

Aerial photos of **VIBR log structure 7**. Photo from 2009 is on the left and 2013 is on the right. The minor changes to the structure include the removal of the two alcove spanning logs and the log in the dry side channel. Other logs were reagrranged slightly.

Aerial photos of **VIBR log structure 10**. Photo from 2009 is on the left and 2013 is on the right. This log structure was completely washed away and the alcove has been filled.

Aerial photos of **VIBR log structure 11**. Photo from 2009 is on the left and 2013 is on the right. This minor changes to the structure are the removal of serveral logs from within the structure an on the bank.

Aerial photos of **VIBR log structure 16**. Photo from 2009 is on the left and 2013 is on the right. The minor changes to the structure include the removal of several loose bar top logs.

Aerial photos of **RABE log structure 8**. Photo from 2009 is on the left and 2013 is on the right. The minor change to the structure was the removal of one loose log in the structure.

Aerial photos of **RABE log structure 10**. Photo from 2009 is on the left and 2013 ison the right. The major changes to the structure include the removal and addition of many logs along with the complete rearangment of the existing logs.

Aerial photos of **RABE log structure 16**. Photo from 2009 is on the left and 2013 is on the right. The log structure was completely removed and the bar was washed out.

APPENDIX E

DATA FROM THE LOG STRUCTURE COMPOSITION SURVEY

	Log Jam Type	Channel BF Width (m)	Structure Length (m)	Structure Width (m)	Structure Height (m)	Area of LS (m^2)	Volume of LS (m^3)	Area of survey (m^2)
Vibr 1	MJ	8.1	12.4	3.1	1.83	38.44	70.15	146.19
Vibr 2	MJ	6.6	5.6	2.4	1.60	13.44	21.50	124.27
Vibr 3	BKJ	6.5	7.6	1.4	1.30	10.64	13.83	118.93
Vibr 4	MJ	10.2	6.3	2.5	1.20	15.75	18.90	134.32
Vibr 5	BKJ	7.7	4.3	3.2	1.75	13.76	24.08	110.99
Vibr 6	BKJ	8.4	6.7	4.1	1.50	27.47	41.20	61.47
Vibr 7	AJ	7.1	3.8	1.8	1.80	6.84	12.31	130.53
Vibr 8	BKJ	5.2	4.2	1.9	1.70	7.98	13.56	73.77
Vibr 9	MJ	6.2	2.6	4.6	1.45	11.96	17.34	103.51
Vibr 11	AJ	6.6	2.2	3.6	1.00	7.92	7.92	57.10
Vibr 12	MJ	7.3	3.5	3	1.35	10.5	14.17	62.24
Vibr 13	MJ	6.6	4.8	4.8	1.80	23.04	41.47	84.46
Vibr 14	AJ	9.2	1.6	2.2	2.00	3.52	7.04	99.29
Vibr 15	MJ	5.1	3	1.8	0.90	5.4	4.86	66.90
Vibr 16	BTJ	24	5.2	3.6	0.80	18.72	14.97	90.44
Vibr 17	MJ	5.5	5.3	1.6	0.80	8.48	6.78	83.48
Rabe 1	BKJ	10	8.6	4.8	2.00	41.28	82.56	197.35
Rabe 2	MJ	21.3	19.2	3.5	2.60	67.2	174.72	324.8
Rabe 4	BKJ	13.1	5.6	4.1	2.30	22.96	52.80	136.2
Rabe 6	BKJ	13.5	6.8	4.1	1.90	27.88	52.97	207.69
Rabe 7	BKJ	15.8	7.2	3.9	2.00	28.08	56.16	222.87
Rabe 8	BKJ	12.4	4.5	3.4	1.90	15.3	29.07	199.47
Rabe 9	MJ	12.5	13.4	4.1	2.10	54.94	115.37	339.81
Rabe 10	BKJ	15.1	8.7	3.2	0.95	27.84	26.45	387.56
Rabe 11	MJ	12.6	11.7	2.8	2.50	32.76	81.9	249.85
Rabe 12	BAJ	14	5	0.7	0.70	3.5	2.45	423.11
Rabe 16	BAJ	13	1.1	1.5	0.00	1.65	0	263.02

BF = Bankfull, LS = Log Structure

Note: BF = Bankfull	**Total logs**	**Total Logs not in BF**	**Anchored Logs in BF /not BF**		**Woven Logs in BF/not BF**		**Loose Logs in Bf /not BF**		**Perpendicular logs in BF/ not BF**		**Logs in Bed Contact**	**Rootwads in BF/ not BF**	
Vibr 1	17	5	6	1	5	0	1	4	3	0	3	8	1
Vibr 2	14	3	5	0	6	2	0	1	4	0	1	4	0
Vibr 3	9	5	3	0	0	2	1	3	2	0	3	3	3
Vibr 4	8	1	5	0	2	0	0	1	2	0	2	3	0
Vibr 5	9	2	3	0	4	2	0	0	4	0	2	3	1
Vibr 6	9	5	1	0	3	3	0	2	1	0	0	1	0
Vibr 7	3	2	0	0	0	1	1	1	1	2	0	0	2
Vibr 8	9	3	3	0	3	2	0	1	4	0	3	3	2
Vibr 9	7	0	2	0	4	0	1	0	4	0	2	3	0
Vibr 11	2	0	2	0	0	0	0	0	0	0	2	2	0
Vibr 12	6	0	4	0	2	0	0	0	3	0	2	3	0
Vibr 13	6	0	2	0	3	0	1	0	1	0	2	3	0
Vibr 14	4	1	3	0	0	0	0	1	1	0	1	2	0
Vibr 15	3	0	3	0	0	0	0	0	1	0	3	3	0
Vibr 16	7	0	3	0	4	0	0	0	2	0	2	4	0
Vibr 17	2	0	2	0	0	0	0	0	1	0	1	1	0
Rabe 1	27	2	9	0	14	1	2	1	6	0	11	9	0
Rabe 2	31	2	14	0	13	1	2	1	7	0	12	12	0
Rabe 4	15	0	10	0	5	0	0	0	5	0	3	7	0
Rabe 6	11	1	4	0	6	1	0	0	3	0	2	6	0
Rabe 7	17	0	10	0	6	0	1	0	3	0	7	5	0
Rabe 8	9	0	6	0	3	0	0	0	3	0	3	5	0
Rabe 9	21	0	13	0	7	0	1	0	6	0	8	10	0
Rabe 10	5	2	3	0	0	0	0	2	2	0	2	3	0
Rabe 11	25	0	14	0	8	0	3	0	6	0	4	7	0
Rabe 12	1	0	1	0	0	0	0	0	0	0	1	1	0
Rabe 16	0	0	1	0	0	0	0	0	0	0	0	1	0

APPENDIX F

PRINCIPAL COMPONENT ANALYSIS PLOTS AND LOADINGS

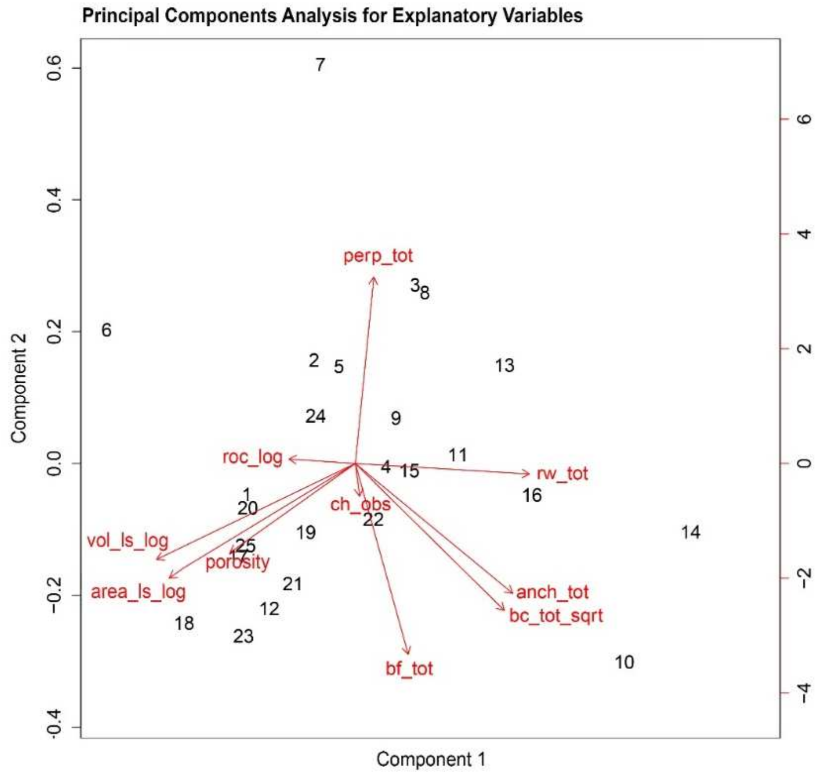

PCA biplot showing the loadings of the explanatory variables (red arrows show direction and length of arrow shows relative loadings). The plotted numbers display how each observation relates to component one and two. Variable descriptions are shown in Table 3 in the text

	Comp1	**Comp2**	**Comp3**
Standard Deviation	1.82	1.63	1.17
Loadings:			
area_ls_log	-0.445	-0.301	0.058
vol_ls_log	-0.476	-0.256	0.079
porosity	-0.300	-0.237	-0.211
anch_tot	0.377	-0.346	0.2237
rw_tot	0.417	-0.028	-0.001
perp_tot	0.044	0.497	-0.024
bc_tot	0.357	-0.392	0.067
bf_tot	0.127	-0.508	-0.075
ch_obs	0.010	-0.088	-0.715
roc_log	-0.156	0.011	.607

Table shows the standard deviation for the three components considered significant in this study (standard deviation >1). The table also shows the loadings of each variable on each of the three significant components.

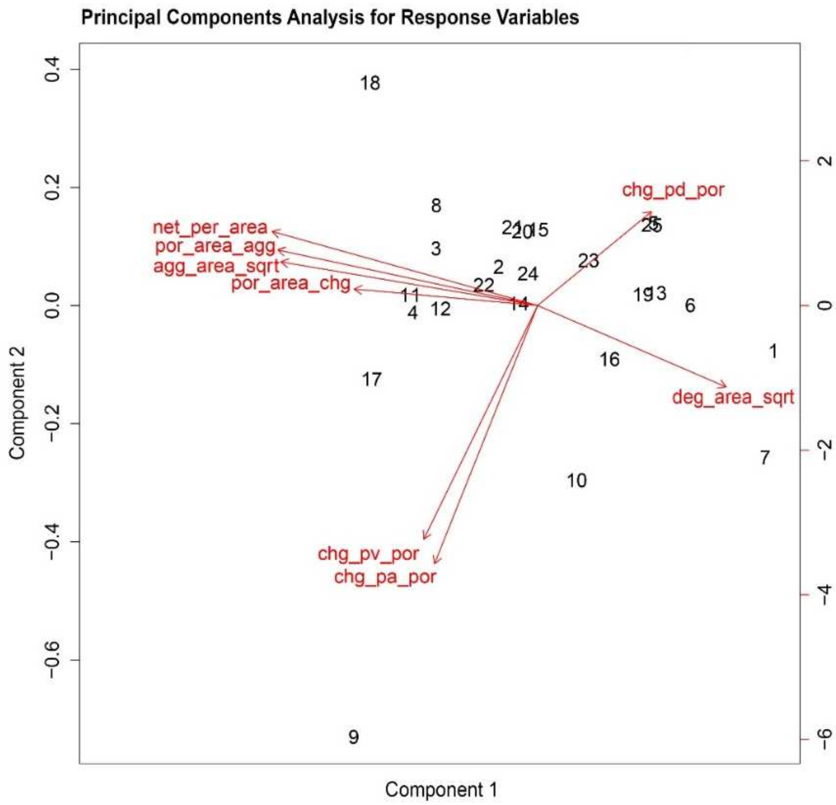

PCA biplot showing the loadings of the response variables (red arrows show direction and length of arrow shows relative loadings). The plotted numbers display how each observation relates to component one and two. Variable descriptions are shown in Table 3 in the text.

	Comp1	**Comp2**	**Comp3**
Standard Deviation	1.93	1.33	1.05
Loadings:			
por_area_chg	-0.337	0.044	-0.584
por_area_agg	-0.466	0.145	0.206
agg_area_sqrt	-0.460	0.114	-0.190
deg_area_sqrt	0.338	-0.212	-0.535
net_per_area	-0.476	0.193	0.067
chg_pd_por	0.204	0.244	0.463
chg_pa_por	-0.185	-0.672	0.097
chg_pv_por	-0.204	-0.608	0.257

Table shows the standard deviation for the three components considered significant in this study (standard deviation >1). The table also shows the loadings of each variable on each of the three significant components.

REFERENCES CITED

Abbe, T. B., Brooks, A. P., & Montgomery, D. R. (2003). Wood in River Rehabilitation and Management. The Ecology and Management of Wood in World Rivers.

Abbe, T. B., & Montgomery, D. R. (1996). Large woody debris jams, channel hydraulics and habitat formation in large rivers. Regulated Rivers Research & Management, 12(23), 201–221.

Bandow, J. R. (2004). Holocene Alluvial History of the Middle Fork John Day River, Oregon. University of Oregon.

Bernhardt, E. S., Palmer, M., Allan, J. D., Alexander, G., Barnas, K., Brooks, S., others. (2005). Synthesizing U. S. river restoration efforts. Science (Washington), 308(5722), 636–637.

Bernhardt, E. S., Sudduth, E. B., Palmer, M. A., Allan, J. D., Meyer, J. L., Alexander, G., … others. (2007). Restoring rivers one reach at a time: results from a survey of US river restoration practitioners. Restoration Ecology, 15(3), 482–493.

Beschta, R. L. (1983). The effects of large organic debris upon channel morphology: a flume study. In Proceedings of the DB Simons Symposium on erosion and sedimentation (Vol. 8). Simons, Li Associates: Fort Collins, CO.

Biron, P. M., Robson, C., Lapointe, M. F., & Gaskin, S. J. (2005). Three-dimensional flow dynamics around deflectors. River Research and Applications, 21(9), 961–975.

Brooks, A. P., Gehrke, P. C., Jansen, J. D., & Abbe, T. B. (2004). Experimental reintroduction of woody debris on the Williams River, NSW: geomorphic and ecological responses. River Research and Applications, 20(5), 513–536.

Brooks, A. P., Howell, T., Abbe, T. B., & Arthington, A. H. (2006). Confronting hysteresis: wood based river rehabilitation in highly altered riverine landscapes of south-eastern Australia. Geomorphology, 79(3), 395–422.

Buffington, J. M., Lisle, T. E., Woodsmith, R. D., & Hilton, S. (2002). Controls on the size and occurrence of pools in coarse-grained forest rivers. River Research and Applications, 18(6), 507–531.

Bureau of Land Management. (n.d.). John Day River. Retrieved from www.blm.gov/or/resources/recreation/johnday/index

Bureau of Reclamation. (2007). Forrest Conservation Property Restoration, Engineering Designs. Department of Interior.

Bureau of Reclamation. (2008a). Middle Fork and Upper John Day River tributary assessments Grant County, Oregon. U.S. Department of the Interior.

Bureau of Reclamation. (2008b). Oxbow Conservation Property Restoration, Engineering Designs. Department of Interior.

Bureau of Reclamation. (2008c). Rock Removal and Large Woody Debris Installation - Beaver to Ragged; Columbia/Snake River Salmon Recovery Program, Oregon.

Bureau of Reclamation. (2009). Geomorphology and hydraulic model analysis of the Oxbow Conservation Area, Middle Fork John Day River, Grant County, Oregon. U.S. Department of the Interior.

Bureau of Reclamation. (2010). Forrest Conservation Area Reach Assessment, Middle Fork John Day River, Grant County, Oregon.

Cherry, J., & Beschta, R. L. (1989). Coarse Woody Debris and Channel Morphology: A Flume Study. Wiley Online Library.

Curry, C., Bennett, S., & Bouwes, N. (2011). Upper Middle Fork John Day River Intensively Monitored Watershed: Experimental Design and Implementation Plan, Draft.

Daniels, M. D., & Rhoads, B. L. (2004). Effect of large woody debris configuration on three-dimensional flow structure in two low-energy meander bends at varying stages. Water Resources Research, 40(11).

Dietrich, J. (2014). Applications of Structure-from-Motion Photogrammetry to Fluvial Geomorphology. Ph.D. Dissertation, University of Oregon.

Drury, T. A., Petroff, C., Abbe, T. B., Montgomery, D. R., & Pess, G. R. (1999). 'Evaluation of engineered log jams as a soft bank stabilization technique: North Fork Stillaguamish River, Washington. In Proc., 1999 Water Resources Engineering Conf.

Gippel, C. J., O'Neill, I. C., Finlayson, B. L., & Schnatz, I. (1996). Hydraulic guidelines for the re-introduction and management of large woody debris in lowland rivers. Regulated Rivers: Research & Management, 12(2-3), 223–236.

Gomez, B. (2000). Book Review: River management: the Australasian experience. Progress in Physical Geography, 24(4), 615–616.

Hillman, M., & Brierley, G. (2005). A critical review of catchment-scale stream rehabilitation programmes. Progress in Physical Geography, 29(1), 50–76.

Jett, S. (1998). Alluvial Fan Development in a Confined Montane Valley, Middle Fork John Day River, Eastern Oregon. Master's Thesis, University of Oregon.

Katz, S. L., Barnas, K., Hicks, R., Cowen, J., & Jenkinson, R. (2007). Freshwater habitat restoration actions in the Pacific Northwest: a decade's investment in habitat improvement. Restoration Ecology, 15(3), 494–505.

Keller, E. A., & Swanson, F. J. (1979). Effects of large organic material on channel form and fluvial processes. Earth Surface Processes, 4(4), 361–380.

Lisle, T. (1987). Using "residual depths" to monitor pool depths independently of discharge. U.S. Forest Service.

Manners, R. B., & Doyle, M. W. (2008). A mechanistic model of woody debris jam evolution and its application to wood-based restoration and management. River Research and Applications, 24(8), 1104–1123.

McDowell, P. (Pers. Comm.). Monitoring Hypothesis Table.

McDowell, P. F. (2000). Human impacts and river channel adjustment, northeastern Oregon: implications for restoration. Riparian Ecology and Management in Multi-Land Use Watersheds. TPS-00-2, American Water Resources Association, Middleburg, VA, 257–261.

McDowell, P. F. (2001). Spatial variations in channel morphology at segment and reach scales, Middle Fork John Day River, Northeastern Oregon. Geomorphic Processes and Riverine Habitat, 159–172.

Middle Fork Intensively Monitored Watershed. (n.d.). Retrieved from www.middleforkimw.org

Milan, D. J., Heritage, G. L., Large, A. R., & Fuller, I. C. (2011). Filtering spatial error from DEMs: Implications for morphological change estimation. Geomorphology, 125(1), 160–171.

Montgomery, D. R., Buffington, J. M., Smith, R. D., Schmidt, K. M., & Pess, G. (1995). Pool spacing in forest channels. Water Resources Research, 31(4), 1097–1105.

Nakamura, F., & Swanson, F. J. (1993). Effects of coarse woody debris on morphology and sediment storage of a mountain stream system in western Oregon. Earth Surface Processes and Landforms, 18(1), 43–61.

Nanson, G. C., & Croke, J. C. (1992). A genetic classification of floodplains. Geomorphology, 4(6), 459–486.

NOAA Fisheries. (n.d.). Stream and Rivers Restoration. US Department of Commerce. Retrieved from www.habitat.noaa.gov/restoration/techniques/srrestoration

Oregon Department of Geology and Mineral Industries. (n.d.). Oregon: A Geologic History. State of Oregon. Retrieved from www.oregongeology.org/sub/publications/ims/ims-028/constructing

Orr, E. L., & Orr, W. N. (2012). Oregon Geology. Oregon State University Press.

Pess, G. R., Liermann, M. C., McHenry, M. L., Peters, R. J., & Bennett, T. R. (2012). Juvenile salmon response to the placement of engineered log jams (ELJs) in the

Elwha River, Washington State, USA. River Research and Applications, 28(7), 872–881.

Roni, P., Beechie, T. J., Bilby, R. E., Leonetti, F. E., Pollock, M. M., & Pess, G. R. (2002). A review of stream restoration techniques and a hierarchical strategy for prioritizing restoration in Pacific Northwest watersheds. North American Journal of Fisheries Management, 22(1), 1–20.

Russell, K., & Bauer, T. (2009). Using High Resolution Balloon Photography to Provide Topographic Data. AGU, Fall Meeting, Abstract H51A–0745.

Shields, F. D., Knight, S. S., & Stofleth, J. M. (2006). Large wood addition for aquatic habitat rehabilitation in an incised, sand-bed stream, Little Topashaw Creek, Mississippi. River Research and Applications, 22(7), 803–817.

Shields, F. D., Morin, N., & Kuhnle, R. A. (2001). Effect of large woody debris structures on stream hydraulics. In Wetlands Engineering & River Restoration 2001 (pp. 1–12). ASCE.

Svoboda, C. D., & Russell, K. (2011). Flume analysis of engineered large wood structures for scour development and habitat. In World Environmental and Water Resources Congress (pp. 2572–2581).

US Fish and Wildlife Service. (n.d.). Endangered Species. Retrieved from www.fws.gov/endangered

Wheaton, J. M., Brasington, J., Darby, S. E., & Sear, D. A. (2010). Accounting for uncertainty in DEMs from repeat topographic surveys: improved sediment budgets. Earth Surface Processes and Landforms, 35(2), 136–156.

Wohl, E. (2005). Compromised rivers: understanding historical human impacts on rivers in the context of restoration. Ecology and Society, 10(2), 2.

Wohl, E., Angermeier, P. L., Bledsoe, B., Kondolf, G. M., MacDonnell, L., Merritt, D. M., Tarboton, D. (2005). River restoration. Water Resources Research, 41(10).